
Volatility Clustering in Financial Markets: Empirical Facts and Agent-Based Models

Rama Cont*

Centre de Mathématiques appliquées, Ecole Polytechnique
F-91128 Palaiseau, France Rama.Cont@polytechnique.fr

To appear in: A Kirman & G Teyssiere (eds.): *Long memory in economics*, Springer (2005).

Summary. Time series of financial asset returns often exhibit the *volatility clustering* property: large changes in prices tend to cluster together, resulting in persistence of the amplitudes of price changes. After recalling various methods for quantifying and modeling this phenomenon, we discuss several economic mechanisms which have been proposed to explain the origin of this volatility clustering in terms of behavior of market participants and the news arrival process. A common feature of these models seems to be a switching between low and high activity regimes with heavy-tailed durations of regimes. Finally, we discuss a simple agent-based model which links such variations in market activity to threshold behavior of market participants and suggests a link between volatility clustering and investor inertia.

1 Introduction

The study of statistical properties of financial time series has revealed a wealth of interesting stylized facts which seem to be common to a wide variety of markets, instruments and periods [12, 16, 25, 47]:

- **Excess volatility:** many empirical studies point out to the fact that it is difficult to justify the observed level of variability in asset returns by variations in “fundamental” economic variables. In particular, the occurrence of large (negative or positive) returns is not always explainable by the arrival of new information on the market [15].
- **Heavy tails:** the (unconditional) distribution of returns displays a heavy tail with positive excess kurtosis.

* The author thanks Alan Kirman and Gilles Teyssière for their infinite patience and participants in the CNRS Summer School on Complex Systems in the Social Sciences (ENS Lyon, 2004) for their stimulating feedback. The last section of this paper is based on joint work with F. Ghoulmie and J.P. Nadal.

- **Absence of autocorrelations in returns:** (linear) autocorrelations of asset returns are often insignificant, except for very small intraday time scales ($\simeq 20$ minutes) where microstructure effects come into play.
- **Volatility clustering:** as noted by Mandelbrot [40], “large changes tend to be followed by large changes, of either sign, and small changes tend to be followed by small changes.” A quantitative manifestation of this fact is that, while returns themselves are uncorrelated, absolute returns $|r_t|$ or their squares display a positive, significant and slowly decaying autocorrelation function: $\text{corr}(|r_t|, |r_{t+\tau}|) > 0$ for τ ranging from a few minutes to a several weeks.
- **Volume/volatility correlation:** trading volume is positively correlated with market volatility. Moreover, trading volume and volatility show the same type of “long memory” behavior [36].

Among these properties, the phenomenon of volatility clustering has intrigued many researchers and oriented in a major way the development of stochastic models in finance –GARCH models and stochastic volatility models are intended primarily to model this phenomenon. Also, it has inspired much debate as to whether there is long-range dependence in volatility. We review some of these issues in Section 2. As noted by the participants of this econometric debate [54, 46], statistical analysis alone is not likely to provide a definite answer for the presence or absence of long-range dependence phenomenon in stock returns or volatility, unless economic mechanisms are proposed to understand the origin of such phenomena.

Some insights into these economic mechanisms are given by agent-based models of financial markets. Agent-based market models attempt to explain the origin of the observed behavior of market prices in terms of simple, stylized, behavioral rules of market participants [11, 38, 39, 32]: in this approach a financial market is modeled as a system of heterogeneous, interacting agents and several examples of such models have been shown to generate price behavior similar to those observed in real markets. We review some of these approached in Section 3 and discuss how they lead to volatility clustering.

Most of these agent-based models are complex in structure and have been studied using Monte Carlo simulations. As noted also by LeBaron [31], due to the complexity of such models it is often not clear *which* aspect of the model is responsible for generating the stylized facts and whether all the ingredients of the model are indeed required for explaining empirical observations. In Section 4 we present an agent-based model capable of generating time series of asset returns with properties similar to the stylized facts above, but which is simple enough in structure so the origins of volatility clustering can be traced back to agents behavior. This model points to a link between investor inertia and volatility clustering and provide an economic explanation for the switching mechanism proposed in the econometrics literature as an origin of volatility clustering.

2 Volatility clustering in financial time series

Denote by S_t the price of a financial asset — a stock, an exchange rate or a market index — and $X_t = \ln S_t$ its logarithm. Given a *time scale* Δ , the log return at scale Δ is defined as:

$$r_t = X_{t+\Delta} - X_t = \ln\left(\frac{S_{t+\Delta}}{S_t}\right). \quad (1)$$

Δ may vary between a minute (or even seconds) for tick data to several days. Observations are sampled at discrete times $t_n = n\Delta$. Time lags will be denoted by the Greek letter τ ; typically, τ will be a multiple of Δ in estimations. For example, if $\Delta = 1$ day, $\text{corr}[r_{t+\tau}, r_t]$ denotes the correlation between the daily return at period t and the daily return τ periods later.

2.1 Empirical behavior of autocorrelation functions

A typical display of daily log-returns is shown in figure 1: the volatility clustering feature is seen graphically from the presence of sustained periods of high or low volatility. As noted above, the autocorrelation of returns is typically insignificant at lags between a few minutes and a month. An example is shown in figure 2 (left). This “spectral whiteness” of returns can be attributed to the activity of arbitrageurs who exploit linear correlations in returns via trend following strategies [41]. By contrast, the autocorrelation function of absolute returns remains positive over lags of several weeks and decays slowly to zero: figure 2 (right) shows this decay for SLM stock (NYSE). This observation is remarkably stable across asset classes and time periods and is regarded as a typical manifestation of volatility clustering [8, 13, 16, 25]. Similar behavior is observed for the autocorrelation of squared returns [8] and more generally for $|r_t|^\alpha$ [16, 17, 13] but it seems to be most significant for $\alpha = 1$ i.e. absolute returns [16].

GARCH models [8, 19] were among the first models to take into account the volatility clustering phenomenon. In a GARCH(1,1) model the (squared) volatility depends on last periods volatility:

$$r_t = \sigma_t \varepsilon_t \quad \sigma_t^2 = a_0 + a\sigma_{t-1}^2 + b\varepsilon_t^2 \quad 0 < a + b < 1 \quad (2)$$

leading to positive autocorrelation in the volatility process σ_t , with a rate of decay governed by $a + b$: the closer $a + b$ is to 1, the slower the decay of the autocorrelation of σ_t . The constraint $a + b < 1$ allows for the existence of a stationary solution, while the upper limit $a + b = 1$ corresponds to the case of an integrated process. Estimations of GARCH(1,1) on stock and index returns usually yield $a + b$ very close to 1 [8]. For this reason the volatility clustering phenomenon is sometimes called a “GARCH effect”; one should keep in mind however that volatility clustering is a “non-parametric” property and is not intrinsically linked to a GARCH specification.

BMW stock daily returns

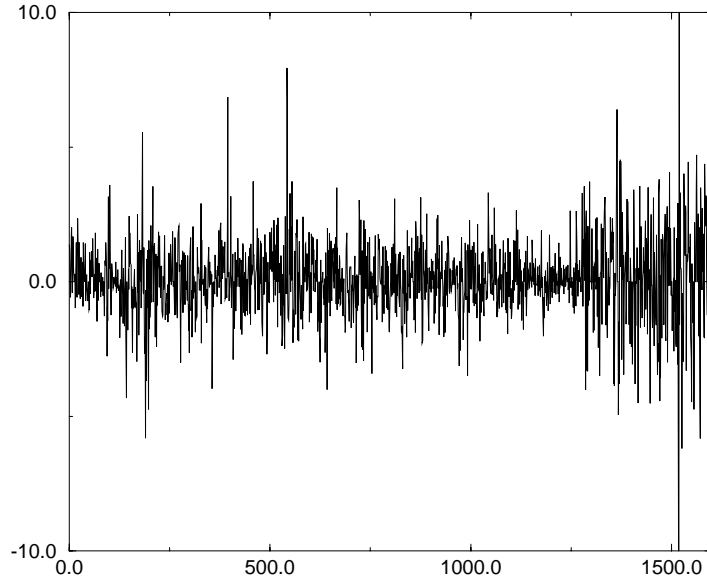


Fig. 1. Large changes cluster together: BMW daily log-returns. $\Delta = 1$ day.

While GARCH models give rise to exponential decay in autocorrelations of absolute or squared returns, the empirical autocorrelations are similar to a power law [13, 25]:

$$C_{|r|}(\tau) = \text{corr}(|r_t|, |r_{t+\tau}|) \simeq \frac{c}{\tau^\beta}$$

with an exponent $\beta \leq 0.5$ [13, 9], which suggests the presence of “long-range” dependence in amplitudes of returns, discussed below.

2.2 Long range dependence

Let us recall briefly the commonly used definitions of long range dependence, based on the autocorrelation function of a process:

Definition 1 (Long range dependence). *A stationary process Y_t (with finite variance) is said to have long range dependence if its autocorrelation function $C(\tau) = \text{corr}(Y_t, Y_{t+\tau})$ decays as a power of the lag τ :*

$$C(\tau) = \text{corr}(Y_t, Y_{t+\tau}) \underset{\tau \rightarrow \infty}{\sim} \frac{L(\tau)}{\tau^{1-2d}} \quad 0 < d < \frac{1}{2} \quad (3)$$

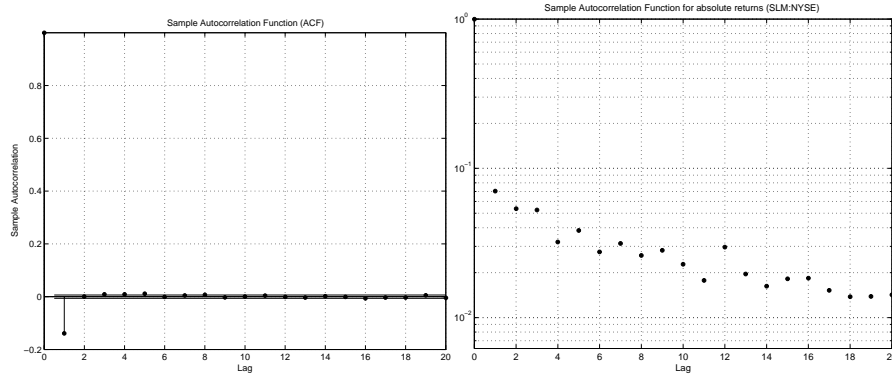


Fig. 2. SLM stock, NYSE, $\Delta = 5$ minutes. Left: autocorrelation function of log-returns. Right: autocorrelation of absolute log-returns.

where L is slowly varying at infinity, i.e. verifies $\forall a > 0, \frac{L(at)}{L(t)} \rightarrow 1$ as $t \rightarrow \infty$.

By contrast, one speaks of “short range dependence” if the autocorrelation function decreases at a geometric rate:

$$\exists K > 0, c \in]0, 1[, |C(\tau)| \leq Kc^\tau \quad (4)$$

Obviously, (3) and (4) are not the only possibilities for the behavior of the autocorrelation function at large lags: there are many other possible decay rates, intermediate between a power decay and a geometric decay. However, it is noteworthy that in all stochastic models used in the financial modeling literature, the behavior of returns and their absolute values fall within one of the two categories.

The long range dependence property (3) hinges upon the behavior of the autocorrelation function at *large* lags, a quantity which may be difficult to estimate empirically [7]. For this reason, models with long-range dependence are often formulated in terms of self-similar processes, which allow to extrapolate across time scales and deduce long time behavior from short time behavior, which is more readily observed. A stochastic process $(X_t)_{t \geq 0}$ is said to be self-similar if there exists $H > 0$ such that for any scaling factor $c > 0$, the processes $(X_{ct})_{t \geq 0}$ and $(c^H X_t)_{t \geq 0}$ have the same law:

$$(X_{ct})_{t \geq 0} \stackrel{d}{=} (c^H X_t)_{t \geq 0}. \quad (5)$$

H is called the self-similarity exponent of the process X . Note that a self-similar process cannot be stationary, so the above definition of long-range dependence cannot hold for a self-similar process, but eventually for its increments (if they are stationary). The typical example of self-similar process

whose increments exhibit long range dependence is fractional Brownian motion [43].

But self-similarity does not imply long-range dependence in any way: α -stable Lévy processes provide examples of self-similar processes with *independent* increments. Nor is self-similarity implied by long range dependence: Cheridito [10] gives several examples of Gaussian semimartingales with the same long range dependence features as fractional Brownian noise but with no self-similarity (thus very different “short range” properties and sample path behavior). The example of fractional Brownian motion is thus misleading in this regard, since it conveys the idea that these two properties are associated. When testing for long range dependence in a model based on fractional Brownian motion, we thus test the joint hypothesis of self-similarity *and* long-range dependence and strict self-similarity is not observed to hold in asset returns [12, 13].

A fallacy often encountered in the literature is that long range dependence in returns is incompatible with absence of (continuous-time) arbitrage. Again, the origin of this idea can be traced back to models based on fractional Brownian motion: since fractional Brownian motion is not a semimartingale, a model in which the (log)-price are described by a fractional Brownian motion is not arbitrage-free (in the continuous-time sense) [51]. This result (and the fact that fractional Brownian motions fails to be a semimartingale) crucially depends on the *local* behavior of its sample paths, not on its long range dependence property. Cheridito [10] gives several examples of Gaussian processes with the same long range dependence features as fractional Brownian motion, but which are semimartingales and lead to arbitrage-free models.

2.3 Dependence in stock returns

The volatility clustering feature indicates that asset returns are not independent across time; on the other hand the absence of linear autocorrelation shows that their dependence is nonlinear. Whether this dependence is “short range” or “long range” has been the object of many empirical studies.

The idea that stock returns could exhibit long range dependence was first suggested by Mandelbrot [41] and subsequently observed in many empirical studies using R/S analysis [42]. Such tests have been criticized by Lo [37] who pointed out that, after accounting for short range dependence, they might yield a different result and proposed a modified test statistic. Lo’s statistic highly depends on the way “short range” dependence is accounted for and shows a bias towards rejecting long range dependence [53]. The final empirical conclusions are therefore less clear [54].

However, the absence of long range dependence in returns may be compatible with its presence in absolute returns or “volatility”. As noted by Heyde [26], one should distinguish long range dependence in signs of increments, when $\text{sign}(r_t)$ verifies (3), from long range dependence in amplitudes, when $|r_t|$ verifies (3). Asset returns do not seem to possess long range dependence

in signs [26]. Many authors have thus suggested models, such as FIGARCH [4], in which returns have no autocorrelation but their amplitudes have long range dependence [4, 18].

It has been argued [33, 5] that the decay of $C_{|r|}(\tau)$ can also be reproduced by a superposition of several exponentials, indicating that the dependence is characterized by multiple time scales. In fact, an operational definition of long range dependence is that the time scale of dependence in a sample of length T is found to be of the order of T : dependence extends over the whole sample. Interestingly, the largest time scale in [33] is found to be of the order of...the sample size, a prediction which would be compatible with long-range dependence!

Many of these studies test for long range dependence in returns, volatility,.. by examining sample autocorrelations, Hurst exponents etc. but if time series of asset returns indeed possess the two features of heavy tails *and* long range dependence, then many of the standard estimation procedures for these quantities may fail to work [50]. For example, sample autocorrelation functions may fail to be consistent estimators of the true autocorrelation of returns in the price generating process: Resnick and van der Berg [49] give examples of such processes where sample autocorrelations converge to *random* values as sample size grows! Also, in cases where the sample ACF is consistent, its estimation error can have a heavy-tailed asymptotic distribution, leading to large errors. The situation is even worse for autocorrelations of squared returns [45]. Thus, one must be cautious in identifying behavior of *sample* autocorrelation with the autocorrelations of the return process.

Slow decay of sample autocorrelation functions may possibly arise from other mechanism than long-range dependence. For example, Mikosch & Starica [46] note that nonstationarity of the returns may also generate spurious effects which can be mistaken for long-range dependence in the volatility. However, we will not go to the extreme of suggesting, as in [46], that the slow decay of sample autocorrelations of absolute returns is a pure artefact due to non-stationarity. “Non-stationarity” does not suggest a modeling approach and it seems highly unlikely that unstructured non-stationarity would lead to such a robust, stylized behavior for the sample autocorrelations of absolute returns, stable across asset classes and time periods. The robustness of these empirical facts call for an explanation, which “non-stationarity” does not provide. Of course, these mechanisms are not mutually exclusive: a recent study by Granger and Hyng [24] illustrates the interplay of these two effects by combining an underlying long memory process with occasional structural breaks.

Independently of the econometric debate on the “true nature” of the return generating process, one can take into account such empirical observations without pinpointing a specific stochastic model by testing for similar behavior of sample autocorrelations in agent-based models (described below), and using sample autocorrelations for indirect inference [22] of the parameters of such models.

3 Mechanisms for volatility clustering

While GARCH, FIGARCH and stochastic volatility models propose statistical constructions which mimick volatility clustering in financial time series, they do not provide any economic explanation for it. We discuss here possible mechanisms which have been proposed for the origin of volatility clustering.

3.1 Heterogeneous arrival rates of information

Heterogeneity in agent's time scale has been considered as a possible origin for various stylized facts [25]. Long term investors naturally focus on long-term behavior of prices, whereas traders aim to exploit short-term fluctuations.

Granger [23] suggested that long memory in economic time series can be due to the aggregation of a cross section of time series with different persistence levels. This argument was proposed by Andersen & Bollerslev [1] as a possible explanation for volatility clustering in terms of aggregation of different information flows.

The effects of the diversity in time horizons on price dynamics have also been studied by Lebaron [32] in an artificial stock market, showing that the presence of heterogeneity in horizons may lead to an increase in return variability, as well as volatility-volume relationships similar to those of actual markets.

3.2 Evolutionary models

Several studies have considered modeling financial markets by analogy with ecological systems where various trading strategies co-exist and evolve via a "natural selection" mechanism, according to their relative profitability [2, 3, 34, 32]. The idea of these models, the prototype of which is the Santa Fe artificial stock market [3, 34], is that a financial market can be viewed as a population of agents, identified by their (set of) decision rules. A decision rule is defined as a mapping from an agents information set (price history, trading volume, other economic indicators) to the set of actions (buy, sell, no trade). The evolution of agents decision rule is often modeled using a genetic algorithm [27]. The specification and simulation of such evolutionary models can be quite involved and specialized simulation platforms have been developed to allow the user to specify variants of agents strategies and evolution rules. Other evolutionary models represent the evolution by a deterministic dynamical system which, through the complex price dynamics it generate, are able to mimick some "statistical" properties of the returns process, including volatility clustering [28].

Though the Santa Fe market model is capable of qualitatively replicating some of the stylized facts [34], precise comparisons with empirical observations are still lacking. Indeed, given the large number of parameters, it is not possible to calibrate the parameters in order to interpret the time periods

in the simulations as “days” or “minutes” etc. thereby leading to a lack of reference for empirical comparisons.

More importantly, the competition between numerous strategies in such complex simulation models does not allow to pinpoint a single mechanism as being responsible for volatility clustering or other stylized properties. Models in which a dominant mechanism is at work are more helpful in this respect; we will now discuss some instances of such models.

3.3 Behavioral switching

The economic literature contains examples where switching of economic agents between two behavioral patterns leads to large aggregate fluctuations [29]: in the context of financial markets, these behavioral patterns can be seen as trading rules and the resulting aggregate fluctuations as large movements in the market price i.e. heavy tails in returns. Recently, models based on this idea have also been shown to generate volatility clustering [30, 39].

Lux and Marchesi [39] study an agent-based model in which heavy tails of asset returns and volatility clustering arise from behavioral switching of market participants between fundamentalist and chartist behavior. Fundamentalists expect that the price follows the fundamental value in the long run. Noise traders try to identify price trends, which results in a tendency to herding. Agents are allowed to switch between these two behaviors according to the performance of the various strategies. Noise traders evaluate their performance according to realized gains, whereas for the fundamentalists, performance is measured according to the difference between the price and the fundamental value, which represents the anticipated gain of a “convergence trade”. This decision-making process is driven by an exogenous fundamental value, which follows a Gaussian random walk. Price changes are brought about by a market maker reacting to imbalances between demand and supply. Most of the time, a stable and efficient market results. However, its usual tranquil performance is interspersed by sudden transient phases of destabilization. An outbreak of volatility occurs if the fraction of agents using chartist techniques surpasses a certain threshold value, but such phases are quickly brought to an end by stabilizing tendencies. This behavioral switching is believed to be the cause of volatility clustering, long memory and heavy tails in the Lux-Marchesi model [39].

Kirman and Teyssière [30] have proposed a variant of [29] in which the proportion $\alpha(t)$ of fundamentalists in the market follows a Markov chain, of the type used in epidemiological models, describing herding of opinions. Simulation of this model exhibit autocorrelation patterns in absolute returns with a behavior similar to that described in Section 2.

3.4 The role of investor inertia

As argued by Liu [35], the presence of a Markovian regime switching mechanism in volatility can lead to volatility clustering, is not sufficient to generate

long-range dependence in absolute returns. More important than the switching is the fact the time spent in each regime –the duration of regimes– should have a heavy-tailed distribution [48, 52]. By contrast with Markov switching, which leads to short range correlations, this mechanism has been called “renewal switching”.²

Bayraktar et al. [6] study a model where an order flow with random, heavy-tailed, durations between trades leads to long range dependence in returns. When the durations τ_n of the inactivity periods have a distribution of the form $\mathbb{P}(\tau_n \geq t) = t^{-\alpha}L(t)$, conditions are given under which, in the limit of a large number of agents randomly submitting orders, the price process in this models converges to a process with Hurst exponent $H = (3 - \alpha)/2 > 1/2$. In this model the randomness (and the heavy tailed nature) of the durations between trades are both exogenous ingredients, chosen in a way that generates long range dependence in the returns. However, as noted above, empirical observations point to clustering and persistence in *volatility* rather than in returns so such a result does not seem to be consistent with the stylized facts.

By contrast, as noted above, regime switching in *volatility* with heavy-tailed durations could lead to volatility clustering. Although in the agent-based models discussed above, it may not be easy to speak of well-defined “regimes” of activity, but Giardina and Bouchaud [21] argue that this is indeed the mechanism which generates volatility clustering in the Lux-Marchesi [39] and other models discussed above. In these models, agents switch between strategies based on their relative performance; Giardina and Bouchaud argue that this (cumulative) relative performance index actually behaves in time like a random walk, so the switching times can be interpreted as times when the random walk crosses zero: the interval between successive zero-crossings is then known to be heavy-tailed, with a power-law decay of exponent $3/2$.

4 Volatility clustering and threshold behavior

While switching between high and low volatility states is probably the mechanism leading to volatility clustering in many of the agent-based models discussed above, this explanation is not easy to trace back to the level of agent behavior, partly because the models described above contain various other ingredients whose contribution to the overall behavior is thus blurred. We now discuss a simple model [14] reproducing several stylized empirical facts, where the origin of volatility clustering can be clearly traced back to investor inertia, caused by threshold response of investors to news arrivals.

² See the chapter by Giraitis, Leipus and Surgailis in this volume for a review on renewal switching models.

4.1 An agent-based model for volatility clustering

Our model describes a market where a single asset, whose price is denoted by S_t , is traded by N agents. Trading takes place at discrete periods $t = 0, 1, 2, \dots$. We will see that, provided the parameters of the model are chosen in a certain range, we will be able to interpret these periods as “trading days”. At each period, agents have the possibility to send an order to the market for buying or selling a unit of asset: denoting by $\phi_i(t)$ the demand of the agent, we have $\phi_i(t) = 1$ for a buy order and $\phi_i(t) = -1$. We allow the value $\phi_i(t)$ to be zero; the agent is then inactive at period t . The inflow of public information is modeled by a sequence of IID Gaussian random variables $(\epsilon_t, t = 0, 1, 2, \dots)$ with $\epsilon_t \sim N(0, D^2)$. ϵ_t represents the value of a common signal received by all agents at date $t-1$. The signal ϵ_t is a forecast of the future return r_t and each agent has to decide whether the information conveyed by ϵ_t is significant, in which case she will place a buy or sell order according to the sign of ϵ_t .

The trading rule of each agent $i = 1, \dots, N$ is represented by a (time-varying) decision threshold $\theta_i(t)$. The threshold $\theta_i(t)$ can be viewed as the agents (subjective) view on volatility. The trading rule we study may be seen as a stylized example of threshold behavior: without sufficient external stimulus ($|\epsilon_t| \leq \theta_i(t)$), an agent remains inactive $\phi_i(t) = 0$ and if the external signal is above a certain threshold, the agent will act: if $\epsilon_t > \theta_i(t)$, $\phi_i(t) = 1$, if $\epsilon_t < -\theta_i(t)$, $\phi_i(t) = -1$. The corresponding demand generated by the agent is therefore given by:

$$\phi_i(t) = 1_{\epsilon_t > \theta_i(t)} - 1_{\epsilon_t < -\theta_i(t)}. \quad (6)$$

The excess demand is then given by $Z_t = \sum_{i=1}^N \phi_i(t)$. A non-zero value of Z produces a change in the price given by

$$r_t = \ln \frac{S_t}{S_{t-1}} = g\left(\frac{Z_t}{N}\right) \quad (7)$$

where the price impact function $g : \mathbb{R} \mapsto \mathbb{R}$ is an increasing function with $g(0) = 0$. We define the (normalized) market depth λ by $g'(0) = \frac{1}{\lambda}$. Examples are a linear price impact $g(z) = z/\lambda$ or $g(z) = \arctan(z/\lambda)$, both having been used in various disequilibrium models.

Initially, we start from a population distribution F_0 of thresholds: $\theta_i(0)$, $i = 1..N$ are positive IID variables drawn from F_0 . Updating of strategies is *asynchronous*: at each time step, any agent i has a probability $0 \leq s \leq 1$ of updating her threshold $\theta_i(t)$. Thus, in a large population, q represents the fraction of agents updating their views at any period; $1/q$ represents the typical time period during which an agent will hold a given view $\theta_i(t)$. If periods are to be interpreted as days, q is typically a small number $s \simeq 10^{-1} - 10^{-3}$. When an agent updates her threshold, she sets it to be equal to the recently observed absolute return, which is an indicator of recent volatility $|r_t| = \left| \ln \frac{S_t}{S_{t-1}} \right|$. Introducing IID random variables $u_i(t)$, $i = 1..N, t \geq 0$ uniformly distributed on $[0, 1]$, which indicate whether agent i updates her threshold or not:

$$\theta_i(t) = 1_{u_i(t) < s} |r_t| + 1_{u_i(t) \geq s} \theta_i(t-1) \quad (8)$$

This way of updating can be seen as a stylized version of various estimators of volatility based on moving averages of absolute or squared returns. It is also corroborated by a recent empirical study by Zovko and Farmer [55], who show that traders use recent volatility as a signal when placing orders.

The asynchronous updating scheme proposed here avoids introducing an artificial ordering of agents as in sequential choice models. As noted above, the heterogeneity of time scales of intervention of agents is a feature believed to be important for generating persistence in volatility [1, 23, 31]. The random nature of updating in this model is a parsimonious way to introduce heterogeneity in time scales without introducing extra parameters. Given this random updating scheme, even if we start from an initially homogeneous population $\theta_i(0) = \theta_0$, heterogeneity creeps into the population through the updating process and evolves in a random manner, leading to a history-dependent disordered system.

Let us recall the main ingredients of the model. At each time period:

1. agents receive a common signal $\epsilon(t) \sim N(0, D^2)$
2. each agent i compares the signal to her threshold $\theta_i(t)$
3. if $|\epsilon(t)| > \theta_i(t)$ the agent considers the signal as significant and generates an order $\phi_i(t)$ according to (6).
4. The market price is impacted by the excess demand and moves according to (7).
5. Each agent updates, with probability q , her threshold according to (8).

Compared to most agent-based models considered in the literature, there is no exogenous “fundamental price” process and we do not distinguish between “fundamentalist” and “chartist” traders. Also, the same information is available to all agents but they differ in the way they *process* the information. We do not introduce any “social interaction” among agents: no notion of locality, lattice or graph structure is introduced. The model has very few parameters: q describes the average updating frequency, D the standard deviation of the noise representing the news arrival process, the market depth λ and the number of agents N which is typically large. We will observe nevertheless that this simple model generates time series of returns with interesting dynamics and properties similar to empirically observed properties of asset returns.

4.2 Simulation results

In order for a direct comparison with empirical stylized facts to be meaningful, we compute sample moments as in the case of empirical data, by averaging over the (single) sample path. After simulating a sample path of the price S_t for $T = 10^4$ periods, we compute the time series of returns $r_t = \ln(S_t/S_{t-1})$, $t = 1..T$, their histogram, a moving average estimator of the

standard deviation of returns (“volatility”), the sample autocorrelation function of returns and the sample autocorrelation function of absolute returns. In order to decrease the sensitivity of results to initial conditions, we allow for a transitory regime and discard the first 10^3 periods before averaging.

In order to interpret the trading periods as “days” and compare the results with properties of daily returns, we note that when g is linear $|r_t| \leq \frac{1}{\lambda}$ and choose $5 \leq \lambda \leq 20$ which allows a (maximal) range of daily returns between 5% and 20%. Also, the amplitude D of the input noise can be chosen such as to reproduce a realistic range of values for the (annualized) volatility: this leads to choosing D in the range $10^{-3} - 10^{-2}$. Let us emphasize that we are discussing the calibration of the *order of magnitude* of parameters, not fine-tuning them to a set of critical values. The results discussed in the sequel are generic within this range of parameters. Figures 3 and 4 illustrate typical sample paths obtained with different parameter values: they all generate series of returns with realistic ranges and realistic values of annualized volatility. For each series, we represent the histogram of returns both in linear and logarithmic scales, the ACF of returns C_r , the ACF of absolute returns $C_{|r|}$. The return series obtained possess regularities which match the properties

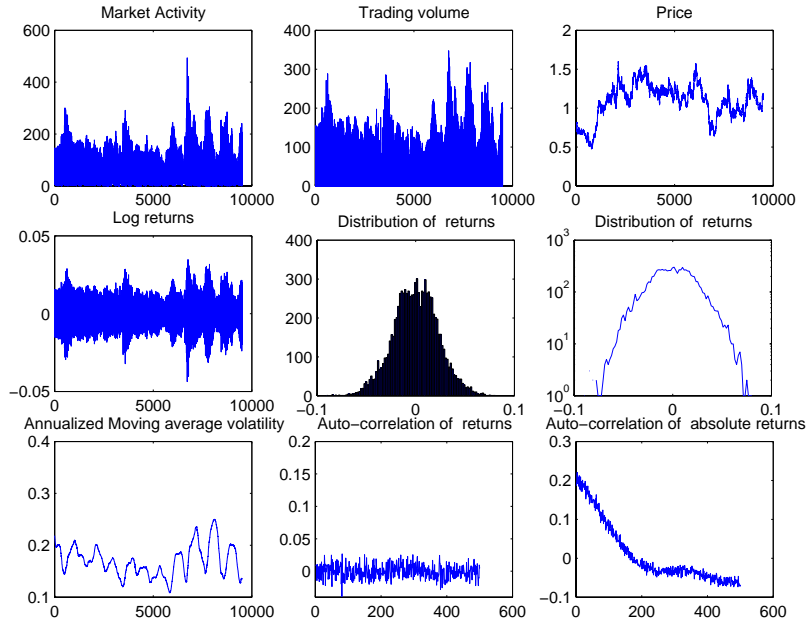


Fig. 3. Numerical simulation of the model with updating frequency $q = 0.01$ (average updating period: 100 “days”) $N = 1000$ agents, $D = 0.001$ and $\lambda = 10$.

outlined in the introduction [14]:

1. Excess volatility: the sample standard deviation of returns can be much larger than the standard deviation of the input noise representing news arrivals $\hat{\sigma}(t) \gg D$.
2. Mean-reverting volatility: the market price fluctuates endlessly and the volatility, as measured by the moving average estimator $\hat{\sigma}(t)$, does neither to zero nor to infinity and displays a mean-reverting behavior.
3. The simulated process generates a leptokurtic distribution of returns with (semi)heavy tails, with an excess kurtosis around $\kappa \simeq 7$. As shown in the logarithmic histogram plots in figures 3–4, the tails exhibit an approximately exponential decay, as observed in various studies of daily returns [16].
4. The returns are uncorrelated: the sample autocorrelation function of the returns exhibits an insignificant value (very similar to that of asset returns) at all lags, indicating the absence of linear serial dependence in the returns.
5. Volatility clustering: the autocorrelation function of absolute returns remains significantly positive over many time lags, corresponding to persistence of the amplitude of returns a time scale $\simeq 1/q$.

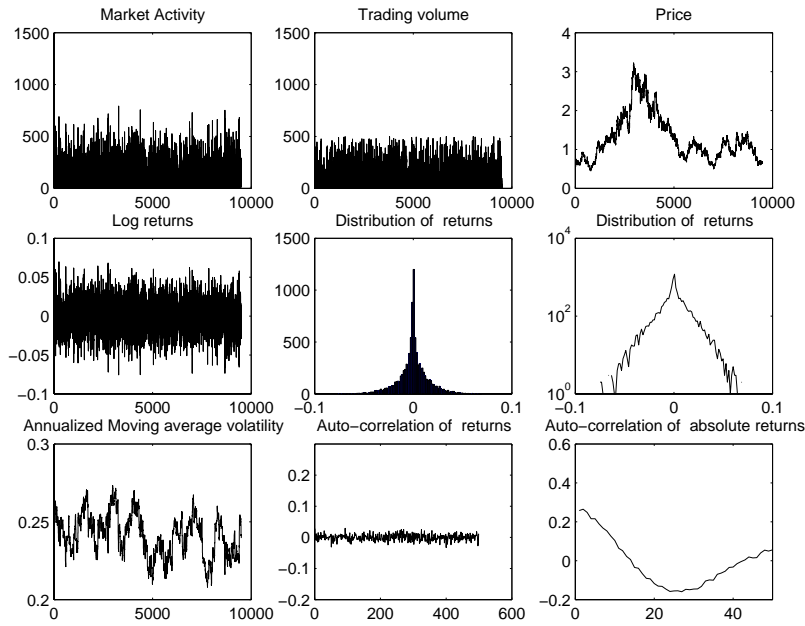


Fig. 4. Numerical simulation of the model with updating frequency $q = 0.1$ (average updating period: 10 “days”) $N = 1500$ agents, $D = 0.001$ and $\lambda = 10$.

4.3 Theoretical analysis

Contrarily to some of the models discussed above, this model is simple enough to allow for a theoretical study of its qualitative studies [14]. Let us begin by examining two limiting cases:

1. **Feedback without heterogeneity:** In the case where $q = 1$, all agents synchronously update their threshold at each period. Consequently, the agents have the same thresholds, given by the last periods absolute return: $\theta_i(t) = |r_{t-1}|$ and will therefore generate the same order: $Z_t = N\phi_1(t) \in \{0, N, -N\}$. So, the return r_t depends on the past only through the absolute return $|r_{t-1}|$:

$$r_t = f(|r_{t-1}, \epsilon_t|) = g(N)1_{\epsilon_t > |r_{t-1}|} + g(-N)1_{\epsilon_t < -|r_{t-1}|},$$

a dependence structure typical of ARCH models [19], leading to uncorrelated returns and volatility clustering. In this case, the distribution of r_t conditional on $|r_{t-1}|$ is actually a trinomial distribution: $r_t \in \{0, g(N), g(-N)\}$, which is not realistic. Simulation studies show that a similar behavior persists for $1 - q \ll 1$, leading to tri-modal distributions. This confirms our intuition that the updating probability q should be chosen small.

2. **Heterogeneity without feedback:** In the case where $q = 0$, no updating takes place: the trading strategies, given by the thresholds θ_i , are unaffected by the price behavior and the *feedback* effect is not present anymore. Heterogeneity is still present: the distribution of the thresholds remains identical to what it was at $t = 0$. The return r_t depends only on ϵ_t :

$$r_t = g\left(\frac{1}{N} \sum_{i=1}^N 1_{\epsilon_t > \theta_i} - 1_{\epsilon_t < -\theta_i}\right) = F(\epsilon_t)$$

We conclude therefore that the returns are IID random variables, obtained by transforming the Gaussian IID sequence (ϵ_t) by the nonlinear function F given in (9), whose properties depend on the (initial) distribution of thresholds $(\theta_i, i = 1..N)$. The log-price then follows a (non-Gaussian) random walk and the model does not exhibit volatility clustering.

The two limiting cases above show that, in order to obtain the interesting statistical properties observed in the simulated examples shown above, it is necessary to have $0 < q \ll 1$: both feedback and heterogeneity are essential ingredients. In the general case we have the following properties:

- **Markovian dynamics:** the thresholds $[\theta_i(t), i = 1..N]$ follow a Markov chain in $\{g(k), k = 0..N\}$. We have $\theta_i(t+1) = \theta_i(t)$ with probability $1 - q$ and

$$\theta_i(t+1) = |r_t| = \left| g\left(\frac{1}{N} \sum_{i=1}^N [1_{\epsilon_t > \theta_i} - 1_{\epsilon_t < -\theta_i}]\right) \right| \quad \text{with probability } q. \quad (9)$$

In fact given that agents are indistinguishable and only the empirical distribution of threshold values affects the returns, defining $N_k(t) = \sum_{i=1}^N 1_{[0, a_k]}(\theta_i(t))$ then $(N_k(t), k = 0..N-1)_{t=0,1,..}$ evolves as a Markov chain in $\{0, \dots, N\}^N$. $N(t) = (N_k(t), k = 0..N-1)$ is none other than the (cumulative) population distribution of the thresholds. The fact that $N(t)$ itself follows a Markov chain means that the population distribution of thresholds is a *random measure* on $\{0, \dots, N\}$, which is characteristic of disordered systems [44], even if we start from a deterministic set of values for the initial thresholds (even identical ones). Here the disorder is endogenous and is generated by the random updating mechanism.

- **Excess volatility:** In this model, the volatility of the news arrival process is quantified by D which is the standard deviation of the external noise ϵ_t , whereas the volatility of the returns can be measured a posteriori as the (conditional or unconditional) standard deviation of r_t . As seen from the nonlinear relation between ϵ_t and r_t ,

$$r_t = g\left(\frac{\sum_{i=1}^N 1_{\epsilon_t > \theta_i(t)} - 1_{\epsilon_t < -\theta_i(t)}}{\lambda N}\right) \quad (10)$$

even after conditioning on the current states of agents $\theta_i(t), i = 1..N$, Eq. (10) yields a nonlinear relation between the input noise ϵ_t and the returns which can have the effect of amplifying the noise by an order of magnitude or more. In the simulation example shown in figure 3, $D = 10^{-3}$ which corresponds to an annualized volatility of 1.6%, while the annualized volatility of returns is in the range of 20%, an order of magnitude larger: the order of magnitude of the volatility of returns may be quite different from that of the input noise.

- **Absence of autocorrelation**

From the dynamic equations of the model

$$Z_t = \frac{1}{N} \sum_{i=1}^N \phi_i(t) = \frac{1}{N} \sum_{i=1}^N [1_{\epsilon_t > \theta_i} - 1_{\epsilon_t < -\theta_i}] \quad (11)$$

$$r_t = g(Z_t) = g\left(\frac{1}{N} \sum_{i=1}^N [1_{\epsilon_t > \theta_i} - 1_{\epsilon_t < -\theta_i}]\right) \quad (12)$$

one can deduce that, if g is an odd function (in particular if g is linear) then asset returns $(r_t)_{t \geq 0}$ are uncorrelated: $\text{cov}(r_t, r_{t+1})=0$. This is due to the fact that the trading/ nontrading decision is based only on the amplitude of the signal, not its sign. The sign of the return is determined by the sign of the common signal, which is independent across periods.

- **Investor inertia**

Except in times of crisis or market crash, at a given point in time only

a small proportion of stockholders are actually trading in the market. As a result, the (daily) order flow for a typical stock can be much smaller than the market capitalization. This phenomenon, sometimes referred to as *investor inertia*, is a generic outcome in our model due to threshold behavior of agents. Starting from an initial holding of $\pi_i(0)$, the quantity of asset held by agent i is given by $\pi_i(t) = \sum_{\tau=0}^t \phi_i(\tau)$. Figure 4.3 displays the evolution of the portfolio $\pi_i(t)$ of a typical agent: short periods of activity (trading) are separated by long periods of inertia, where the portfolio remains constant. This “inertia” increases in periods of high volatility, an

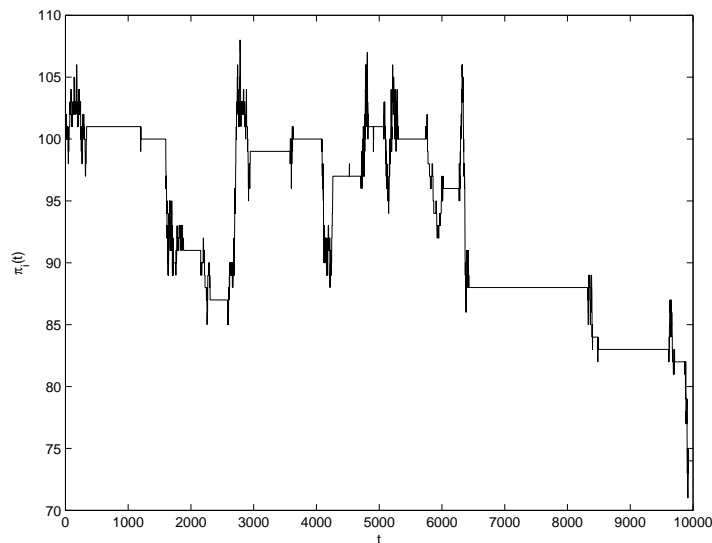


Fig. 5. Evolution of the portfolio of a typical agent, with long periods of inactivity punctuated by bursts of activity.

effect similar to the behavior of risk-averse agent.

- **Mean reversion and clustering of volatility**

Many market microstructure models –especially those with learning or evolution– converge over large time intervals to an equilibrium where prices and other aggregate quantities cease to fluctuate randomly. By contrast, in the present model, prices fluctuate endlessly and the volatility exhibits mean-reverting behavior. Suppose we are in a period of “low volatility”; the amplitude $|r_t|$ of returns is small. Agents who update their thresholds will therefore update them to small values, become more sensitive to news arrivals, thus generating higher excess demand and thus increasing the amplitude of returns. Conversely, in a period of high volatility, agents will update their threshold values to high values and become less reactive to

the incoming signal: this increase in investor inertia will thus decrease the amplitude of returns. The mean reversion time in the volatility corresponds here to the time it takes for agents to adjust their thresholds to current market conditions, which is of order $\tau_c = 1/q$.

When the amplitude of the noise is small it can be shown [14] that volatility decays exponentially in time and increases through upward “jumps”. This behavior is actually similar to that of a class of stochastic volatility models, introduced by Barndorff-Nielsen and Shephard [5] and successfully used to describe various econometric properties of returns.

5 Conclusion

Volatility clustering is recognized as a stylized property present in most financial time series. Agent-based models seek to explain volatility clustering in terms of behavior of market participants, described in terms of simple rules. We have discussed several agent-based models capable of generating volatility clustering. A common feature of these models seems to be the “switching” of the market between periods of high and low activity, with long durations of periods. Models differ in the mechanism which leads to this switching at the level of agents.

While the econometric debate on the short range or long range nature of dependence in volatility still goes on (and may probably never be resolved), agent-based models can provide motivation for choosing between alternative econometric specifications which are otherwise equally plausible in statistical terms, thus providing a useful complement to econometric analysis.

References

1. T. Andersen and T. Bollerslev, Heterogeneous information arrivals and returns volatility dynamics, *Journal of finance*, 52 (1997), pp. 975–1005.
2. J. Arifovic and R. Gencay, Statistical properties of genetic learning in a model of exchange rate, *Journal of Economic Dynamics and Control*, 24 (2000), pp. 981–1005.
3. Arthur, W., Holland, J., LeBaron, B., Palmer, J. and Tayler, P. (1997). Asset pricing under heterogeneous expectations in an artificial stock market, in: *The Economy as an Evolving Complex System*. Perseus Books, Reading MA, pp. 15–44.
4. Baillie, R.T. (1996). Long memory processes and fractional integration in econometrics. *Journal of Econometrics*, **73**, 5–59.
5. O. E. Barndorff-Nielsen and N. Shephard (2001) Non-Gaussian Ornstein-Uhlenbeck based models and some of their uses in financial econometrics, *Journal of the Royal Statistical Society B*, 63, pp. 167–241.
6. E. Bayraktar, U. Horst, and K. R. Sircar, A limit theorem for financial markets with inert investors, working paper, Princeton University, 2003.

7. J. Beran, *Statistics for long memory processes*, Chapman and Hall, New York, 1994.
8. T. Bollerslev, R. Chou, and K. Kroner, ARCH modeling in finance, *Journal of Econometrics*, 52 (1992), pp. 5–59.
9. F. Breidt, N. Crato, and P. De Lima, The detection and estimation of long memory in stochastic volatility, *Journal of Econometrics*, 83 (1998), pp. 325–348.
10. P. Cheridito, Gaussian moving averages, semimartingales and option pricing, *Stochastic Process. Appl.*, 109 (2004), pp. 47–68.
11. C. Chiarella, M. Gallegatti, R. Leombruni, and A. Palestini, Asset price dynamics among heterogeneous interacting agents, *Computational Economics*, 22 (2003), pp. 213–223.
12. R. Cont, Empirical properties of asset returns: Stylized facts and statistical issues, *Quantitative Finance*, 1 (2001), pp. 1–14.
13. R. Cont, J.-P. Bouchaud, and M. Potters, Scaling in financial data: Stable laws and beyond, in: B. Dubrulle, F. Graner, and D. Sornette (eds.) *Scale Invariance and Beyond*, Springer, Berlin, 1997.
14. R. Cont, F. Ghoulmie, and J.-P. Nadal, Threshold behavior and volatility clustering in financial markets, Working paper, Ecole Polytechnique, 2004.
15. D. Cutler, J. Poterba, and L. Summers, What moves stock prices?, *Journal of Portfolio Management*, (1989), pp. 4–12.
16. Z. Ding, C. Granger, and R. Engle, A long memory property of stock market returns and a new model, *Journal of empirical finance*, 1 (1983), pp. 83–106.
17. Z. Ding and C. W. J. Granger, Modeling volatility persistence of speculative returns: a new approach, *Journal of Econometrics*, 73 (1996), pp. 185–215.
18. P. Doukhan, G. Oppenheim, and M. S. Taqqu, eds., *Theory and applications of long-range dependence*, Birkhäuser Boston Inc., Boston, MA, 2003.
19. R. Engle, *ARCH models*, Oxford University Press, Oxford, 1995.
20. F. Ghoulmie, R. Cont and J.-P. Nadal, Heterogeneity and feedback in an agent-based market model, *Journal of Physics: Condensed Matter*, **17**, S1259-S1268 (2005).
21. I. Giardina and J.-P. Bouchaud, Bubbles, crashes and intermittency in agent based market models, *Eur. Phys. Journal B .*, 31 (2003), pp. 421–437.
22. C. Gouriéroux, A. Monfort, and E. Renault, Indirect inference, *Journal of Applied Econometrics*, 8 (1993), pp. S85–S118.
23. C. W. J. Granger, Long memory relationships and the aggregation of dynamic models, *Journal of Econometrics*, 14 (1980), pp. 227–238.
24. Granger, C.W.J. and Hyung, N. (2004) Occasional structural breaks and long memory with an application to the S&P 500 absolute stock returns. *Journal of Empirical Finance*, 11, 399-421.
25. D. Guillaume, M. Dacorogna, R. Davé, U. Müller, R. Olsen, and O. Pictet, From the birds eye view to the microscope: A survey of new stylized facts of the intraday foreign exchange markets, *Finance and Stochastics*, 1 (1997), pp. 95–131.
26. C. C. Heyde, On modes of long-range dependence, *Journal of Applied Probability*, 39 (2002), pp. 882–888.
27. J. Holland, *Adaptation in Natural and Artificial Systems*, Bradford Books, 1992.
28. C. H. Hommes, A. Gaunersdorfer, and F. O. Wagener, Bifurcation routes to volatility clustering under evolutionary learning, working paper, CenDEF, 2003.

29. A. Kirman, Ants, rationality, and recruitment, *Quarterly Journal of Economics*, 108 (1993), pp. 137–156.
30. A. Kirman and G. Teyssiere, Microeconomic models for long-memory in the volatility of financial time series, *Studies in nonlinear dynamics and econometrics*, 5 (2002), pp. 281–302.
31. B. LeBaron, Agent-based computational finance : suggested readings and early research, *Journal of Economic Dynamics and Control*, 24 (2000), pp. 679–702.
32. ———, Evolution and time horizons in an agent-based stock market, *Macroeconomic Dynamics*, 5 (2001), pp. 225–254.
33. ———, Stochastic volatility as a simple generator of apparent financial power laws and long memory, *Quantitative Finance*, 1 (2001), pp. 621–631.
34. B. LeBaron, B. Arthur, and R. Palmer, Time series properties of an artificial stock market, *Journal of Economic Dynamics and Control*, 23 (1999), pp. 1487–1516.
35. M. Liu, Modeling long memory in stock market volatility, *Journal Econometrics*, 99 (2000), pp. 139–171.
36. Lobato, I. and Velasco, C. (2000) Long memory in stock market trading volume. *Journal of Business and Economic Statistics*, 18, 410-427.
37. A. Lo Long-term memory in stock market prices, *Econometrica*, 59 (1991), pp. 1279–1313.
38. T. Lux, The socio-economic dynamics of speculative markets : interacting agents, chaos, and the fat tail of return distributions, *Journal of Economic Behavior and Organization*, 33 (1998), pp. 143–65.
39. T. Lux and M. Marchesi, Volatility clustering in financial markets : a micro simulation of interacting agents, *International Journal of Theoretical and Applied Finance*, 3 (2000), pp. 675–702.
40. B. B. Mandelbrot (1963) The variation of certain speculative prices, *Journal of Business*, XXXVI (1963), pp. 392–417.
41. B. B. Mandelbrot (1971) When can price be arbitrated efficiently? A limit to the validity of the random walk and martingale models, *Rev. Econom. Statist.*, 53 (1971), pp. 225–236.
42. B. B. Mandelbrot and M. S. Taqqu, Robust R/S analysis of long-run serial correlation, in Proceedings of the 42nd session of the International Statistical Institute, Vol. 2 (Manila, 1979), vol. 48, 1979, pp. 69–99.
43. B. B. Mandelbrot and J. Van Ness, Fractional Brownian motion, fractional noises and applications, *SIAM Review*, 10 (1968), pp. 422–437.
44. M. Mézard, G. Parisi, and M. Virasoro, *Spin glass theory and beyond*, World Scientific, 1984.
45. T. Mikosch and C. Stărică, Limit theory for the sample autocorrelations and extremes of a GARCH (1,1) process, *Ann. Statist.*, 28 (2000), pp. 1427–1451.
46. ———, Long-range dependence effects and ARCH modeling, in Theory and applications of long-range dependence, Birkhäuser Boston, Boston, MA, 2003, pp. 439–459.
47. A. Pagan (1986). The econometrics of financial markets, *Journal of empirical finance*, 3, pp. 15–102.
48. M. Pourahmadi (1988) Stationarity of the solution of $X_t = A_t X_t + 1$ and analysis of non-Gaussian dependent variables. *Journal of Time Series Analysis*, 9, 225–239.
49. S. Resnick, G. Samorodnitsky, and F. Xue, How misleading can sample ACFs of stable MAs be? (Very!), *Ann. Appl. Probab.*, 9 (1999), pp. 797–817.

50. S. I. Resnick, Why non-linearities can ruin the heavy-tailed modeler's day, in *A practical guide to heavy tails* (Santa Barbara, CA, 1995), Birkhäuser Boston, Boston, MA, 1998, pp. 219–239.
51. L. Rogers, Arbitrage with fractional Brownian motion, *Mathematical Finance*, 7 (1997), pp. 95–105.
52. M. Taqqu and J. Levy, Using renewal processes to generate long range dependence and high variability, in *Dependence in probability and statistics*, E. Eberlein and M. Taqqu, eds., Birkhauser, Boston, 1986, pp. 73–89.
53. V. Teverovsky, M. S. Taqqu, and W. Willinger, A critical look at Lo's modified R/S statistic, *J. Statist. Plann. Inference*, 80 (1999), pp. 211–227.
54. W. Willinger, M. S. Taqqu, and V. Teverovsky, Long range dependence and stock returns, *Finance and Stochastics*, 3 (1999), pp. 1–13.
55. I. Zovko and J. D. Farmer, The power of patience: a behavioral regularity in limit order placement, *Quantitative Finance*, 2 (2002), pp. 387–392.

VOLATILITY CLUSTERING IN FINANCIAL MARKETS: A MICRO-SIMULATION OF INTERACTING AGENTS

Thomas Lux and Michele Marchesi

Department of Economics, University of Bonn and
Department of Electrical and Electronic Engineering, University of Cagliari

Abstract: The finding of clustered volatility and ARCH effects is ubiquitous in financial data. This paper presents a possible explanation of this phenomenon within a multi-agent framework of speculative activity. In the model, both chartist and fundamentalist strategies are considered with agents switching between both behavioural variants according to observed differences in pay-offs. Price changes are brought about by a market maker reacting on imbalances between demand and supply. Most of the time, a stable and efficient market results. However, its usual tranquil performance is interspersed by sudden transient phases of destabilisation. Outbreak of volatility occurs if the fraction of agents using chartist techniques surpasses a certain threshold value, but such phases are quickly brought to an end by stabilising tendencies. Formally, this pattern can be understood as an example of a new type of dynamic behaviour denoted on-off intermittency in physics literature. Statistical analysis of simulated time series shows that the main stylised facts (unit roots in levels together with heteroscedasticity and leptokurtosis of returns) can be found in this „artificial“ market. *Copyright © 1998 IFAC*

Keywords: volatility clustering, interacting agents, on-off intermittency

1. INTRODUCTION

Both foreign exchange markets and national stock markets share a number of stylised facts for which a satisfactory explanation is still lacking in standard theories of financial markets (see Pagan, 1996, and de Vries, 1994, for recent surveys of the time series properties of financial data). In this paper, we will introduce a behavioural model of speculative activity whose time series characteristics conform with the most important empirical regularities.

To set the stage, we first provide a short account of the ubiquitous characteristics of financial data:

- first, standard statistical procedures are usually not able to reject the hypothesis that financial prices follow a random walk. If levels (or logs) obey a unit root dynamics, returns or differences of logs should be stationary. In fact, this has been confirmed throughout the literature. However, certain distributional characteristics of returns also count as well-established facts which - in the wording of de Vries (1994) - „have a sound statistical basis but for which no convincing economic explanation has been established“.
- the first of these is the *clustering of volatility*. More formally, this can be identified with what is now known as ARCH effects: non-homogeneity of volatility together with highly significant autocorrelation in all measures of volatility despite insignificant autocorrelation in raw returns.

- the third stylised fact is the *fat tail phenomenon*: exchange rate changes or stock returns at weekly, daily and higher frequencies exhibit more probability mass in the tails and in the centre of the distribution than does the standard Normal.

Though these three properties characterise the behaviour of almost all financial prices, behavioural explanations of these features of financial data are sparse.

2. THE MODEL

The model presented in this paper is close in economic content to the ones analysed in Lux (1995, 1997, 1998). This approach shares features of both Kirman's (1993) and Day and Huang's (1990) models of speculative activity. We consider an ensemble of interacting agents who may pursue a chartist or fundamentalist strategy. Furthermore, the chartist group is composed of two subgroups containing individuals who are optimistic or pessimistic about the future development of the market.

The dynamics of the model are governed by both endogenous changes of agents' behaviour and price reactions brought about by a market maker who coordinates demand and supply. In detail, we have the following elements of the dynamics:

(1) chartists switching between the optimistic and pessimistic subgroup under the influence of the majority opinion as well as the observed price trend,

(2) switching of agents between chartist and fundamentalist strategy. These behavioural changes are modelled in the following way: agents meet individuals from the other group, compare (myopic) excess profits from both strategies and with a probability depending on the pay-off differential switch to the more successful strategy.

(3) endogenous price formation by a market maker who reacts on imbalances between demand and supply in the usual manner. Demand and supply functions themselves are derived from the activities and dispositions of speculators.

All potential changes of behaviour (from optimistic to pessimistic disposition and *vice versa*, from fundamentalism to chartism and *vice versa*) as well as the price adjustment by the market maker are formalised using Poisson transition probabilities. It is, thus, assumed that changes of behaviour occur *asynchronously* in our model.

3. MAIN RESULTS

In contrast to earlier articles, here we are not interested in the potential of cyclic or chaotic time paths but will concentrate on investigating the system's dynamics in the presence of *stable 'fundamental' equilibria* in which the price is (on average) equal to the fundamental value of the asset. However, using a combination of theoretical tools and micro-simulations it is demonstrated that an otherwise stable fundamental equilibrium can be subject to sudden transient phases of destabilisation. The characteristic features of these periods are bursts of severe fluctuations around the equilibrium which, however, quickly die out in the course of events the system returning to a stable and calm state again.

Fig. 1 shows the time development of returns and z , the fraction of chartist traders, from a typical micro-simulation.

The trajectory of returns, plotted over 3,000 time steps, clearly shows that we do *not* only find the small homogenous disturbances with a given variance that one would usually expect in the presence of a stable equilibrium. Instead we see long calm periods punctuated with sudden bursts of clustered volatility in returns.

In the bottom diagram we depict the trajectory of the fraction of chartists, denoted by z , together with the theoretically derived suspected bifurcation value \bar{z} where the fundamental equilibrium loses stability. Looking at both the upper and lower part of the figure, the following interplay between both variables can be observed: As long as z is far from \bar{z} , the time development of z appears quite random. It is accompanied by small fluctuations of returns around zero whose magnitude appears to be correlated with the number of chartists, z . However, once z approaches \bar{z} , overproportionally strong price changes set in. The reason is that, with a certain dominance of chartist practices, deviations from the fundamental equilibrium become self-reinforcing and the system cannot maintain its local stability any more.

Nevertheless, the dynamics is globally stable: deviations are checked after some time presumedly because of the superior performance of fundamentalists. Hence, sooner or later the market returns to its usual tranquil mode of operation after any outbreak of instability.

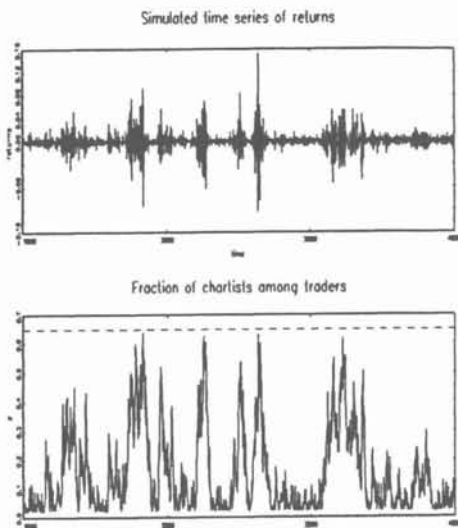


Fig. 1: Upper part: typical simulated time series of returns, bottom part: simultaneous development of the fraction of chartists, z , within the population of speculators. The broken line indicates the critical value $z = 0.65$ where a loss of stability is expected.

It is quite obvious that the behaviour of the simulated time series in the upper part of Fig. 1 conforms with empirical observations in a number of aspects: first, returns appear to be stationary and are also distributed rather symmetrically around zero. Second, they exhibit occasionally sudden, strong deviations which appear to come in clusters.

We conducted a series of statistical tests using the time series from several simulation runs with different parameter sets (see the paper for details). They confirmed that our artificial time paths for prices and returns share the basic characteristics of real-life markets: non-rejection of unit roots in levels together with heteroscedasticity and leptokurtosis of returns.

4. A BROADER PERSPECTIVE

The phenomenon of volatility bursts has also been found in a somewhat different economic context recently by Youssefmir and Huberman (1997) who dealt with the evolution of resource utilisation by adaptive agents. In their paper, they conjectured that the same mechanism may serve as an explanation for volatility clustering in financial markets. The present paper confirms this conjecture.

In recent natural science literature, a number of papers with qualitatively similar dynamic behaviour can be found which may, however, result

from very different types of models (see e.g., Fujisaka and Yamada, 1986; Heagy et al., 1994). The phenomenon under study has been denoted *on-off intermittency*. Loosely speaking, the unifying feature of all examples of its occurrence is an attracting state (which may not always be a fixed point) becoming *temporally* unstable due to a local bifurcation, i.e. some key variable surpassing some stability threshold. This destabilisation may be generated in a deterministic manner (e.g. through weak coupling to another dynamics) or may occur stochastically. In any case, there will be no lasting deviation from the equilibrium as the system is driven back to stability by some endogenous mechanism.

In our model of chartist/fundamentalist interaction, the bifurcation parameter is the time-varying fraction of traders pursuing a chartist strategy. In general, agents are allowed to switch between a chartist and a fundamentalist trading strategy after comparing the respective profits. However, in the vicinity of the equilibrium the price (on average) equals the fundamental value and no price trend can be identified and exploited so that neither strategy is superior. As a consequence, then, switching between strategies occurs in an unsystematic manner and depends, so to say, on idiosyncratic motivation which is captured using transition *probabilities* instead of a deterministic modelling device. Hence, the fraction of agents pursuing one or the other strategy follows a random walk and, sooner or later, leaves the region warranting a stable market. The ensuing destabilisation is characterised by an outbreak of severe fluctuations with a large fraction of traders switching to chartism and pursuing destabilising trend-following strategies. However, this situation does not last very long, as the temporary advantage of chartists disappears when the ensuing price bubble breaks down. Afterwards, fundamentalists gain on average higher profits which leads to a conversion of chartists to the other strategy. This makes oscillations diminish and the state variables are pushed towards a stable market constellation again. However, every once in a while, the pattern will repeat. More picturesque, one may describe the market as being stable (and efficient) to a large extent, but inherently nervous with the potential of sudden, unforecastable eruptions.

Although we are able to provide some intuition and mathematical insight for the phenomenon of volatility bursts using tools from mean-field theory and local stability analysis, their appearance can only be demonstrated using numerical simulation. We believe that our findings extend beyond the stylised model of speculative behaviour analysed in this paper. Considering our results as well as those obtained in a different context by Youssefmir and Huberman the key ingredients for the emergence of volatility bursts (in models with many interacting

agents) seem to be the following: (i) indeterminacy of the population composition in equilibrium (i.e. no strategy has an advantage within a stationary environment) and (ii) dependence of stability of the equilibrium itself on the composition of the population. We believe that these conditions are met by various economic models. In any case, the similarity between the phenomenon of on-off intermittency and the behaviour of the successful ARCH time series models developed in financial econometrics seems remarkable and may point to an explanation of the underlying phenomena.

REFERENCES

- Day, R. and W. Huang, 1990, Bulls, Bears, and Market Sheep, *Journal of Economic Behavior and Organization* 14, pp. 299 - 329
- Fujisaka, H. and T. Yamada, 1986, Stability Theory of Synchronized Motion in Coupled-Oscillator Systems IV, *Progress of Theoretical Physics* 75, pp. 1087 - 1104.
- Heagy, J.F, N. Platt and S.M. Hammel, 1994, Characterization of on-off Intermittency, *Physical Review E* 49, pp. 1140 - 1150.
- Kirman, A., 1993, Ants, Rationality, and Recruitment, *Quarterly Journal of Economics* 108, pp. 137 - 156
- Lux, T., 1995a, Herd Behaviour, Bubbles and Crashes. *Economic Journal* 105, pp. 881 - 896
- , 1997a, Time Variation of Second Moments from a Noise Trader/Infection Model. *Journal of Economic Dynamics and Control* 22, pp. 1 - 38.
- , 1998, The Socio-Economic Dynamics of Speculative Markets: Interacting Agents, Chaos, and the Fat Tails of Return Distributions, *Journal of Economic Behavior and Organization* 33, pp. 143 - 165.
- Pagan, A., 1996, The Econometrics of Financial Markets, *Journal of Empirical Finance* 3, pp. 15 - 102.
- Vries, C.G. de, 1994, Stylized Facts of Nominal Exchange Rate Returns, pp. 348 - 89 in: van der Ploeg, F., ed., *The Handbook of International Macroeconomics*. Blackwell: Oxford.
- Youssefmir, M. and B. Huberman, 1997, Clustered Volatility in Multiagent Dynamics, *Journal of Economic Behavior and Organization* 32, pp. 101 - 118.

Received October 27, 2020, accepted November 7, 2020, date of publication November 10, 2020, date of current version December 1, 2020.

Digital Object Identifier 10.1109/ACCESS.2020.3037240

Analyses on Volatility Clustering in Financial Time-Series Using Clustering Indices, Asymmetry, and Visibility Graph

KYUNGWON KIM¹ AND JAE WOOK SONG²

¹AI Center, Samsung Research, Samsung Electronics Seoul Research and Development Campus, Seoul 06765, South Korea

²Department of Industrial Engineering, Hanyang University, Seoul 04763, South Korea

Corresponding author: Jae Wook Song (jwsong@hanyang.ac.kr)

This work was supported by the research fund of Hanyang University under Grant HY-2019.

ABSTRACT The volatility clustering has critical implications in financial risk management. This paper aims to analyze the existence and cause of volatility clustering in financial time-series using different measures simultaneously. Specifically, we utilize the clustering indices, asymmetry measures, and the power of the scale freeness in the visibility graph. For the experiment, we utilize four representing financial time-series, including the S&P500, one-year US Treasury Constant Maturity rate, Euro-Dollar exchange rate, and Crude oil for the stock, bond, exchange, and commodity markets, respectively. The duration of the experiment is from 2009 to 2018, which is divided into two sub-periods: crisis and post-crisis periods. At first, we identify the positive and slowly decaying non-linear autocorrelation in all markets, which indicates the power-law decay. Also, the autocorrelation of the simulated time-series suggests that the order of return-series with respect to its magnitude contributes more to the volatility clustering than the heavy-tailed distributions. Secondly, we detect that the scale of the return contributes more to volatility clustering than the sign of the return. Lastly, we observe that the clustering and asymmetry measures are more robust measures to the return distribution changes than the PSVG to analyze the volatility clustering.

INDEX TERMS Clustering asymmetry, clustering index, finance, pattern clustering, power-law decay, statistical analysis, time series analysis, visibility graph, volatility clustering.

I. INTRODUCTION

The financial time-series and its associated return distribution, representing the market's volatility, are of great interest to both researchers and investors. In general, the financial time series are assumed to be independent and identically distributed (iid) generated from random walks [1]. Therefore, the probability density function of the return should follow the Gaussian distribution. However, the clustering of the large fluctuations in financial price-series is observed accompanying the return distribution's heavy tail property [2], [3]. In other words, a large fluctuation is likely to follow a previous large fluctuation, whereas a small fluctuation is likely to follow a previous small fluctuation, which rejects the iid assumption. Such a phenomenon is called the volatility clustering. The financial market is characterized by unexpected shocks. In this milieu, the volatility clustering has

critical implications in financial risk management, especially in calculating the Value-at-Risk or Expected Shortfall of the portfolio. When an unexpected shock is realized, the volatility of a financial market dramatically increases. Furthermore, the existence of volatility clustering suggests the persistence of extreme volatility for a while. Given that the risk measures are estimated based on the historical return series, investors must adjust the estimates to adequately manage and ensure the institution's capability against the additional risk. Hence, it is important and necessary to analyze the existence and causes of volatility clustering in the financial time-series.

From Econometrics's perspective, the traditional method to detect the causes of the volatility clustering is the Autoregressive Conditionally Heteroscedastic (ARCH) [3], which is extended to GARCH (Generalized ARCH) [4]. These methods are robust and descriptive approaches to analyze the volatility clustering, but neither of these models explains why such distribution appears. Also, both methods assume a specific distribution for a financial time-series, which even

The associate editor coordinating the review of this manuscript and approving it for publication was Md. Asaduzzaman¹.

makes the standard estimation process difficult since the long-memory or heavy-tailed characteristics of the financial time-series is changing over time [5]–[7].

From Econophysics' perspective, many researchers have discovered several stylized facts in financial markets. In particular, the heavy tail and aggregated normal distribution of the asset return distribution [8]–[14], asymmetry on rises and falls of the price dynamics, long-range autocorrelation or cross-correlation [7], [15]–[20], volatility clustering [21]–[24] have been studied, which generally suggest the rejection of the traditional normality assumption on the return distribution [25]–[29]. In this context, the volatility clustering has been studied as one of the major stylized facts [5], [23].

At first, the quantitative method can be used to capture the volatility clustering based on the autocorrelations of the return series [2]. Significantly, the evidence of volatility clustering is the positive and slowly decaying (a.k.a. power-law decay) autocorrelation. Note that such power-law decay is observed in the absolute or squared return series, often referred to as the non-linear autocorrelation, rather than the plain log-returns. It is known that the slowly decaying non-linear autocorrelation is mainly due to the correlation between the large fluctuation of volatility clusters. However, it is difficult to assert that the slow decay of nonlinearity implies the long memory tendency of volatility [5]. Nevertheless, if a particular time series has long memory property, or if the distribution of returns is close to non-normality, many statistical estimates tend to possess the autocorrelation or power-law decay [7], [19], [23].

Secondly, there is a network-driven method to detect the volatility clustering based on the fact that the dynamic properties of the time series can be preserved in the network framework. Specifically, many researchers have developed the methods to explain the geometrical structure of the time series, including the cycle approach [30], correlation approach [31], visibility graph [32], recurrence network [33], and isometric network [34]. Also, the monitoring of different patterns of the complex systems in the time-series has been studied [35]–[38]. Among them, we consider the visibility graph to analyze the clustering behavior of the financial time-series based on the following reasons. At first, the visibility graph is known to map the time series into the network values and successfully inherits the time series's properties. In particular, it is known that the visibility graph transforms the random series into a random graph, the periodic series into a regular graph [39], and the fractal series into a scale-free graph [40]–[43]. In this regard, the visibility graph has been utilized in various domains, including the geometric structure of traffic pattern [44], analyzing exchange rate series [45], and reflecting the geometric structure of the two-dimensional Ising algorithm [46]. Secondly, the visibility graph has fast computing time with a simple algorithmic structure, while most complex network-based algorithms require long computing time. Besides, the most recent development of the visibility graph is the Power of Scale-freeness of Visibility Graph (PSVG). Note that this method's feature does not

require an infinite time series, so it is easy to implement in the practical usages since the real-world time-series is always finite. Hence, we employ the PSVG for the analyses.

The non-linear autocorrelation and visibility graphs are useful methods to analyze the volatility clustering in the financial time-series. However, there has been a limited attempt to simultaneously incorporate both methods to explain the volatility clustering phenomenon in detail. Therefore, in this study, we suggest the measures for reliable estimation and explanation of the volatility clustering and provide the relevance between two approaches by comparing variations in clustering and fractality measures. In particular, we utilized the clustering and asymmetry measures presented in [22], [24]. Moreover, it is also necessary to measure the degree of influence when the causes of clustering are related. Hence, we analyze the values obtained from the measures of volatility clustering effect. Specifically, we analyze the influence of positive/negative values, large/small fluctuations, and each fluctuation ratio. In addition, the associated asymmetry measures are included to identify the different causes. Note that there are studies on the asymmetry degree, clustering degree, or scale difference according to rising and falling, which are also included in this research [47]–[50].

The rest of this paper is organized as follows. At first, Section 2 presents the methods and measures used in this paper where the Section 2.1, 2.2, and 2.3 explains the clustering index and asymmetric volatility measures, the PSVG approach, and the measures for their variations in different conditions of return distributions, respectively. Then, Section 3 presents the statistical properties and descriptive information of fractality of four representing financial markets, and Section 4 analyzes and discusses the results of the experiments, including the effects on clustering of the distributional features, clustering and asymmetry effects by the scale and sign of the data, and variations effects appear in sequence. Lastly, Section 5 concludes.

II. METHODS

A. CLUSTERING INDEX AND ASYMMETRY

The volatility clustering in the financial time series can be analyzed based on the daily log-return series. Let S_t be the daily closing price of a financial asset at time t , then the daily log-return, R_t , can be defined as

$$R_t = \ln \left(\frac{S_t}{S_{t-1}} \right). \quad (1)$$

The volatility clustering can be quantitatively studied by observing the positive and slowly decaying autocorrelation of the absolute daily log-return series, which indicates the power-law decay behavior. We follow the procedures defined in [22], [24]. Let $C(x_t, x_{t+\tau})$ be the autocorrelation function of time-series variable x for some time interval τ , then

$$C(x, x_{t+\tau}) \equiv \frac{\mathbb{E}[(x_t - \mathbb{E}[x_t])(x_{t+\tau} - \mathbb{E}[x_{t+\tau}])]}{\sqrt{\mathbb{E}[x_t^2] - (\mathbb{E}[x_t])^2} \sqrt{\mathbb{E}[x_{t+\tau}^2] - \mathbb{E}[x_{t+\tau}]^2}}. \quad (2)$$

Note that the autocorrelation is analyzed to detect the factor contributing to the volatility clustering by comparing the original and Gaussian-rearranged financial return series. The rearrangement procedure can be summarized as follows. At first, we define the Gaussian distribution with its mean and standard deviation analogous to those of the original return series. Secondly, we draw an equal number of data from this Gaussian distribution and refer it as Gaussian simulated series. Thirdly, we sort both the empirical and the simulated series in the descending order according to absolute returns. Lastly, we substitute values in the empirical series by the simulated series one by one from the largest one to the smallest one.

Then, we utilize the clustering index to analyze the volatility clustering in the financial time series. Let c denotes the degree of volatility clustering, indicating the largest $p\%$ within a time window of size n . Given that c is calculated by sliding the moving window with a specified time step, a clustering index, CI_n , for time window n can be defined in terms of the ratio of standard deviation c series such that,

$$CI_n \equiv \frac{\sigma_O}{\sigma_G} \tag{3}$$

where σ_O and σ_G are the standard deviations of the original and Gaussian-rearranged return series for the time window n , respectively. In this regard, CI_n indicates the ratio of clustering patterns within the current data compared to the simulated Gaussian distribution. In case when the clustering is more similar to the original than the simulated Gaussian distribution, the larger the time window size from 1 to 100, the higher the number of largest $p\%$ included in the window. Also, the larger the time window size, the smaller the standard deviation represents the heavier tail. As a result, the larger CI_n is, the higher the degree of volatility clustering is compared to the Gaussian distribution, which indicates the comparatively higher kurtosis and heavier tail. Besides, the theoretical upper limit of the clustering index, CI_n^{lim} , can be derived as described in [22], [24]. Simply put, we can derive a standard deviation of m clustering values using the probability that m corresponding to largest $p\%$ are involved within the window of size n such that,

$$\begin{aligned} \sigma_G &= \sqrt{\sum_{m=0}^n \left(m - \frac{p}{100}n\right)^2 \left(\frac{p}{100}\right)^m \left(1 - \frac{p}{100}\right)^{n-m}} \\ &= \sqrt{n \left(\frac{p}{100}\right) \left(1 - \frac{p}{100}\right)} \end{aligned} \tag{4}$$

where $\frac{p}{100}n$ indicates a mean value of c series about window of size n . In this context, the limit of a standard deviation can be defined as follows. For the time series of length N ,

$$\begin{aligned} &\frac{1}{N - n + 1} \left[\left(\frac{p}{100}N - n\right) \left(n - \frac{p}{100}n\right)^2 \right. \\ &\quad \left. + \left(\left(1 - \frac{p}{100}\right)N - n\right) \left(\frac{p}{100}n\right)^2 \right. \\ &\quad \left. + \sum_{m=0}^n \left(m - \frac{p}{100}n\right)^2 \right]. \end{aligned} \tag{5}$$

Since $\frac{p}{100}N$ and $(1 - \frac{p}{100})N$ are larger than n , Eq.(5) converges to $n^2(\frac{p}{100})(1 - \frac{p}{100})$. As $N \rightarrow \infty$, the theoretical limit of the standard deviation, σ_{lim} , converges to

$$\sigma_{\text{lim}} = \sqrt{n^2 \left(\frac{p}{100}\right) \left(1 - \frac{p}{100}\right)}. \tag{6}$$

Finally, the theoretical upper limit of clustering index, CI_n^{lim} , is,

$$CI_n^{\text{lim}} = \frac{\sigma_{\text{lim}}}{\sigma_G} = \frac{\sqrt{n^2(\frac{p}{100})(1 - \frac{p}{100})}}{\sqrt{n(\frac{p}{100})(1 - \frac{p}{100})}} = \sqrt{n} \tag{7}$$

In general, the persistence of the volatility can be detected using the GARCH estimation [4], [51], [52], which is widely used to measure the degree of the volatility clustering. However, the GARCH-model only provides the existence of clustering or persistence of the volatility with difficulties in determination of the parameter order, error distribution, the significance of estimated coefficients, and convergence of the algorithm. In contrast, the clustering index does not require such an estimation process. Therefore, the clustering index has its advantage in measuring the degree of volatility clustering in time-series.

Furthermore, the asymmetry of clustering also can be measured. In this study, we employ two asymmetry measures as defined in [22], [24]. The first measure, A_{scale} , evaluates the asymmetry between the largest values and smallest values of the clustering index such that

$$A_{\text{scale}} = \frac{CI^L - CI^S}{CI^L + CI^S} \tag{8}$$

where CI^L and CI^S indicate the clustering indices due to large and small values, respectively. Therefore, the measure shows which of large or small fluctuation contains more clustering as the window size increases. That is, the more large (small) values clustering, the closer A_{scale} is to positive (negative) value. The second measure, A_{sign} , calculates the asymmetry between large positive values and large negative values.

$$A_{\text{sign}} = \frac{CI^+ - CI^-}{CI^+ + CI^-} \tag{9}$$

where CI^+ and CI^- indicate the clustering indices due to large positive returns and large negative returns, respectively. Therefore, we can determine the degree of clustering due to window size and large positive or large negative values. Likewise, positive A_{sign} refers to the existence of more clustering in the positive return series.

B. VISIBILITY GRAPH ALGORITHM

It is possible to map the volatility in times series to its visibility graph [10]. In this graph, the node corresponds to the volatility values, whereas the undirected edge represents the connection between two volatility values when the two nodes satisfy the following condition of the equation.

Let X_i be the i -th point of the time series, then the condition for the existence of the edge is

$$X_{t_c} \leq X_{t_b} + (X_{t_a} - X_{t_b}) \frac{X_{t_b} - X_{t_c}}{X_{t_b} - X_{t_a}} \quad (10)$$

where t_a and t_b correspond to the node for specific time(node) in time series, with $t_c(t_a \leq t_c \leq t_b)$. Note that more detailed procedure can be found in [53]. Based on the constructed visibility graph, we count the number of connections in $X_i(i = t_a, \dots, t_c, \dots, t_b)$, which can be defined as the k degree of the each node in the undirected graph. In this context, the degree distribution($P(k) = n_k/n$) can be obtained by calculating the ratio of the total number of nodes(n) to frequency n_k for each k . The degree distribution is known to follow the power-law behaviour, and the power-law exponent(λ) is called as the Power of the Scale freeness in Visibility Graph (PSVG) such that

$$P(k) \sim k^{-\lambda}. \quad (11)$$

The PSVG is closely related to the complexity and fractality in time series. The PSVG has an inverse relationship with the Hurst exponent($H(0 < H < 1)$), which is also related to the autocorrelation in time series. The time-series has the characteristic of the fractional Brownian Motion(fBM) when the λ and H are related as,

$$\lambda = 3 - 2H \quad (12)$$

where $H = 0.5$, $H > 0.5$, and $H < 0.5$ indicate the non-correlated, correlated(persistent), and anti-correlated (anti-persistent) time-series, respectively.

C. MEASURES OF VARIATIONS IN CLUSTERING, ASYMMETRY, AND POWER-LAW EXPONENTS

For instance, if the largest $p\%$ for the measure is set to be 20%, the results of the measures only represent relatively high-risk investments, including extremely large positive and negative returns, which excludes the empirical evidence from the relatively smaller returns. Therefore, we suggest investigating the clustering pattern of volatility in more detail by analyzing the variations within the proposed clustering and asymmetry measures when $p\%$ is changed. In this research, we obtain the variations in measures by comparing the largest 20% and 40%. For the clustering indices (CI^L, CI^S, CI^+, CI^-) and asymmetry measures (A_{scale}, A_{sign}), the variations can be simply obtained by subtracting the values of 40% from those of 20%.

In addition, we also investigate the variations in PSVG, the power-law coefficients, λ , in visibility graph. If the power-law coefficient is denoted by $\lambda^L(p)$ for largest $p\%$, it can be defined by the coefficient ratio of original data and Gaussian simulated so that the results can be comparable with those of $CI^L, CI^S, CI^+, CI^-, A_{scale}$ and, A_{sign} . Therefore, the measures regarding the largest $p\%$ ($\lambda^L(p)$), smallest $p\%$ ($\lambda^S(p)$), largest positive $p\%$ ($\lambda^+(p)$), and smallest

negative $p\%$ ($\lambda^-(p)$) can be defined such that,

$$\begin{aligned} \lambda^L(p) &= \frac{\lambda_O^L(p)}{\lambda_G^L(p)} \\ \lambda^S(p) &= \frac{\lambda_O^S(p)}{\lambda_G^S(p)} \\ \lambda^+(p) &= \frac{\lambda_O^+(p)}{\lambda_G^+(p)} \\ \lambda^-(p) &= \frac{\lambda_O^-(p)}{\lambda_G^-(p)} \end{aligned} \quad (13)$$

where the subscripts O and G on the right-hand side of the equations indicate the original and Gaussian simulated, respectively. Also, the relative difference between largest and smallest value λ_p^{scale} , and that of large positive and large negative value λ_p^{sign} are similarly defined as follows.

$$\begin{aligned} \lambda^{scale}(p) &= \lambda^L(p) - \lambda^S(p) \\ \lambda^{sign}(p) &= \lambda^+(p) - \lambda^-(p) \end{aligned} \quad (14)$$

Based on the above measures, we can explore the variations in power-law coefficients by subtracting the values of 40% from those of 20%. The methods used in this research are summarized in Figure 1.

III. DATA AND DESCRIPTIVE STATISTICS

In this study, we investigate the four representing financial time-series from different markets including the S&P500(S&PCOMP) for the stock market, one year US Treasury Constant Maturity rate bond(FRTCMI1Y) for the bond market, Euro-Dollar exchange rate(EUDOLLR) for the exchange market, and the crude oil price(CRUOIL) for the commodity markets. Each data obtained from the Thomson Reuters Datastream includes the ten years of daily closing prices from 2009 to 2018, resulting in 2608 observations. For the analysis, we divide the ten years into two sub-periods with equal size. The first sub-period (SP1) is from 2009-01-01 to 2013-12-31, which includes the outbreak of the sub-prime mortgage crisis and the European debt crisis, whereas the second sub-period (SP2) is from 2014-01-01 to 2018-12-31, which does not include any major financial crisis. In this context, the division of sub-period can provide empirical evidence of the volatility clustering in different market conditions. Note that this paper focuses on the impact of the magnitude(large and small values) and the sign(positive and negative values) of volatility on the volatility clustering or fractality by considering the daily return in percent to represent the volatility.

Figure 2 shows the time-varying properties of the financial price and return series. Specifically, the red and yellow lines on the left are the daily returns and absolute return series, respectively, in percent. The black lines on the right are the rearranged Gaussian simulated returns. Note that the vertical dotted lines in each figure represent the division point of the sub-periods. Interestingly, we observe the repeated pattern

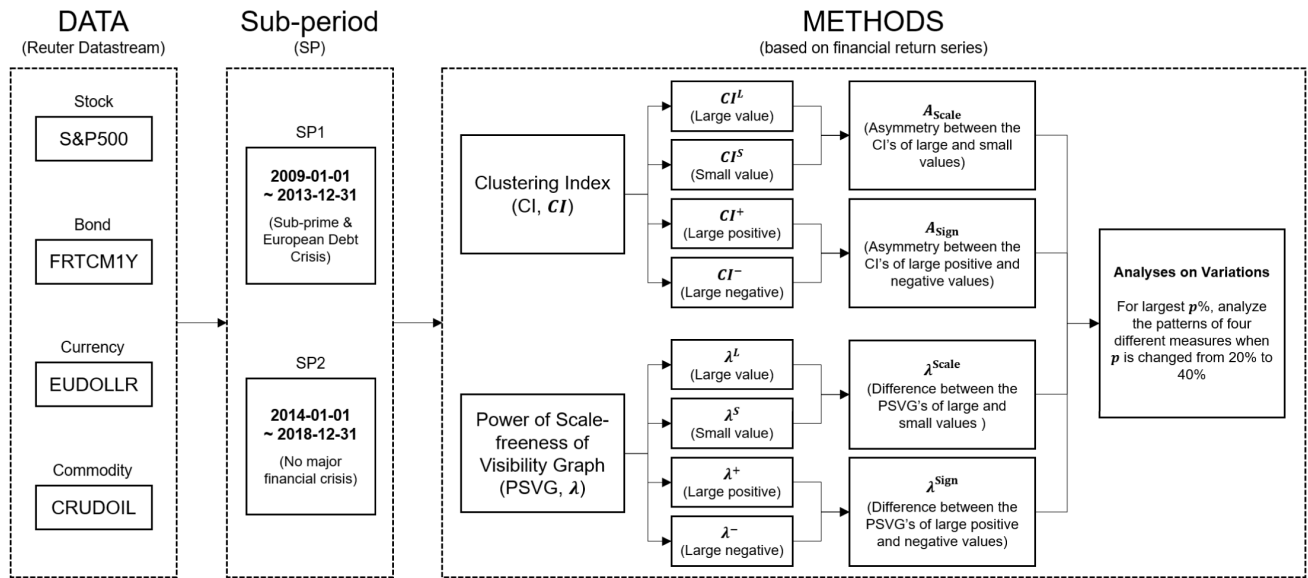


FIGURE 1. Flow chart of the methods used in analyses.

TABLE 1. Descriptive Statistics of return series.

Statistics	S&PCOMP		FRTCM1Y		EUDOLLR		CRUDOIL	
	SP1	SP2	SP1	SP2	SP1	SP2	SP1	SP2
Mean	0.06	0.02	-0.07	0.23	0.00	0.02	0.06	-0.06
Stdev	1.21	0.82	5.94	4.65	0.66	0.52	2.14	2.32
Skewness	-0.26	-0.50	0.18	0.09	-0.25	-0.07	-0.02	0.05
Kurtosis	4.35	4.01	2.52	5.80	2.32	2.23	5.29	2.72
K-S	0.1***	0.15***	0.28***	0.2***	0.12***	0.18***	0.12***	0.15***
Jarque-Bera	1031.35***	917.95***	349.5***	1814.23***	303.65***	268.22***	1504.79***	398.6***
ARCH(10)	207.98***	168.9***	100.74***	116.94***	47.14***	68.57***	258.7***	149.99***
ARCH(20)	298.63***	189.53***	122.72***	154.45***	46.0***	89.92***	300.02***	180.05***
LB(10)	33.83***	16.52*	39.61***	32.74***	5.62	13.44	20.93**	16.14*
LB(20)	50.71***	25.51	69.59***	51.66***	13.42	25.07	35.62**	25.24
LB(10) ²	563.04***	354.1***	211.04***	230.31***	64.12***	99.36***	537.29***	318.98***
LB(20) ²	948.79***	421.48***	391.29***	415.85***	95.2***	170.32***	963.55***	557.0***
ADF	-16.8***	-17.27***	-8.53***	-8.34***	-36.47***	-36.39***	-18.43***	-39.59***

Note: K-S, LB, and ADF are abbreviations for the Kolmogorov-Smirnov, Ljung-Box, and Augmented Dickey-Fuller tests, respectively.

for large or small absolute returns for all markets and sub-periods, which indicates the volatility clustering property. Specifically, S&PCOMP in Figure 2(a) shows the relatively high volatility in SP1 than that in the SP2. The highest volatility can be found in 2008, which indicates the sub-prime mortgage crisis. Some high volatility points exist in the second sub-period, but it has a much smaller magnitude with shorter duration. In the case of FRTCM1Y in Figure 2(b), constant high volatility is observed from 2008 to 2015, which covers the entire SP1 and the one-third of the SP2. Then, the volatility gradually decreases and becomes extremely small at the end of the SP2. EUDOLLR and CRUDOIL in Figure 2(c,d) show repeated patterns of large and small volatility for both sub-periods. Thus, the various volatility pattern is observed in different financial markets.

The descriptive statistics in Table 1 also shows the different volatility patterns in different financial markets. In the case of S&PCOMP, the mean and standard deviation of the volatility, defined as the daily return series, in SP1 is higher than those of SP2, as suggested in Figure 2(a). The volatility in SP2 was more left-skewed than that of SP1. The volatility in SP1 showed auto-correlation by the Ljung-Box test in lag 10 and 20, whereas the volatility in SP2 shows the weaker auto-correlation. Note that the test statistics on auto-correlation implies that the volatility clustering is higher in SP1 than SP2. In the case of FRTCM1Y, a kurtosis in SP2 is twice larger than that in SP1, whereas the skewness in SP2 is half of that in SP1. In the case of EUDOLLR, unlike other financial assets, the statistics in SP1 and SP2 are analogous in values. In addition, EUDOLLR shows no auto-correlation

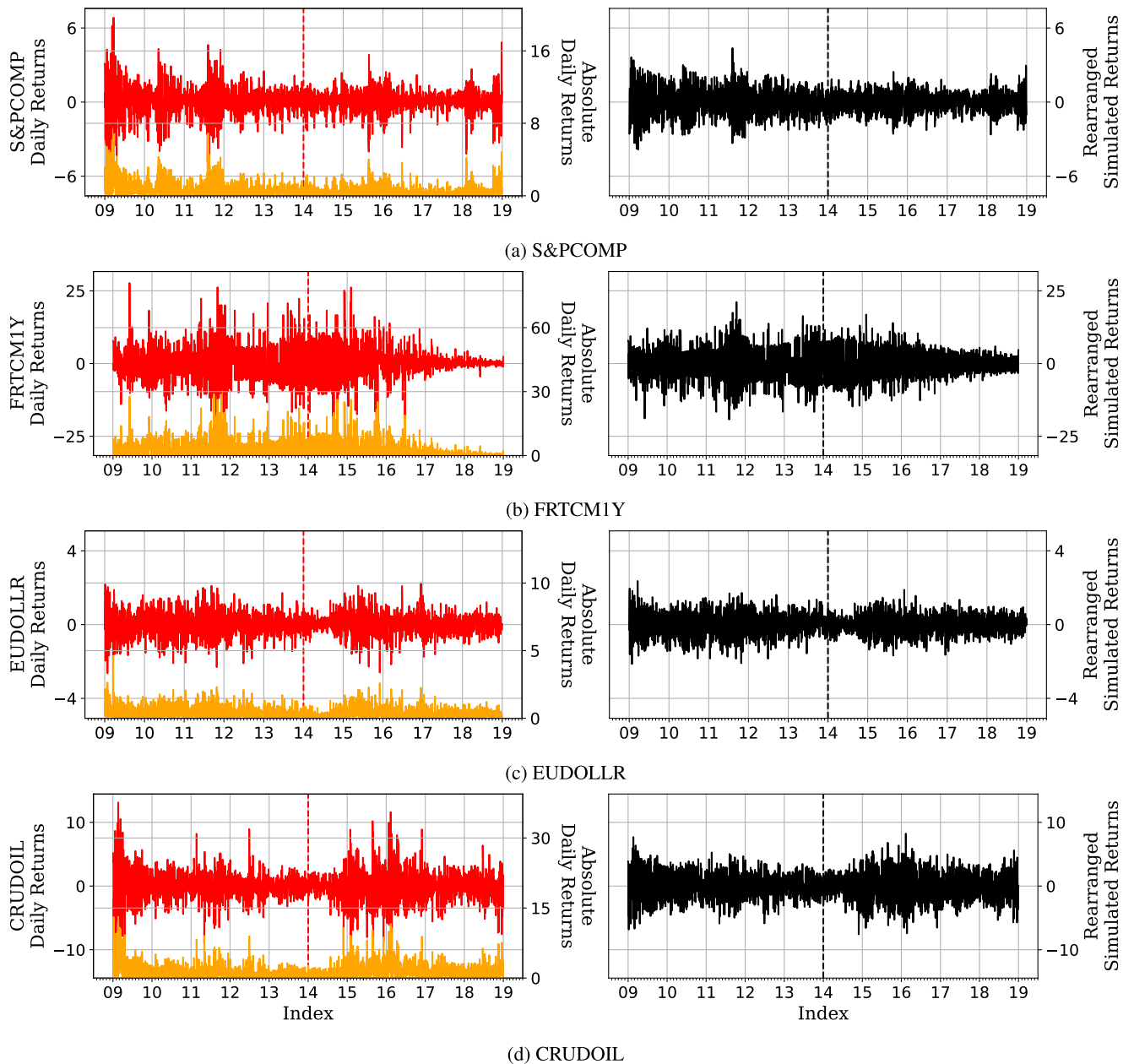


FIGURE 2. Time series of returns(left) and absolute returns(right) by sub-periods.

in both sub-period. Lastly, in CRUDOIL, the kurtosis in SP1 is twice greater than that in SP2. Also, the Ljung-Box auto-correlation test indicates weaker auto-correlation in SP2.

Then, we infer the clustering pattern based on the connectedness among distinct volatility values(nodes). At first, Figure 3 illustrates the linear fit to estimate the PSVG on four markets. The horizontal axis is the logarithm of degree k ($1/k$ for minus value), while the vertical axis indicates the logarithm of degree distribution $P(k)$. In addition, blue and red dashed lines result from linear fitting for SP1 and SP2, respectively, with layered areas representing standard error

of them. The results show that the degree distribution for each market follows the power-law. The detailed statistics are summarized in Table 2. At first, the PSVGs expressed as a mean±standard deviation are around 1.6 for all markets and sub-periods. Also, the PSVGs of all markets follow the fractional Brownian motion, whose values can be ranged from 0 to 1. Note that the values of fractional Brownian motion for all markets are ranged between 0.6 and 0.75, implying a persistence behavior. While the descriptive statistics on volatility show significantly different patterns among markets and sub-periods, the descriptive statistics on fractality show similar patterns regardless of market and sub-period.

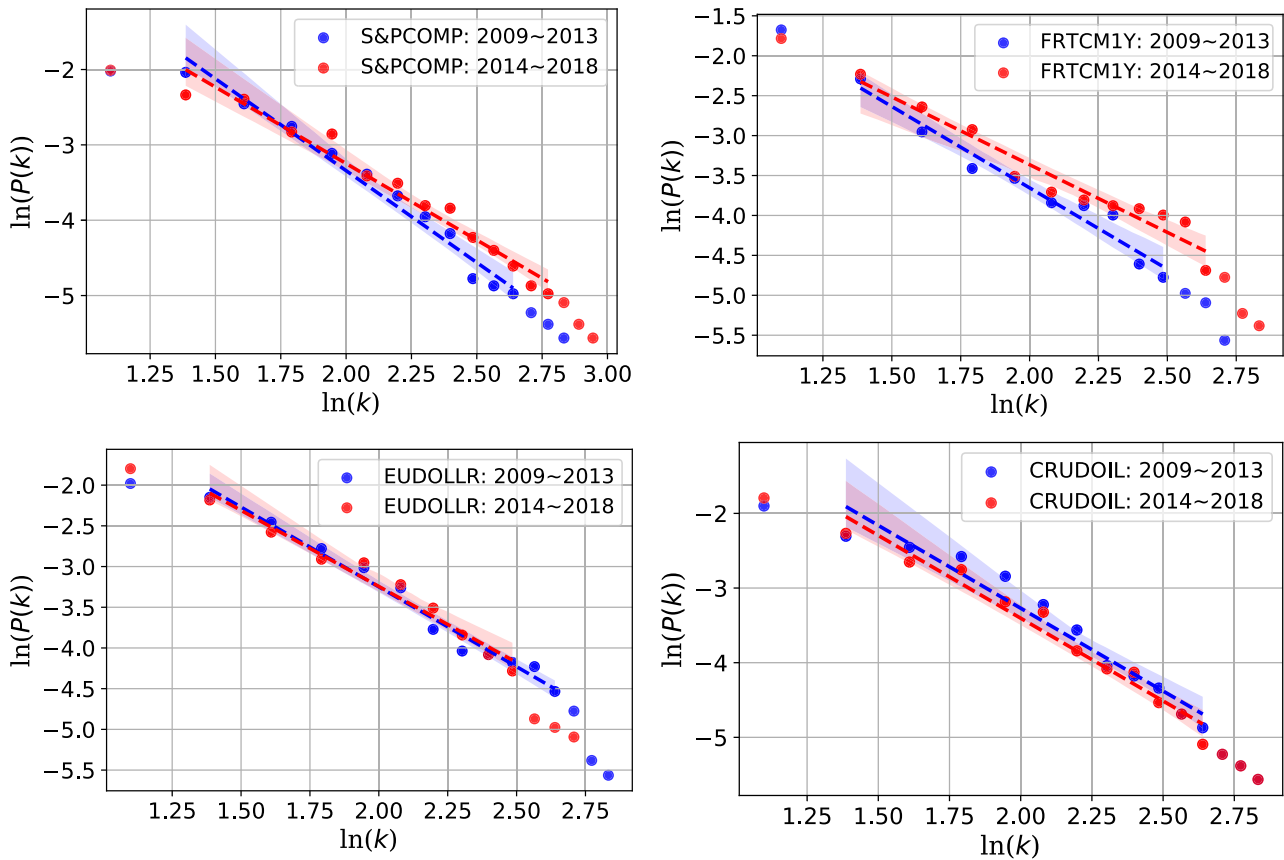


FIGURE 3. The distribution and slope of linear fit (λ_p) for each sub-period.

TABLE 2. Descriptive statistics on fractality.

Market	Sub-periods	power-law	fBM
S&PCOMP	SP1	1.6843±0.1609	0.6579
	SP2	1.5771±0.1362	0.7115
FRTCM1Y	SP1	1.7505±0.1507	0.6247
	SP2	1.5590±0.1418	0.7205
EUDOLLR	SP1	1.6045±0.1607	0.6978
	SP2	1.5913±0.1957	0.7043
CRUDOIL	SP1	1.6593±0.1702	0.6704
	SP2	1.6933±0.1508	0.6534

Note: fBM refers to the fractional Brownian motion.

IV. EMPIRICAL RESULTS AND DISCUSSIONS

A. CLUSTERING DUE TO THE POSITION OF THE DATA IN TIME AND DISTRIBUTIONAL CHARACTERISTICS

Based on the results in Section III, the financial time series shows a high kurtosis or heavy-tail behavior. Thus, it is reasonable to assume that its non-Gaussian distributional property might cause volatility clustering. Figure 4 shows the histograms of the original and Gaussian simulated time-series of four markets. Based on the results, the Gaussian series is simulated correctly, considering the Gaussian fitting on the histogram for all markets and sub-periods.

Also, the histogram of the original series is different from the Gaussian simulated series for all markets and sub-periods.

Figure 5 shows the auto-correlation of the absolute return series for the original (red), Gaussian simulated (black), and rearranged Gaussian simulated (blue) data in four markets. For all markets, the original and rearranged Gaussian simulated returns show the positive and slowly decaying behavior, which indicates the existence of volatility clustering. Furthermore, the Gaussian simulated returns' auto-correlation whose values revolve around zero is different from those of the original and rearranged Gaussian simulated returns in all markets and sub-periods. The fact that the auto-correlation of the rearranged Gaussian simulated series is more analogous to that of the original series than that of the Gaussian simulated series implies that the position of the return series' magnitude in time causes the volatility clustering more significantly than its distribution characteristics.

B. VOLATILITY CLUSTERING AND ASYMMETRY DUE TO THE DATA SCALE AND SIGN

We observe that the position of the magnitude of the volatility (absolute return) in time is a significant factor contributing to the volatility clustering. In this regard, we further investigate the factor for different types of returns. At first, we examine

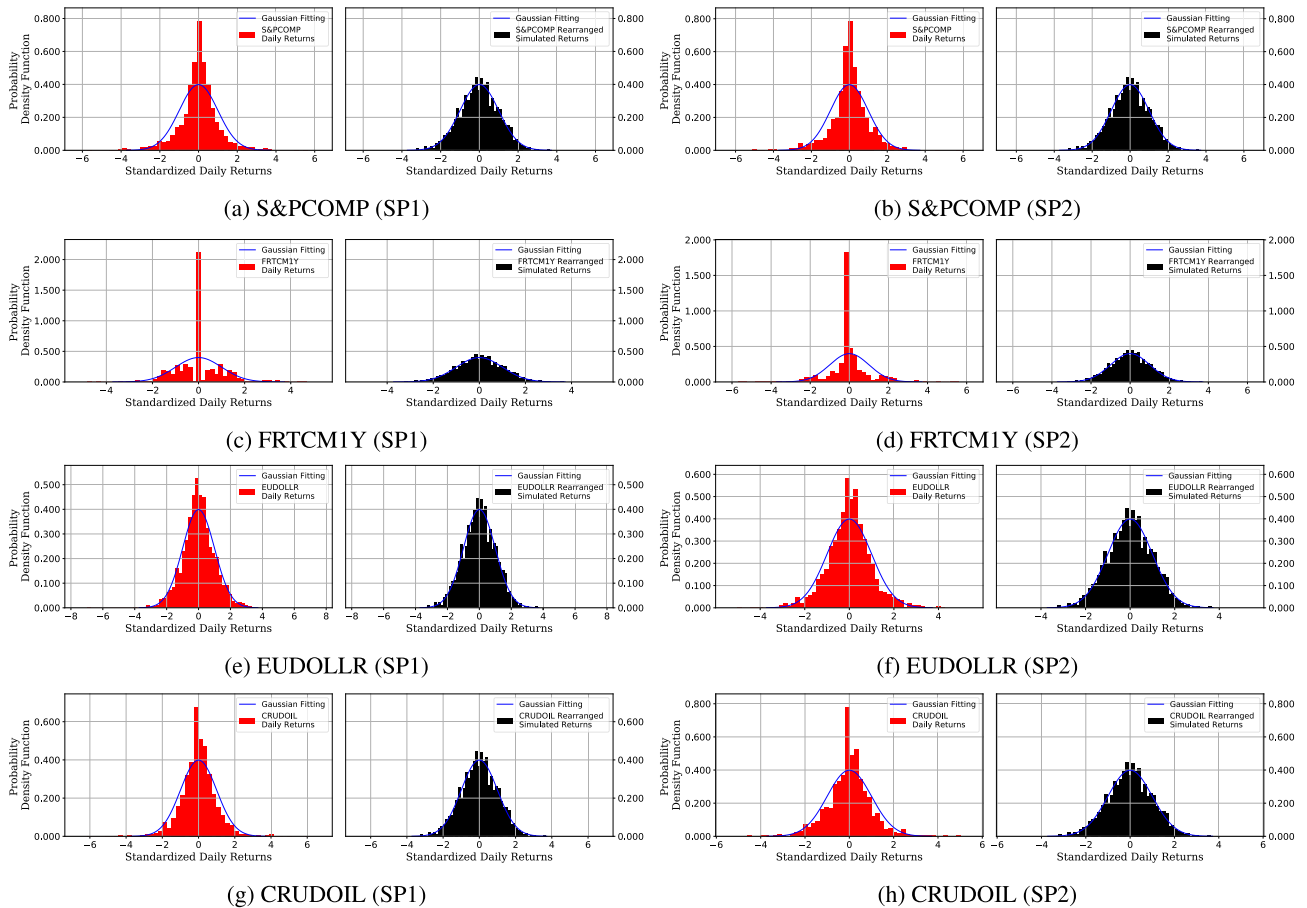


FIGURE 4. Comparison of histogram plots between the origin time series return(left) and gaussian simulated return(right).

the clustering effect due to large or small absolute returns. Then, we examine the clustering effect due to the large positive and negative absolute returns. Figure 6 and 7 show the volatility clustering affected by the scale and sign during the SP1 and SP2, respectively, based on the clustering index. Note that the solid black line is the theoretical limit, CI_n^{lim} , and the blue and red lines in the left figures are the CI^L and CI^S , respectively, whereas the blue and red lines in the right figures are the CI^+ and CI^- , respectively. That is, the blue lines indicate how many large returns exist within clustering data(time window) compared to Gaussian distribution, whereas the red lines indicate how many small returns exist within clustering data(time window) compared to Gaussian distribution. Also, the dashed lines indicate the clustering index when $p = 0.2$ (top 20% of the large or small returns), whereas the dash-dotted lines indicate the clustering index when $p = 0.4$ (top 40% of the large or small returns). For all markets and sub-periods, the original data, which exhibits the volatility clustering, possesses more of both large and small returns than the Gaussian distribution. The results imply that large or small returns promote the volatility clustering. Also, there are more of both positive and negative returns in large asset returns ($p = 0.2$). Therefore, the large positive

and large negative returns promote the volatility clustering. Note that there are relatively more large returns than small returns in the original data. Besides, the proportion of positive and negative returns in clustering is due to large returns. In summary, the contribution to the clustering effect within top 40% clustering data is Large > Small > Large(-) > Large(+).

The above results separate the contribution of large and small returns(scale) to the clustering effect from that of positive and negative returns(sign) within large returns. Therefore, it is necessary to compare the scale and the sign simultaneously and investigate the difference between sub-periods. In this context, the asymmetry measures are shown in Figure 8. A_{scale} , plotted as the blue line, indicates which of the large returns and small returns has more impact on the clustering, and A_{sign} , plotted as the red line, indicates which of the positive returns and negative returns has more impact on the clustering. During the SP1, the top 20% asset return tends to have many large returns than small returns, with slightly more positive returns than negative returns. In addition, the top 40% volatility also has many large returns with comparatively more negative returns than positive returns. Lastly, as time window size increases, A_{scale} with $p = 0.4$ is

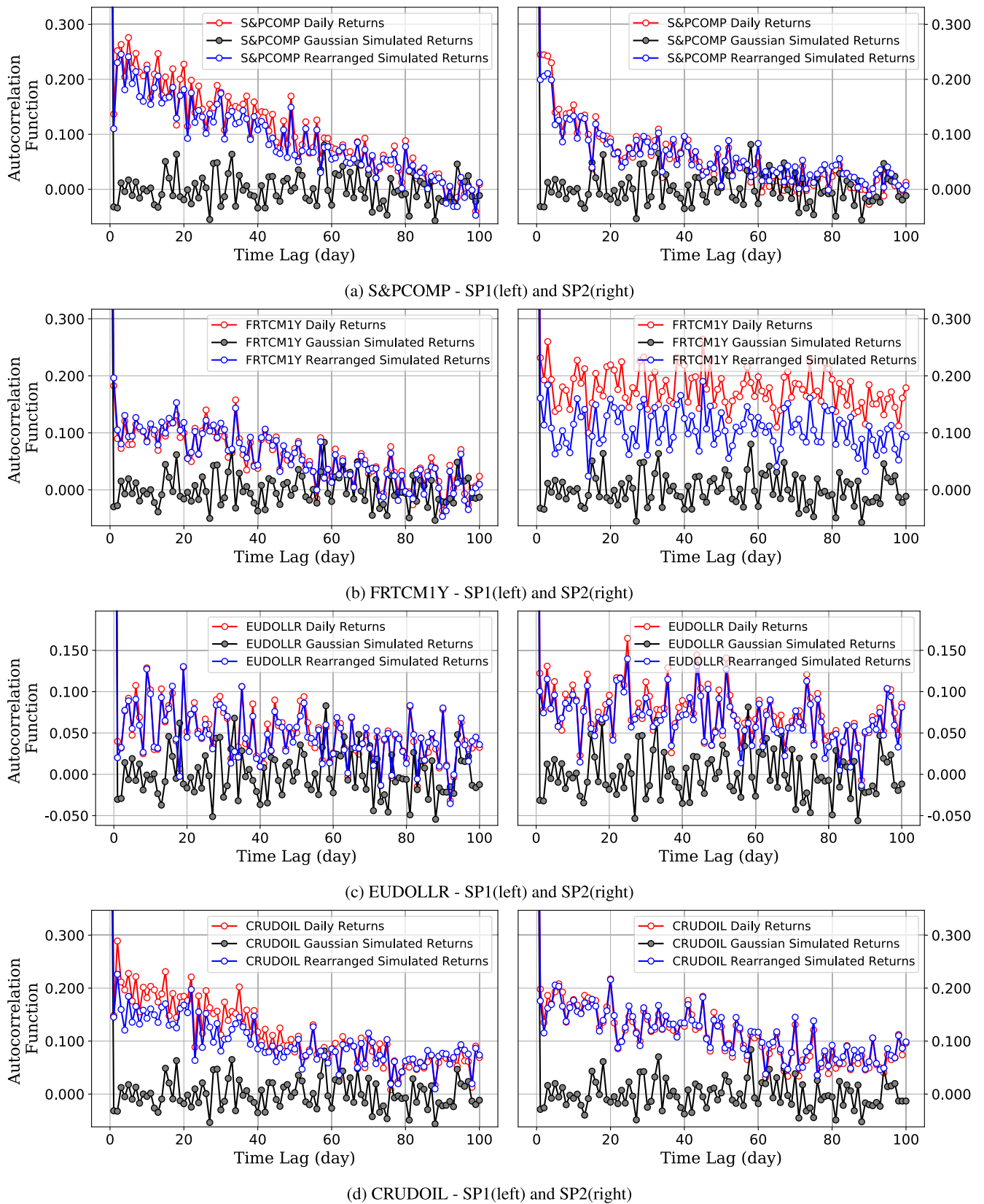


FIGURE 5. Auto-correlation plots on daily, Gaussian simulated, and rearranged Gaussian simulated returns.

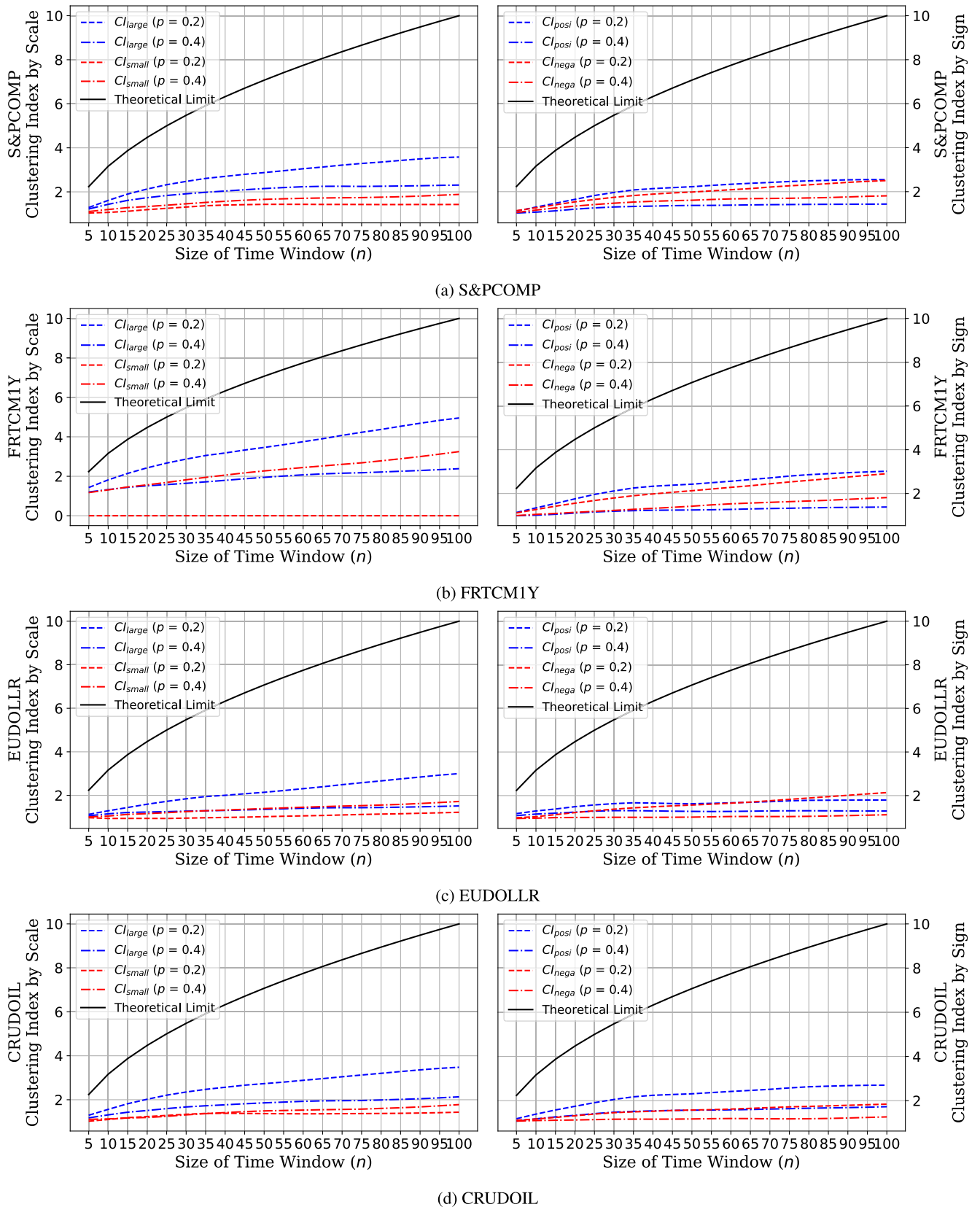


FIGURE 6. Clustering effect by scale(left) and sign(right) during SP1.

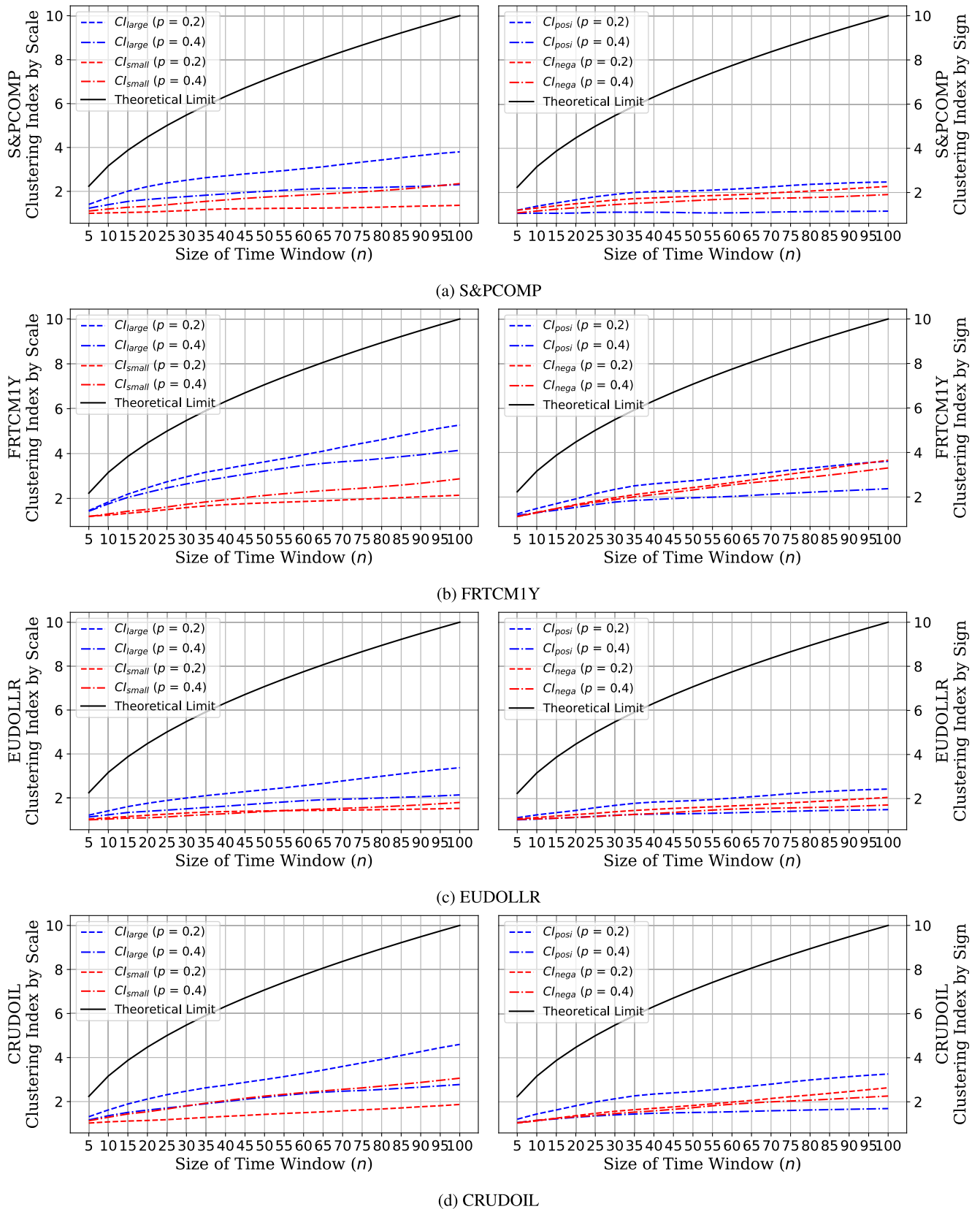


FIGURE 7. Clustering effect by scale(left) and sign(right) during SP2.

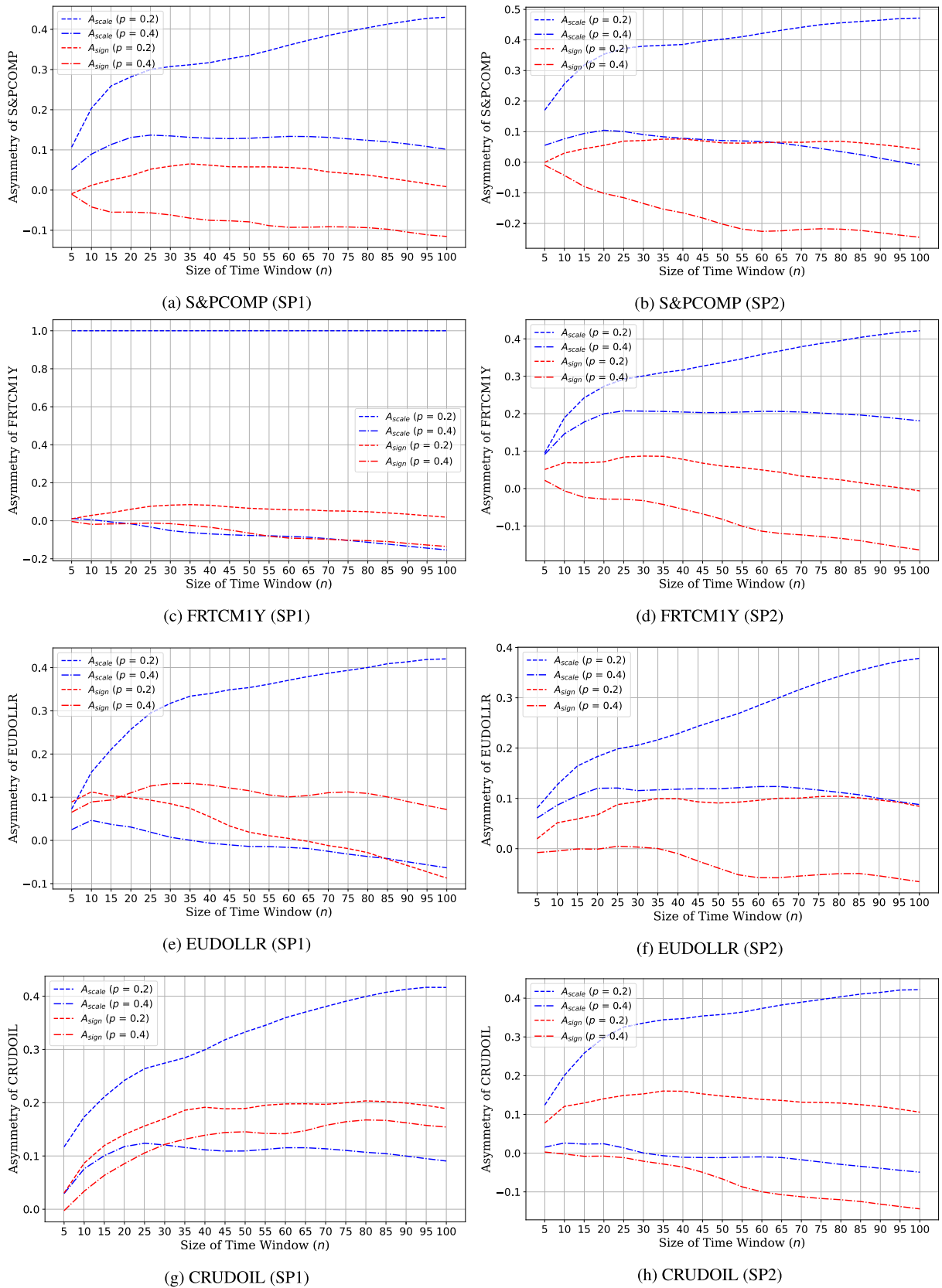


FIGURE 8. Asymmetry by scale and sign sub-periods.

TABLE 3. Median of clustering index and asymmetry on each market and sub-period.

Markets	Sub-periods	Target Return	Clustering Effect				Asymmetry Effect	
			Large	Large(+)	Large(-)	Small	Scale	Sign
S&PCOMP	SP1	Top 20%	2.92	2.26	2.01	1.42	0.34	0.04
		Top 40%	2.17	1.38	1.63	1.67	0.13	-0.08
	SP2	Top 20%	2.91	2.09	1.84	1.23	0.41	0.06
		Top 40%	2.03	1.1	1.65	1.76	0.07	-0.21
FRTCM1Y	SP1	Top 20%	3.53	2.46	2.16	0	1	0.05
		Top 40%	1.98	1.25	1.45	2.31	-0.08	-0.07
	SP2	Top 20%	3.7	2.78	2.48	1.82	0.34	0.05
		Top 40%	3.28	1.98	2.38	2.17	0.2	-0.09
EUDOLLR	SP1	Top 20%	2.18	1.66	1.59	1.03	0.36	0.01
		Top 40%	1.37	1.29	1.02	1.41	-0.01	0.11
	SP2	Top 20%	2.41	1.93	1.61	1.41	0.26	0.09
		Top 40%	1.78	1.33	1.45	1.4	0.12	-0.04
CRUDOIL	SP1	Top 20%	2.77	2.34	1.58	1.37	0.34	0.19
		Top 40%	1.88	1.57	1.17	1.5	0.11	0.14
	SP2	Top 20%	3.07	2.51	1.87	1.44	0.36	0.13
		Top 40%	2.24	1.52	1.78	2.29	-0.01	-0.08

TABLE 4. Top six ordering patterns of the clustering effects and their ratios and cases of market returns.

Order of Clustering Effect	Ratio	Cases of Market Return
Large > Large(+) > Large(-) > Small	50%	Top 20% All Markets
Large > Large(+) > Small > Large(-)	13%	Top 40% FRTCM1Y(SP2) & CRUDOIL(SP1)
Large > Small > Large(-) > Large(+)	13%	Top 40% S&PCOMP(SP1) & S&PCOMP(SP2)
Small > Large > Large(-) > Large(+)	13%	Top 40% FRTCM1Y(SP1) & CRUDOIL(SP2)
Large > Large(-) > Small > Large(+)	6%	Top 40% EUDOLLR(SP2)
Small > Large > Large(+) > Large(-)	6%	Top 40% EUDOLLR(SP1)

more decreased in SP2 than SP1. However, the overall trend is very similar to that of SP1.

Table 3 summarizes the median of the clustering index and the degree of asymmetry. Note that the median is used to ensure the statistical robustness against dramatic change caused by the time window’s small size. In other words, the table shows the degree to which the scale and the sign contribute to the clustering effect of Top 20% and Top 40% returns. In the case of the clustering effect, the clustering effects also become larger when the clustering indices of large, large positive, large negative, and small returns are larger. In the case of the asymmetry effect, the positive(negative) values in the scale column mean small returns have less(more) contribution to clustering in positive(negative) returns. The positive(negative) value in the sign column means positive returns in large return contribute more (less) to clustering than negative return does.

Lastly, the patterns in clustering effect are summarized in Table 4. We reduce the total of sixteen patterns into six major patterns contributing to the volatility clustering. The most frequent pattern, which covers 50%, is the order of Large > Large(+) > Large(-) > Small returns located in the first row. This pattern holds for all markets and sub-periods in the top 20% returns. The larger the asset return and the larger the positive asset return, the higher the volatility clustering and persistent behavior are. In contrast, all the remaining five priority patterns occur in the Top 40% returns. It implies

that when lower returns (larger p) is desired, the factors affecting the volatility clustering and persistent behavior can be different according to the market and period. While S&PCOMP consistently shows the order of Large > Small > Large(-) > Large(+) in Top 40% asset return for SP1 and SP2 as described in the third row, EUDOLLR shows different pattern depending on sub-period as listed in the fifth and sixth rows. In the case of FRTCM1Y and CRUDOIL, both the large and small returns can be the most critical factor to the volatility clustering and persistent behavior depending on the sub-periods in the opposite way as described in the second and fourth rows.

C. VARIATIONS OF VOLATILITY CLUSTERING, ASYMMETRY, AND POWER-LAW PROPERTIES

Previously, we discover the factors contributing to the clustering effect according to different markets and the sub-periods. Especially, we observe the establishment of various patterns regarding the order of contributing factors when p is increased from 0.2 to 0.4. Note that the order is the same for all markets and sub-periods when $p = 0.2$. Furthermore, the detailed results on the variations of clustering and asymmetric properties can be investigated in Table 5. Specifically, the pattern of factors contributing to the clustering when extending from high-returns($p = 0.2$) to low-returns($p = 0.4$) are summarized. The variations in six different measures are presented based on the subtraction of the values of $p =$

TABLE 5. Variations of clustering and asymmetry measures from the top 20% to 40% returns on each sub-period.

Variation of Clustering Effect (Top 20% → 40%)							
Sub-period: SP1							
Statistics	Markets	Large	Large(+)	Large(-)	Small	Scale	Sign
Values	S&PCOMP	-0.75	-0.88	-0.38	0.25	-0.21	-0.12
	FRTCM1Y	-1.55	-1.21	-0.71	2.31	-1.08	-0.12
	EUDOLLR	-0.81	-0.37	-0.57	0.38	-0.37	0.1
	CRUDOIL	-0.89	-0.77	-0.41	0.13	-0.23	-0.05
Directions	S&PCOMP	-	-	-	+	-	-
	FRTCM1Y	-	-	-	+	-	-
	EUDOLLR	-	-	-	+	-	+
	CRUDOIL	-	-	-	+	-	-
Sub-period: SP2							
Statistics	Markets	Large	Large(+)	Large(-)	Small	Scale	Sign
Values	S&PCOMP	-0.88	-0.99	-0.19	0.53	-0.34	-0.27
	FRTCM1Y	-0.42	-0.8	-0.1	0.35	-0.14	-0.14
	EUDOLLR	-0.63	-0.6	-0.16	-0.01	-0.14	-0.13
	CRUDOIL	-0.83	-0.99	-0.09	0.85	-0.37	-0.21
Directions	S&PCOMP	-	-	-	+	-	-
	FRTCM1Y	-	-	-	+	-	-
	EUDOLLR	-	-	-	-	-	-
	CRUDOIL	-	-	-	+	-	-

TABLE 6. Variations of power-law properties from the top 20% to 40% returns on each sub-period.

Variation of PSVG (Top 20% → 40%)							
Sub-period: SP1							
Statistics	Markets	Large	Large(+)	Large(-)	Small	Scale	Sign
Values	S&PCOMP	0.0419	0.0467	0.1409	-0.127	0.695	-0.0580
	FRTCM1Y	0.0540	0.0669	0.4570	-1.2142	2.0159	-0.0812
	EUDOLLR	-0.0378	0.0598	0.1098	-0.0578	0.1383	-0.0499
	CRUDOIL	0.0161	0.0272	0.0412	-0.0468	0.1629	-0.0331
Directions	S&PCOMP	+	+	+	-	+	-
	FRTCM1Y	+	+	+	-	+	-
	EUDOLLR	-	+	+	-	+	-
	CRUDOIL	+	+	+	-	+	-
Sub-period: SP2							
Statistics	Markets	Large	Large(+)	Large(-)	Small	Scale	Sign
Values	S&PCOMP	0.0599	0.2781	0.1624	-0.0550	0.2049	-0.0347
	FRTCM1Y	-0.0095	0.0102	-0.0154	0.0258	-0.0716	0.0822
	EUDOLLR	0.0174	-0.0039	0.0812	-0.0897	0.0364	-0.1208
	CRUDOIL	-0.0189	0.0140	0.0163	-0.0704	0.1603	0.0015
Directions	S&PCOMP	+	+	+	-	+	-
	FRTCM1Y	-	+	-	+	-	+
	EUDOLLR	+	-	+	-	+	-
	CRUDOIL	-	+	+	-	+	+

0.4 from those of $p = 0.2$ with its corresponding direction. At first, we examine the results in SP1. For instance, the results of S&PCOMP show that the volatility clustering due to large returns, including the large, large positive, and large negative returns, decreases as p increases (-0.75, -0.88, -0.38). In contrast, the clustering due to small returns increases (0.25). These results are consistent in the other three markets. In terms of asymmetry measures, the volatility clustering is increased by small and large negative returns

given that the scale and sign are -0.21 and -0.12, respectively. If each market's result is only considered in terms of the direction, the volatility clustering due to small return increases in all markets. In the case of the direction of asymmetry measures, the clustering due to large negative return becomes larger in all the markets except EUDOLLR when p increases. The result of SP2 is analogous to that of SP1. Both small and large negative return increases in all four markets except EUDOLLR when p increases. That is, EUDOLLR

TABLE 7. Directional consistency between the variations in clustering and asymmetry measures and power-law exponents.

Comparison between clustering and power-law (Top 20% → 40%)								
Sub-period: SP1								
Statistics	Markets	Large	Large(+)	Large(-)	Small	Scale	Sign	#T
Consistency	S&PCOMP	FALSE	FALSE	FALSE	FALSE	FALSE	TRUE	1
	FRTCM1Y	FALSE	FALSE	FALSE	FALSE	FALSE	TRUE	1
	EUDOLLR	TRUE	FALSE	FALSE	FALSE	FALSE	FALSE	1
	CRUDOIL	FALSE	FALSE	FALSE	FALSE	FALSE	TRUE	1
Sub-period: SP2								
Statistics	Markets	Large	Large(+)	Large(-)	Small	Scale	Sign	#T
Consistency	S&PCOMP	FALSE	FALSE	FALSE	FALSE	FALSE	TRUE	1
	FRTCM1Y	TRUE	FALSE	TRUE	TRUE	TRUE	FALSE	4
	EUDOLLR	FALSE	TRUE	FALSE	TRUE	FALSE	TRUE	3
	CRUDOIL	TRUE	FALSE	FALSE	FALSE	FALSE	FALSE	1

Note: #T refers to the number of true among the factor of the volatility clustering in each market.

has more large returns than small returns. Although the market volatility is lower in SP2 than SP1 in four markets, the effect of a factor on the volatility clustering remains the same even under the non-Gaussian distribution. In summary, the volatility clustering of the low-returns($p = 0.4$) is more affected by the small return and large negative returns than the high-returns($p = 0.2$).

Furthermore, we summarize the variation of fractality in Eqs.(13) and (14) in Table 6. Similar to the Table 5, we describe how PSVG changes when p increases from 0.2 (high-return) to 0.4 (low-return). Note that the positive value and direction indicate the increases in persistent behavior in volatility clustering, whereas the negative value and direction indicate the increases in anti-persistent behavior. For instance, the result of S&PCOMP in SP1 shows that the large returns (0.0299, 0.0655, 0.1314) increase the persistent behavior in volatility clustering, whereas the small returns contribute to the increase in anti-persistent behavior. The same results can be found on the scale. Also, anti-persistent behavior is more increased by large negative values than large positive values. That is, small and large negative returns, critical factors in the clustering effect, increase the anti-persistent behavior of volatility clustering. Again, all the four markets except EUDOLLR shows the same pattern. Unlike SP1, the variations in PSVG in SP2 are hardly generalized for different markets. While S&PCOMP in SP2 has the same pattern in SP1, all the other markets have distinct fractality patterns. In other words, unlike clustering and asymmetry measures, the PSVG are highly affected by non-Gaussian distribution. Note that the return distribution of SP2 is closer to the Gaussian distribution than that of SP1 for all markets. It implies that the clustering and asymmetry measures are more robust than the PSVG in terms of generalization of the pattern of factors contributing to the volatility clustering.

Lastly, Table 7 summarizes the comparison whether the sign of directions in Table 5 and that of in Table 6 are the same. Given that the number of trues in SP1 is much smaller than that in SP2, we presume that the directions of

clustering and asymmetry measures when p increases from 0.2 to 0.4 and that of PSVG changes in opposite direction when the market is highly volatile.

V. CONCLUSION

The prices of numerous financial products in the market change over time and generate various financial time-series patterns. In particular, volatility clustering exists, indicating the phenomenon that the large (small) fluctuations of the financial time-series consistently occur after the previous large (small) fluctuations. There have been efforts to detect the volatility clustering and explain the causes of the volatility clustering within the market. In this study, we accumulate state-of-the-art methods and analyzed volatility clustering using the non-linear autocorrelation and various clustering and asymmetry measures. We also provide a further explanation of the causes of the volatility clustering when the target return is changed. Note that, to the best of our knowledge, this is the first attempt to utilize clustering and asymmetry measures to analyze the volatility clustering simultaneously, including their variations with respect to the target returns.

The findings of this paper are as follows. In terms of the existence of volatility clustering, we observe that volatility clustering occurs in all representative financial time series of the four financial markets where the return distributions follow the fractional Brownian motion rather than the Gaussian distribution in most markets and sub-periods. Also, we confirm that the data positioning of the return series contributes more to the volatility clustering than the distributional characteristics such as heavy-tails. Specifically, we observe that the four representative financial return-series show the positive and slowly decaying non-linear autocorrelation. Also, we confirm that the Gaussian simulated returns, whose order of returns are rearranged as the underlying real financial time-series, also show the power-law decay.

The results above are further investigated by the clustering and asymmetry measures. In particular, the factors affecting the volatility clustering are studied in detail. At first,

we observe that the order of contributing factors on volatility clustering is Large > Large positive > Large negative > Small returns for high target return (small p). In contrast, the order of contributions of the factors appears differently depending on the market conditions. Secondly, in most markets and sub-periods, we discover that the scale of the return contributes more to volatility clustering than its sign. It implies that the extreme upward or downward price movement might last longer when realized. Thirdly, we find that irrespective of market conditions, the group who obtain high returns tends to keep their high returns where the order of contributing factors are independent of the market or sub-periods since the clustering and asymmetry measures show the similar pattern regardless of market condition. In contrast, the variation of PSVG shows different contributing factors depending on market conditions. During the financial crisis (SP1), the direction of increase or decrease in PSVG is similar for all contributing factors. However, after the financial crisis (SP2), the direction of increase or decrease in PSVG varies depending on the market and contributing factors. Given that the financial crisis and non-financial crisis periods show different return distributions, the PSVG coefficients seem to be affected by the non-Gaussian distribution, unlike clustering and asymmetry measures. Therefore, we presume that clustering and asymmetry measures are more robust measures to distribution for the volatility clustering than PSVG. Lastly, in a highly volatile market, an inverse relationship between the directions of the clustering effect defined by the clustering indices and asymmetry and PSVG is observed when the variation is examined from high returns to low returns.

Based on the empirical evidences, we conclude that the volatility clustering in the financial time-series exists whose contributing factors varies for market condition and target returns. Therefore, as a future work, we are planning to model the Value-at-Risk and Expected Shortfall algorithms, switching with respect to volatility clustering incurred from different causes. Such algorithms can be further implemented in terms of decentralized in financial risk management system.

REFERENCES

- [1] L. Bachelier, "Théorie de la spéculation," in *Annales scientifiques de l'École normale supérieure*, vol. 17, 1900, pp. 21–86.
- [2] Z. Ding, C. W. J. Granger, and R. F. Engle, "A long memory property of stock market returns and a new model," *J. Empirical Finance*, vol. 1, no. 1, pp. 83–106, Jun. 1993.
- [3] R. F. Engle, "Autoregressive conditional heteroscedasticity with estimates of the variance of United Kingdom inflation," *Econometrica, J. Econ. Soc.*, vol. 50, no. 4, pp. 987–1007, 1982.
- [4] T. Bollerslev, "Generalized autoregressive conditional heteroskedasticity," *J. Econometrics*, vol. 31, no. 3, pp. 307–327, Apr. 1986.
- [5] R. Cont, "Volatility clustering in financial markets: Empirical facts and agent-based models," in *Long Memory in Economics*. Berlin, Germany: Springer, 2007, pp. 289–309.
- [6] S. I. Resnick, "Why non-linearities can ruin the heavy-tailed modeler's day," in *A Practical Guide to Heavy Tails: Statistical Techniques and Applications*. Boston, MA, USA: Birkhäuser, 1998, pp. 219–239.
- [7] S. Resnick, G. Samorodnitsky, and F. Xue, "How misleading can sample ACFs of stable MAs be? (very!)," *Ann. Appl. Probab.*, vol. 9, no. 3, pp. 797–817, Aug. 1999.
- [8] R. N. Mantegna and H. E. Stanley, "Scaling behaviour in the dynamics of an economic index," *Nature*, vol. 376, no. 6535, p. 46, 1995.
- [9] B.-H. Wang and P.-M. Hui, "The distribution and scaling of fluctuations for Hang Seng index in Hong Kong stock market," *Eur. Phys. J. B-Condens. Matter Complex Syst.*, vol. 20, no. 4, pp. 573–579, 2001.
- [10] A. Razdan, "Scaling in the Bombay stock exchange index," *Pramana*, vol. 58, no. 3, pp. 537–544, Mar. 2002.
- [11] J. A. Skjeltorp, "Scaling in the Norwegian stock market," *Phys. A, Stat. Mech. Appl.*, vol. 283, nos. 3–4, pp. 486–528, Aug. 2000.
- [12] P. Gopikrishnan, V. Plerou, Y. Liu, L. N. Amaral, X. Gabaix, and H. E. Stanley, "Scaling and correlation in financial time series," *Phys. A, Stat. Mech. Appl.*, vol. 287, nos. 3–4, pp. 362–373, 2000.
- [13] H. E. Stanley, L. A. N. Amaral, P. Gopikrishnan, and V. Plerou, "Scale invariance and universality of economic fluctuations," *Phys. A, Stat. Mech. Appl.*, vol. 283, nos. 1–2, pp. 31–41, Aug. 2000.
- [14] P. Gopikrishnan, M. Meyer, L. A. N. Amaral, and H. E. Stanley, "Inverse cubic law for the distribution of stock price variations," *Eur. Phys. J. B*, vol. 3, no. 2, pp. 139–140, Jul. 1998.
- [15] F. Lillo and J. D. Farmer, "The long memory of the efficient market," *Stud. Nonlinear Dyn. Econometrics*, vol. 8, no. 3, pp. 1–19, Jan. 2004.
- [16] J. Jiang, K. Ma, and X. Cai, "Non-linear characteristics and long-range correlations in Asian stock markets," *Phys. A, Stat. Mech. Appl.*, vol. 378, no. 2, pp. 399–407, May 2007.
- [17] B. Mandelbrot, "New methods in statistical economics," *J. Political Economy*, vol. 71, no. 5, pp. 421–440, Oct. 1963.
- [18] B. B. Mandelbrot, "The variation of certain speculative prices," in *Fractals and Scaling in Finance*. New York, NY, USA: Springer, 1997, pp. 371–418.
- [19] R. Adler, R. Feldman, and M. Taqqu, *A Practical Guide to Heavy Tails: Statistical Techniques and Applications*. Boston, MA, USA: Birkhäuser, 1998.
- [20] B. Podobnik, D. Horvatic, A. M. Petersen, and H. E. Stanley, "Cross-correlations between vol. change, and price change," *Proc. Nat. Acad. Sci. USA*, vol. 106, no. 52, pp. 22079–22084, 2009.
- [21] J. Y. Campbell, A. W. Lo, A. C. MacKinlay, and R. F. Whitelaw, "The econometrics of financial markets," *Macroeconomic Dyn.*, vol. 2, no. 4, pp. 559–562, 1998.
- [22] J.-J. Tseng and S.-P. Li, "Asset returns and volatility clustering in financial time series," *Phys. A, Stat. Mech. Appl.*, vol. 390, no. 7, pp. 1300–1314, Apr. 2011.
- [23] G. Teyssière and A. P. Kirman, *Long Memory in Economics*. Berlin, Germany: Springer, 2006.
- [24] J.-J. Tseng and S.-P. Li, "Quantifying volatility clustering in financial time series," *Int. Rev. Financial Anal.*, vol. 23, pp. 11–19, Jun. 2012.
- [25] R. Cont, "Empirical properties of asset returns: Stylized facts and statistical issues," *Quant. Finance*, vol. 1, no. 2, pp. 223–236, Feb. 2001.
- [26] R. F. Engle and A. J. Patton, "What good is a volatility model?" in *Forecasting Volatility in the Financial Markets*. Amsterdam, The Netherlands: Elsevier, 2007, pp. 47–63.
- [27] A. Chakraborti, I. M. Toke, M. Patriarca, and F. Abergel, "Econophysics: Empirical facts and agent-based models," 2009, *arXiv:0909.1974*. [Online]. Available: <http://arxiv.org/abs/0909.1974>
- [28] R. N. Mantegna and H. E. Stanley, *Introduction to Econophysics: Correlations and Complexity in Finance*. Cambridge, U.K.: Cambridge Univ. Press, 1999.
- [29] J.-P. Bouchaud and M. Potters, *Theory of Financial Risk and Derivative Pricing: From Statistical Physics to Risk Management*. Cambridge, U.K.: Cambridge Univ. Press, 2003.
- [30] J. Zhang and M. Small, "Complex network from pseudoperiodic time series: Topology versus dynamics," *Phys. Rev. Lett.*, vol. 96, no. 23, Jun. 2006, Art. no. 238701.
- [31] Y. Yang and H. Yang, "Complex network-based time series analysis," *Phys. A, Stat. Mech. Appl.*, vol. 387, nos. 5–6, pp. 1381–1386, 2008.
- [32] L. Lacasa, B. Luque, F. Ballesteros, J. Luque, and J. C. Nuño, "From time series to complex networks: The visibility graph," *Proc. Nat. Acad. Sci. USA*, vol. 105, no. 13, pp. 4972–4975, Apr. 2008.
- [33] X. Xu, J. Zhang, and M. Small, "Superfamily phenomena and motifs of networks induced from time series," *Proc. Nat. Acad. Sci. USA*, vol. 105, no. 50, pp. 19601–19605, 2008.
- [34] Y. Zhao, T. Weng, and S. Ye, "Geometrical invariability of transformation between a time series and a complex network," *Phys. Rev. E, Stat. Phys. Plasmas Fluids Relat. Interdiscip. Top.*, vol. 90, no. 1, Jul. 2014, Art. no. 012804.

- [35] S. Mutua, C. Gu, and H. Yang, "Visibility graphlet approach to chaotic time series," *Chaos, Interdiscipl. J. Nonlinear Sci.*, vol. 26, no. 5, May 2016, Art. no. 053107.
- [36] M. Stephen, C. Gu, and H. Yang, "Visibility graph based time series analysis," *PLoS ONE*, vol. 10, no. 11, Nov. 2015, Art. no. e0143015.
- [37] M. McCullough, M. Small, T. Stemler, and H. H.-C. Iu, "Time lagged ordinal partition networks for capturing dynamics of continuous dynamical systems," *Chaos, Interdiscipl. J. Nonlinear Sci.*, vol. 25, no. 5, May 2015, Art. no. 053101.
- [38] J. Zhang, J. Zhou, M. Tang, H. Guo, M. Small, and Y. Zou, "Constructing ordinal partition transition networks from multivariate time series," *Sci. Rep.*, vol. 7, no. 1, pp. 1–13, Dec. 2017.
- [39] M. E. J. Newman, D. J. Watts, and S. H. Strogatz, "Random graph models of social networks," *Proc. Nat. Acad. Sci. USA*, vol. 99, no. 1, pp. 2566–2572, 2002.
- [40] A.-L. Barabási and R. Albert, "Emergence of scaling in random networks," *Science*, vol. 286, no. 5439, pp. 509–512, Oct. 1999.
- [41] R. Albert and A.-L. Barabási, "Statistical mechanics of complex networks," *Rev. Mod. Phys.*, vol. 74, p. 47, Jan. 2002.
- [42] L. Lacasa, B. Luque, J. Luque, and J. C. Nuño, "The visibility graph: A new method for estimating the Hurst exponent of fractional Brownian motion," *Europhys. Lett.*, vol. 86, no. 3, p. 30001, 2009.
- [43] M. Ahmadlou, H. Adeli, and A. Adeli, "Improved visibility graph fractality with application for the diagnosis of autism spectrum disorder," *Phys. A, Stat. Mech. Appl.*, vol. 391, no. 20, pp. 4720–4726, Oct. 2012.
- [44] M. Andjelković, N. Gupte, and B. Tadić, "Hidden geometry of traffic jamming," *Phys. Rev. E, Stat. Phys. Plasmas Fluids Relat. Interdiscip. Top.*, vol. 91, no. 5, May 2015, Art. no. 052817.
- [45] Y. Yang, J. Wang, H. Yang, and J. Mang, "Visibility graph approach to exchange rate series," *Phys. A, Stat. Mech. Appl.*, vol. 388, no. 20, pp. 4431–4437, Oct. 2009.
- [46] L. Zhao, W. Li, C. Yang, J. Han, Z. Su, and Y. Zou, "Multifractality and network analysis of phase transition," *PLoS ONE*, vol. 12, no. 1, Jan. 2017, Art. no. e0170467.
- [47] O. Henry, "Modelling the asymmetry of stock market volatility," *Appl. Financial Econ.*, vol. 8, no. 2, pp. 145–153, Apr. 1998.
- [48] A. Peiró, "Asymmetries and tails in stock index returns: Are their distributions really asymmetric?" *Quant. Finance*, vol. 4, no. 1, pp. 37–44, Feb. 2004.
- [49] J. Chen, H. Hong, and J. C. Stein, "Forecasting crashes: Trading volume, past returns, and conditional skewness in stock prices," *J. Financial Econ.*, vol. 61, no. 3, pp. 345–381, 2001.
- [50] M. M. Pelagatti, "Modelling good and bad volatility," *Stud. Nonlinear Dyn. Econometrics*, vol. 13, no. 1, pp. 1–13, Jan. 2009.
- [51] D. B. Nelson, "Conditional heteroskedasticity in asset returns: A new approach," *Econometrica, J. Econ. Soc.*, vol. 59, no. 2, pp. 347–370, 1991.
- [52] R. T. Baillie, T. Bollerslev, and H. O. Mikkelsen, "Fractionally integrated generalized autoregressive conditional heteroskedasticity," *J. Econometrics*, vol. 74, no. 1, pp. 3–30, Sep. 1996.
- [53] M. Mondal, A. Mondal, J. Mondal, K. K. Patra, A. Deb, and D. Ghosh, "Evidence of centrality dependent fractal behavior in high energy heavy ion interactions: Hint of two different sources," *Chaos, Solitons Fractals*, vol. 113, pp. 230–237, Aug. 2018.



KYUNGWON KIM received the B.Sc. degree in mathematics and physics from Hanyang University, Seoul, South Korea, in 2007, and the M.Sc. degree in computational science and technology (specialized in data mining) and the Ph.D. degree in industrial engineering (specialized in financial engineering) from Seoul National University, Seoul, in 2010 and 2014, respectively. From 2014 to mid-2017, he was a Data Scientist with the Big Data Laboratory, Visual Display Division, Samsung Electronics Company Ltd., South Korea. Then, he moved to the AI Center of Samsung Research and currently working as a Senior Data Scientist, focusing on sales and marketing analytics based on data mining, time-series, and explainable AI.



JAE WOOK SONG received the B.Sc. degree in industrial engineering from the Georgia Institute of Technology, in 2010, and the Ph.D. degree in industrial engineering from Seoul National University, in 2016. Then, he had been working as a Senior Data Scientist with Samsung Electronics Company Ltd., and an Assistant Professor of data science with Sejong University. In 2019, he joined the Department of Industrial Engineering, Hanyang University, where he is currently an Assistant Professor running the Financial Innovation and Analytics Laboratory. His research interests include inter- and multi-disciplinary approaches for data-driven innovations in financial markets, risk management, investment strategies, portfolio management, and business analytics.

• • •



THE RIDDLE OF VOLATILITY CLUSTERS

Bohumil Stádník

*Faculty of Finance and Accounting, The University of Economics in Prague,
W. Churchill Sq. 4, 130 67 Prague 3, Czech Republic
E-mail: bohumil.stadnik@email.cz*

Received 19 September 2013; accepted 22 January 2014

Abstract. In this financial engineering research we evaluate if observed non-normalities in the market price distributions are caused mainly by a volatility clustering or also by another non-clustering mechanism. Such findings allow us to assess according to which rules the market price is actually developing or even make conclusions about market price directional forecasting chances, based on the realistic financial processes which we assign to the clustering and non-clustering mechanisms.

In the research we suggest certain methodology how to recognize these processes behind the market price development. We apply the method to the European government bonds market and for the comparison also to 1 day periods of S&P 500 Index development, with respect to the different time periods.

Based on the findings we confirm the combination of both the volatility clustering and the non-clustering processes to be active inside 1 day periods and to be responsible for measured non-normalities. We also find significant non-clustering mechanism in 30 and 60 minute periods in case of European government bonds.

Keywords: volatility clustering, departures from normality, bond market, Euro-Bund Futures, S&P500, directional and volatility dependence, feedbacks.

JEL Classification: G1, G10, G17.

Introduction

The main contribution of this financial engineering study is to resolve a general question: “Are the departures from normality caused by a volatility clustering or also by another non-clustering mechanism distributing the market price in a non-normal way?” If we find certain situations when empirically measured departures are not caused by volatility clustering we have to logically conclude that these non-normalities must be caused by some non-clustering processes. According to the empirical observations and also simulations we recommend to assign these potential non-clustering processes to the real existing feedback mechanisms which are based on the directional dependency and which will be also discussed later in the text. Such processes allow us to improve directional forecasting, which we cannot basically conclude in the case of volatility clustering process, because the clustering itself

can be also caused by the pure volatility effects without the directional dependency, and in addition: if such mechanism is also hidden (Stádník 2013a) the whole situation is then applicable to the future profit making and such findings do have a certain practical value. A solution of this question is also important for a general assessment of the market functionality, depending on the mechanisms responsible for the departures. In this research we try to answer the above formulated question for Euro Bund Futures, which directly affect the European government bond market, and we study the price distribution inside 1, 5, 10, 30, 60 minute periods and also within 1 day time series as we expect specific economic processes which are dominating inside the short time periods, processes which are significant for the longer periods and we also observe processes which are common for all the periods. In addition and also for the comparison we try to answer the same question for S&P500 index day price development.

1. Literature review

The volatility clustering is nowadays considered to be the main cause of the leptokurtic departures and the clusters itself are usually considered to be caused by a pure volatility dependency effects. The pure volatility dependence process is denoted as the process in which price direction is always independent of the past but the volatility is dependent. Such a process does not allow directional forecasting and it is closely connected to the size of price steps in the given time period. There are more theories of basic research in the area of volatility dependence. For example the Gaussian mixture distribution. Gaussian mixture has an acceptable interpretation: financial market occurs in two regimes with high and low volatility. We can model many non-normal distributions which characteristic depend on the probability of both regimes and their parameters. If the regimes have a Markov law of motion, the mixture is then a hidden Markov model (Baum, Petrie 1966), which is also known as the Markov regime switching model. We find many extensions of the Markov switching model (Krolzig 1997; etc.). Other famous works in this area were done by Bollerslev (1986) GARCH process; Engle (1995) ARCH process. Some new research in the area of volatility dependence was done by Witzany (2013) or Roch (2011). While GARCH, ARCH and other volatility models propose statistical constructions based on volatility clustering in financial time series, they do not provide any financial explanation. The financial explanation of volatility clustering is quite difficult. The simplest possible financial clustering mechanism is just the switching of the market between periods of high and low activity or clustering of economic news. The other idea was the competition between more trading strategies but the simulation does not allow to confirm that the mechanism is responsible for volatility clustering (Cont 2005). Some economic works contain examples where switching of economic agents between two behavioral patterns leads to large volatility. Volatility clustering should also arise from the switching of market participants between fundamentalist and chartist behavior (Lux, Marchesi 2000). Chart traders evaluate their investments using historical development, whereas fundamentalists evaluate their investment opportunity according to the difference between the market price and the fundamental valuation. According to the Lux-Marchesi model the market price development follows the Gaussian random walk until the moment when some chart traders using certain techniques surpass a certain threshold value and at this moment a volatility outbreak occurs. According to Cont 2005, the origin of volatility clustering can also be caused by threshold response of investors to news arrivals. Other new research connected to the volatility clustering were done by Jianga, Lia, Caia (2008) or Tsenga Jie-Jun, Sai-Ping Lia (2011).

Instead of the volatility dependency effects we are able to explain non-normalities using pure directional dependency effects. This way considers the price development direction

to be dependent on the past and allows certain forecasting chances in comparison to the volatility dependency. There are many case studies based on the directional dependency but comprehensive modeling of the departures from normality in this way is not so frequent. For example the commonly used technical trading rules are based on a market price direction forecasting according to the past. We can consider Technical Analysis to be the prediction tool, but its benefit is still under discussion. We meet many other interesting detailed works or case studies in the area like Henriksson, Merton (1981); Anatolyev, Gerko (2005); Diviš, Teplý (2005); Primbs, Rathinam (2009); Gontis, Ruseckas, Kononovičius (2010); Lux (2011); Džikevičius, Vetrov (2012); Černohorská, Teplý, Vrábel (2012); Janda, Svarovska (2010). Price direction development dependence also takes place in the basic feedback process according to the behavioral finance concept where upward trend is more likely to be followed by another upward movement (Schiller 2003) or in other research as for example momentum studies (Pesaran, Timmermann 1995; Stankevičienė, Gembickaja 2012), short term trend trading strategy in futures market based on chart pattern recognition (Masteika, Rutkauskas 2012) or in the development of the conception of sustainable return investment decisions strategy in capital and money markets (Rutkauskas *et al.* 2008). We have to mention also the work of Larrain 1991, which states that long term memory exists inside the financial market, other similar works of Hsieh (1991), Peters (1989, 1991, and 1994) which focus mainly on measurement of probability diversions from normality.

It is important for our research that the directional dependency way is able to explain the departures without the clustering mechanisms. For example feedbacks system according to the Dynamic Financial Market Model (Stádník 2011) is able to cause sharpness and fat tails in the distribution. Feedbacks increase the value of probability of next price step up or down direction (from 50/50 for the pure symmetrical random walk to for example 51/49) depending on the previous development. The idea of feedback processes is based on the empirical observations that traders, investors and other market participants not only watch present or historical data but according to them they are also placing buy or sell orders and thus influence future development. Feedback which keeps the movement in a certain direction is described in the model as a trend stabilizer feedback. For example traders participating in “momentum trading” try to find instruments that are moving significantly in one direction and in order to realize financial profit on the movement they basically prolong short-term trends. The other important feedback is a price inertia feedback which is pushing the market price back to a certain level and which is resulting from “level trading” where traders believe the price will return to the level which was set after the last economic news of high importance for example.

A special case is volatility clustering which could be well explained using the directional dependency effects like the spring oscillation mechanism (Stádník 2013b) when feedbacks may cooperate and under certain conditions cause volatility clusters as the final result. This is the case when we observe volatility clusters which are not caused by volatility dependence but by directional dependence behind.

2. Methodology

To make the decision between the clustering or non-clustering mechanism responsible for the departures from normality in the price distributions we have to, first of all, assess the impact of both the mechanisms on the character of the price distribution and its departures. The general clustering mechanism causes significant autocorrelation in volatility data series and possibly the departures from normality in the distribution but we have to mention at this point also an artificial case of observing volatility clusters with the resulting Gaussian distribution as it is simulated in the Figure 14 in the appendix. Typical non-clustering mechanisms like the price inertia feedback distribute the price to the initial (level) value and contribute to the sharpness in the distribution. On the other hand the trend stabilizer feedback contributes to the fat tails. In such cases the resulting price distribution is non-normal but the leptokurtic one and the volatility series is without the volatility clusters. To support our ideas about this impact of the feedbacks on the price distribution we have made the simulation (Fig. 15, appendix). In this simulation we simulate the price inertia and the trend stabilizer according to the Dynamic Financial Market Model. The simulation is without any volatility clustering. We can see in the figure that the volatility autocorrelation (0.0236) is insignificant but the value of acuteness (1.665) is significantly high. For the assessment of the price inertia action we have defined *acuteness* (Eq.1) as the ratio of histogram maximum value in the measured distribution over the maximum value of an adequate normal distribution:

$$acuteness = \frac{Max_{measured}}{Max_{normal}} \cdot \quad (1)$$

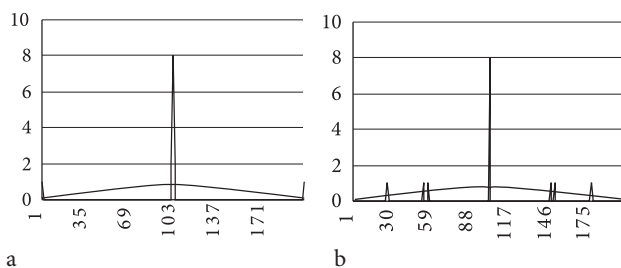


Fig. 1. Distributions (a) and (b) are with the same acuteness but a different kurtosis: 5.285 and 0.096 (source: own research)

The value of acuteness for normal distribution is 1. The value of kurtosis is not a useful quantitative pointer of the sharpness especially in this case when the price inertia is active separately. The case of the same sharpness and the different values of kurtosis are demonstrated in the Figures 1a and 1b.

Based on the previous we can logically conclude into the main methodology steps:

If there is no significant autocorrelation in the volatility data series and the price distribution exhibits certain acuteness then the departures are not caused by the volatility clusters but by some non-clustering mechanism which could for example be the price inertia feedback action.

If there is significant volatility autocorrelation and certain acuteness then the departures in the price distribution may be caused by a clustering mechanism in cooperation with a non-clustering mechanism. In such a case we have to decide if the departures are caused only by the clusters or also by the coexistence of both effects. To answer such a question we suggest the filtering of volatility clusters thus separating from data series the continuous parts without the clusters. We continue filtering until the autocorrelation of volatility time series is insignificant but we also cannot destruct the series (continuous parts without clusters must be left). Autocorrelation is measured on the absolute values of volatility series. After the filtering we are allowed to study the price distribution of the data series without the clusters and also inside the clusters separately. If the price distribution without the clusters is a non-normal one it means the non-clustering mechanism causing the departures is present. In addition to that if the value of kurtosis or acuteness of such distribution is lower than of the original distribution with the clusters we can conclude on coexistence of both the clustering and non-clustering mechanisms in the original distribution. In case that it is not possible to eliminate volatility clusters without the destruction of data series (we cannot separate continuous time periods without clusters) we cannot be sure if the departures are caused only by the volatility clustering or also by non-clustering effects. If we for example eliminate volatility clusters from one day volatility data series of certain investment instrument (stock, bond, etc.) which performs one day non-normal price distribution and if filtered price series is also non-normally distributed, we conclude that there must be present some non-clustering mechanism like for example price inertia feedback (Stádník 2012) distributing the price towards to the initial value and causing departures in the distribution. Such feedback is the typical directional dependency process which allows better directional forecasting (Stádník 2013a).

We apply the suggested methodology to European bond futures which directly affects prices of appropriate government bonds (mainly 10 years maturities), traded on EUREX exchange, contract name: Euro-Bund Futures and also on S&P500 Index. All the data time series in the research have

been downloaded from Reuters system and for the elimination of clusters we have used special software which detects continuous periods of lower and higher volatility.

3. Findings in Euro-Bund Futures 1 min, 5 min and 10 min price distributions

In case of 1, 5 and 10 minute price volatility data series (Figs 2a, 3, 4a) we were not successful in eliminating volatility clusters (to decrease the level of autocorrelation without the destruction of the appropriate time series).

This is why in the case of 1, 5 and 10 minute price development we cannot be sure about reliable conclusions. The departures in the price distributions (Figs 2b and 4b) are probably caused by certain clustering mechanisms (autocorrelations: 0.201, 0.22, 0.183) but we are not able to make any conclusion on non-clustering mechanism based on the measurement of volatility data series in this case. The solution could be reached by the direct market observation and according to the market participants' behavior.

4. Findings in Euro-Bund Futures 30 min, 60 min price distributions

In the 30 and 60 minute price volatility series (Figs 5a, 6a) the volatility has low autocorrelation (0.108 and 0.0966) but the price distributions (Figs 5b, 6b) perform the high acuteness (1.760, 1.765) and also kurtosis.

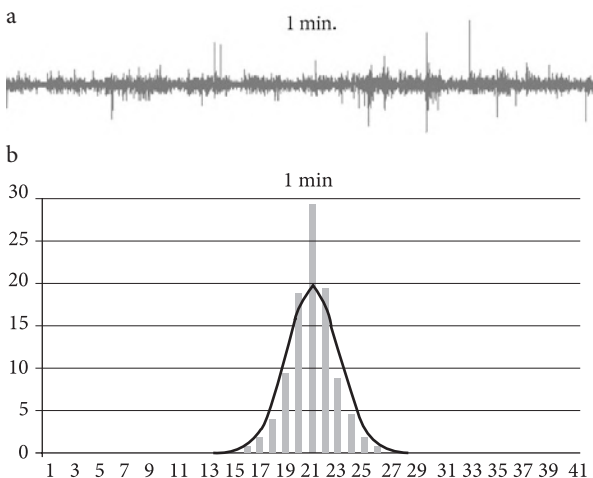


Fig. 2. 1 minute volatility series (a) and price distribution (b) of Euro-Bund Futures, volatility autocor.: 0.201, average value: 0.0000578, skewness: -0.156, kurtosis: 29.369, acuteness: 1.479, data: 2013 (source: own research)

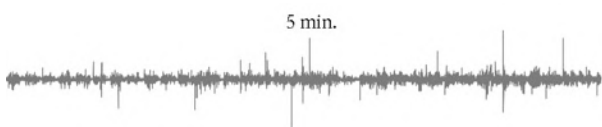


Fig. 3. 5 minutes volatility, volatility autocor.: 0,229, data: 2013 (source: own research)

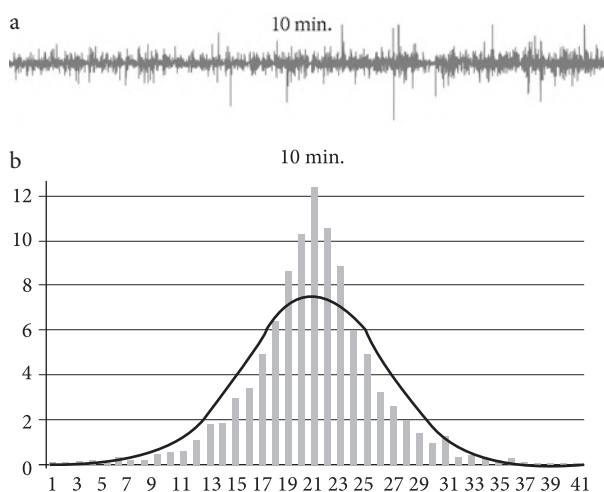


Fig. 4. 10 minutes volatility series (a) and price distribution (b) of Euro-Bund Futures, volatility autocor.: 0,18373, average value: -0.000615, skewness: -0.0852, kurtosis: 9.049, acuteness: 1.631, data: 2013 (source: own research)

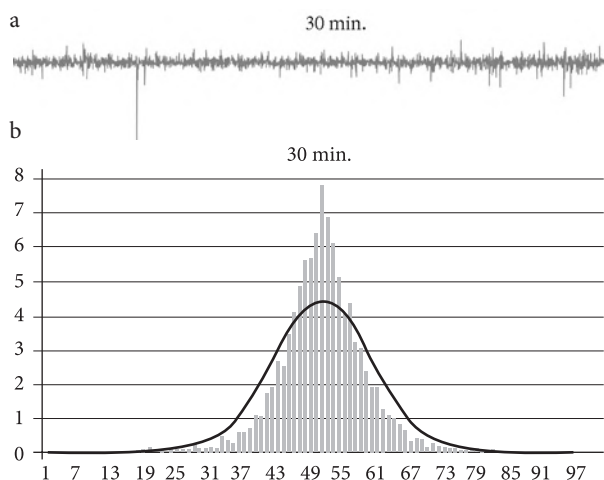


Fig. 5. 30 minutes volatility series (a) and price distribution (b) of Euro-Bund Futures, volatility autocor.: 0.10835, average value: -0.000904, skewness: -4.237, kurtosis: 84.038, acuteness: 1.760, data: 2013 (source: own research)

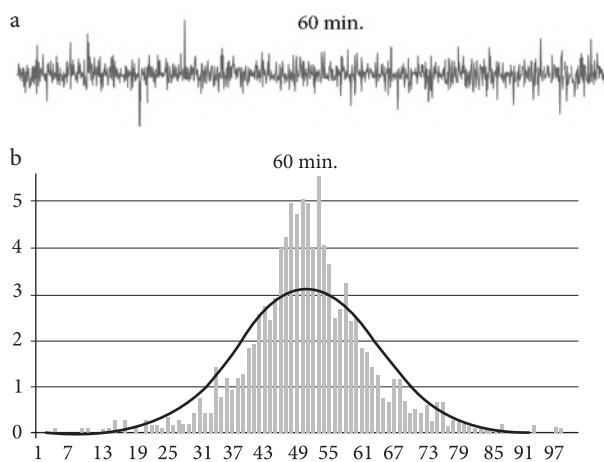


Fig. 6. 60 minutes volatility series (a) and price distribution (b) of Euro-Bund Futures, volatility autocor.: 0.0966, average value: 0.000264, skewness: -2.136, kurtosis: 34.878, acuteness: 1.765, data: 2013 (source: own research)

In this case we can conclude on the directional dependency effects mainly responsible for the departures in the price distributions.

5. Findings in Euro-Bund Futures 1 day price distribution

From 1 day price volatility series (Fig. 7a) we successfully eliminate the volatility clusters (Fig. 8a) thus decreasing

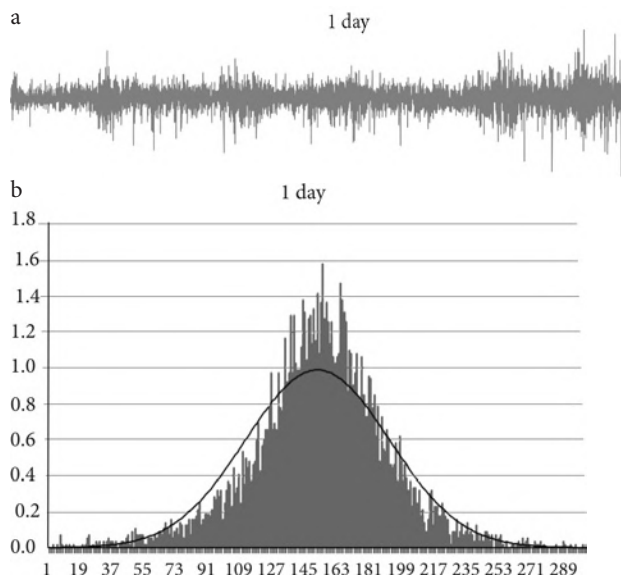


Fig. 7. 1 day volatility series (a) and price distribution (b) of Euro-Bund Futures, volatility autocor. 0.138, average value: 0.0107, skewness: -0.294 , kurtosis: 3.265, acuteness: 1.593, data: 1990–2013 (source: own research)

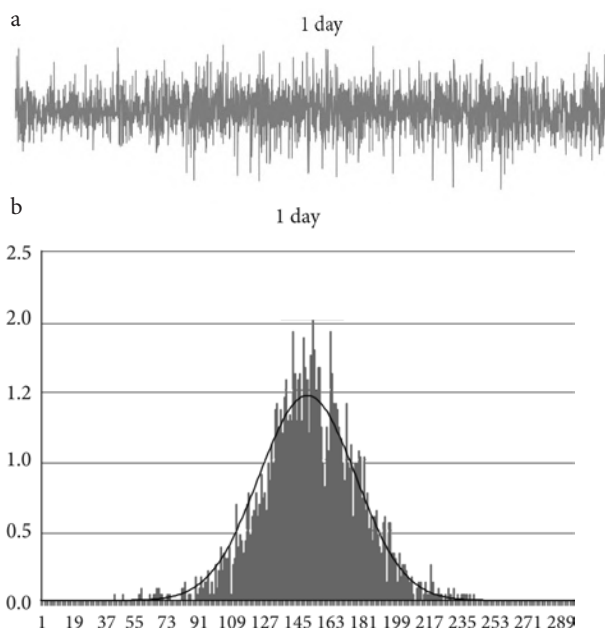


Fig. 8. 1 day volatility series (a) and price distribution (b) of Euro-Bund Futures without VOLATILITY CLUSTERS, volatility autocor.: -0.00502 , average value: 0.02, skewness: -0.06136 , kurtosis: 0.618, acuteness: 1.369, data: 1990–2013 (source: own research)

the volatility autocorrelation to an insignificant level (from 0.138 to -0.00502). There is volatility data series of an independent random walk (autocorrelation 0.0120) in the Figure 13 in the appendix for a comparison. We may conclude that the price distribution which does not involve the clusters (Fig. 8b) also has significant acuteness and therefore there is present a non-clustering mechanism responsible for measured non-normalities in the price distributions.

Also inside the volatility clusters (Fig. 9a) where the volatility autocorrelation is insignificant (0.0185) but the price distribution (Fig. 9b) has significant acuteness we confirm non-clustering mechanisms. As the value of kurtosis of the original distribution (Fig. 7b) is higher than in the cases of the price distributions without the clusters and inside the clusters we conclude on coexistence of both the clustering and the non-clustering mechanisms responsible for the departures in the original price distribution.

6. Findings in S&P500 1 day return distribution

For the comparison we try to eliminate clusters from S&P500 return volatility series (Fig. 10a). In this case we have been successful in eliminating the volatility clusters (Fig. 11a) and thus reduce volatility autocorrelation (from 0.22 to 0.0248). Based on that we can measure that the price distribution which does not involve the clusters (Fig. 11b) has significant acuteness (1.795) and therefore there is also present a non-clustering mechanism which causes the departures from normality.

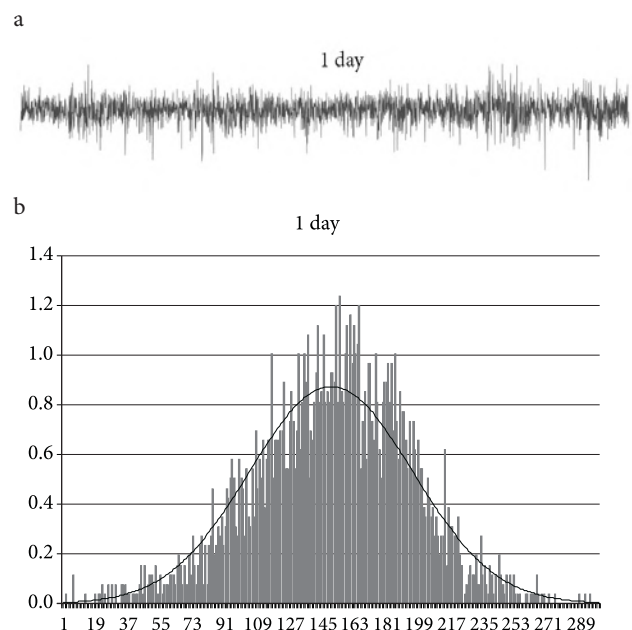


Fig. 9. 1 day volatility series (a) and price distribution (b) of Euro-Bund Futures inside VOLATILITY CLUSTERS, volatility autocor.: 0.0185, average value: 0, skewness: -0.383 , kurtosis: 1.4006, acuteness: 1.416, data: 1990–2013 (source: own research)

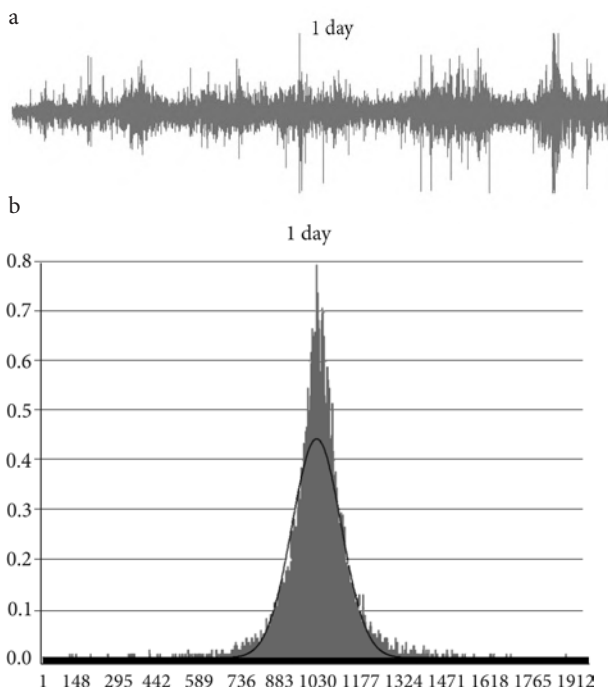


Fig. 10. 1 day volatility series (a) and return distribution (b) of S&P500, volatility autocor.: 0.22, average value: 0.0294, skewness: 0.936, kurtosis: 25.421, acuteness: 1.795, data: 1963–2013 (source: own research)

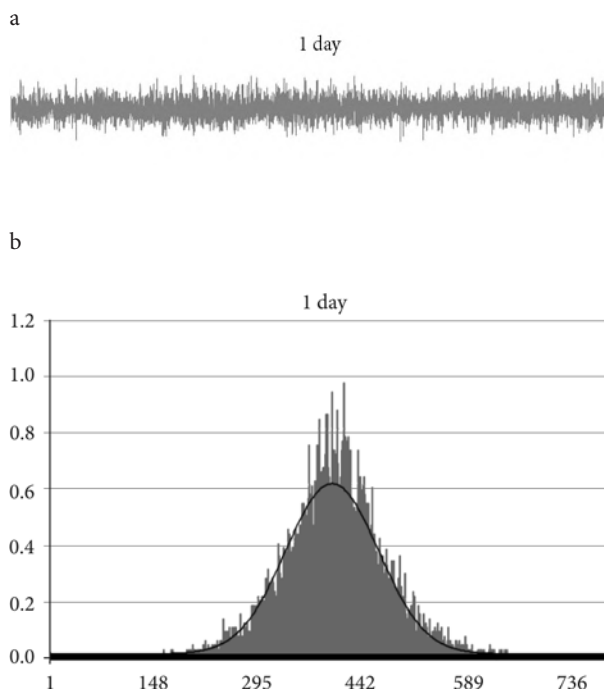


Fig. 11. 1 day volatility series (a) and return distribution of S&P500 (b) without VOLATILITY CLUSTERS, volatility autocor.: 0.0248, average value: 0.0357, skewness: kurtosis 0.0355, acuteness: 1.589, data: 1963–2013 (source: own research)

As the value of kurtosis of the original distribution with the clusters is higher we can also confirm the coexistence of the directional and volatility dependency processes responsible for the departures in the original price distribution as is the case of the Euro-Bund Futures contract. We also confirm a significant non-clustering mechanism causing the departures inside the clusters (Fig. 12a), because the value of autocorrelation is insignificant (0.045) but the acuteness (Fig. 12b) is significantly high (1.858).

7. Main findings summary

For the short time period series of Euro Bund Futures (1, 5, 10 minutes) we were not successful in confirming a non-clustering mechanism according to the suggested methodology and we conclude that the volatility clustering is probably the key factor causing the departures inside these high frequency distributions.

For 30 and 60 minute price distributions we recognize that the volatility autocorrelation is low and due to the significant departures in the price distribution we consider a non-clustering mechanism to be the key reason for the departures from normality.

For the daily distributions we find the coexistence of the clustering and non-clustering mechanisms. We successfully eliminate the volatility clusters from the development and we recognize that the filtered development is also distributed in a non-normal way. Also the price development inside

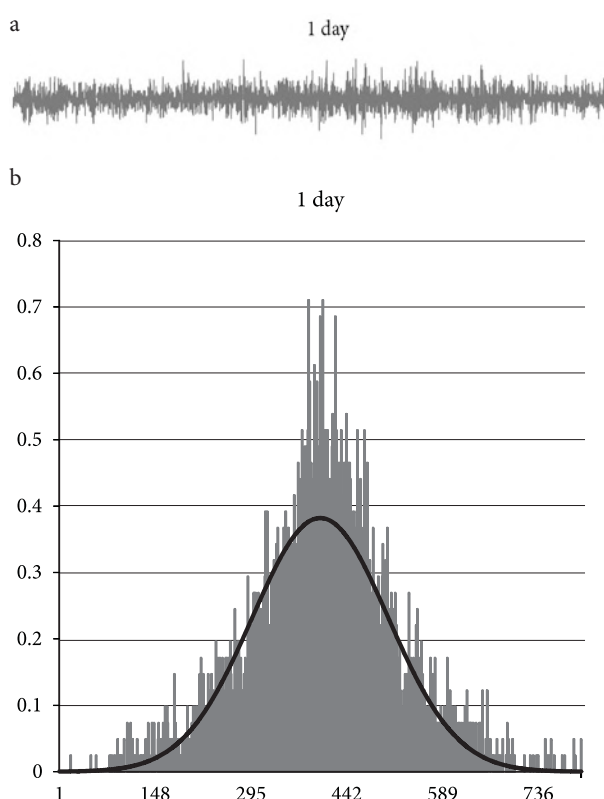


Fig. 12. 1 day volatility series (a) and price distribution (b) of S&P500 inside VOLATILITY CLUSTERS, volatility autocorrelation: 0.045, average value: 0.00629, skewness: 0.127, kurtosis 1.0181, acuteness: 1.858, data: 1963–2013 (source: own research)

the clusters is non-normal. The data set in the case of S&P 500 daily development indicates exactly the same result.

Conclusions and the scientific discussion

In this financial research we propose a certain methodology for the recognition between the clustering and non-clustering processes being responsible for the departures from normality in the price distributions. The methodology is applicable to the worldwide financial investment instruments. From the volatility time series we basically suggest the filtering of volatility clusters and then study the price distributions without the clusters and also inside the clusters separately to make the final conclusions on the existence of certain non-clustering mechanisms distributing the price in a non-normal way. We also define certain quantitative pointer (acuteness) as the measure of expected non-clustering mechanism causing the departures which is the price inertia feedback resulting from the mentioned level trading technique.

In the study we find quite different results with respect to the different time periods. These distinctions could be connected to the various style of trading techniques dominating within certain time periods. We can state that the findings generally support the assumption that the volatility clustering is not the main or the only reason for the departures from normality in the price distributions, but there is also some non-clustering mechanism cooperating, which also causes the departures. From the financial point of view we recommend the mentioned price inertia feedback to be assigned to this non-clustering process. The existence of this feedback is also supported by the direct empirical observations, by the statistical research (Stádník 2012) and by the simulation according to the Figure 15 in the appendix (discussed in the “Methodology” chapter). Such feedback is the typical directional dependency process which is connected to the better directional forecasting (Stádník 2013a) but its practical value is still under the discussion.

In addition we also suspect this feedback to be the reason for the measured non-normalities inside the separated volatility clusters while the clustering itself could be caused by for example the clustering of economic news or trading activities.

Acknowledgements

The research has been supported by the institutional grant VŠE IP 100040.

References

Anatolyev, S.; Gerko, A. 2005. A trading approach to testing for predictability, *Journal of Business and Economic Statistics* 23: 455–461. <http://dx.doi.org/10.1198/073500104000000640>

- Baum, L. E.; Petrie, T. 1966. Statistical inference for probabilistic functions of Finite State Markov Chains, *The Annals of Mathematical Statistics* 37(6): 1554–1563. <http://dx.doi.org/10.1214/aoms/1177699147>
- Bollerslev, T. 1986. Generalized autoregressive conditional heteroskedasticity, *Journal of Econometrics* 31: 307–327. [http://dx.doi.org/10.1016/0304-4076\(86\)90063-1](http://dx.doi.org/10.1016/0304-4076(86)90063-1)
- Černohorská, L.; Teplý, P.; Vrábek, M. 2012. The VT Index as an indicator of market liquidity risk in Slovakia, *Journal of Economics* 60(3): 223–238.
- Cont, R. 2005. Volatility clustering in financial markets: empirical facts and agent-based models, in A. Kirman, G. Teyssiere (Eds.). *Long memory in economics*, Springer. ISBN 978-3-540-22694-9.
- Dzikevičius, A.; Vetrov, J. 2012. Stock market analysis through business cycle approach, *Business: Theory and Practice* 13(1): 36–42.
- Diviš, K.; Teplý, P. 2005. Information efficiency of Central Europe stock exchanges, *Czech Journal of Finance* 10: 471–482.
- Engle, R. F. 1995. *ARCH: selected readings*. Oxford, UK: Oxford University Press.
- Gontis, V.; Ruseckas, J.; Kononovičius, A. 2010. A long-range memory stochastic model of the return in financial markets, *Physica A: Statistical Mechanics and its Applications* 389(1): 100–106.
- Henriksson, R. D.; Merton R. C. 1981. On the market timing and investment performance of managed portfolios II – statistical procedures for evaluating forecasting skills, *Journal of Business* 54(4): 513–533. <http://dx.doi.org/10.1086/296144>
- Hsieh, D. A. 1991. Chaos and nonlinear dynamics: application to financial markets, *Journal of Finance* 46: 1839–1877. <http://dx.doi.org/10.1111/j.1540-6261.1991.tb04646.x>
- Janda, K.; Svarovska, B. 2010. Investing into microfinance, *Journal of Business Economics and Management* 3(11): 483–510. <http://dx.doi.org/10.3846/jbem.2010.24>
- Jianga, J.; Lia, W.; Caia, X. 2008. Cluster behavior of a simple model in financial markets, *Physica A: Statistical Mechanics and its Applications* 387(2–3): 528–536.
- Krolzig, H. M. 1997. International business cycles: regime shifts in the stochastic process of economic growth, in *Applied Economics Discussion Paper 194*. University of Oxford.
- Larrain, M. 1991. Testing Chaos and Nonlinearities in T-bills rates, *Financial Analysts Journal* 47(5): 51–62. <http://dx.doi.org/10.2469/faj.v47.n5.51>
- Lux, T.; Marchesi, M. 2000. Volatility clustering in financial markets: a micro simulation of Interacting agents, *International Journal of Theoretical and Applied Finance* 3: 675–702. <http://dx.doi.org/10.1142/S0219024900000826>
- Lux, T. 2011. Sentiment dynamics and stock returns: the case of the German stock market, *Empirical Economics* 41(3): 663–679. <http://dx.doi.org/10.1007/s00181-010-0397-0>
- Masteika, S.; Rutkauskas, A. V. 2012. Research on futures trend trading strategy based on short term chart pattern, *Journal of Business Economics and Management* 13(5): 915–930. <http://dx.doi.org/10.3846/16111699.2012.705252>
- Pesaran, M. H.; Timmermann, A. 1995. Predictability of stock returns: robustness and economic significance, *Journal of Finance* 50: 1201–1228. <http://dx.doi.org/10.1111/j.1540-6261.1995.tb04055.x>

- Peters, E. 1989. Fractal structure in the capital markets, *Financial Analysts Journal* 45(4): 32–37.
<http://dx.doi.org/10.2469/faj.v45.n4.32>
- Peters, E. 1991. *Chaos and order in the capital markets: a new view of cycles, prices, and market volatility*. New York: John Wiley & Sons.
- Peters, E. 1994. *Fractal market analysis: applying chaos theory to investment and economics*. New York: John Wiley & Sons.
- Primbs, J. A.; Rathinam, M. 2009. Trader behavior and its effect on asset price dynamics, *Applied Mathematical Finance* 16(2): 151–181. <http://dx.doi.org/10.1080/13504860802583444>
- Rutkauskas, A. V.; Miečinskienė A.; Stasytytė, V. 2008. Investment decisions modelling along sustainable development concept on financial markets, *Technological and Economic Development of Economy* 14(3): 417–427.
<http://dx.doi.org/10.3846/1392-8619.2008.14.417-427>
- Roch, A. F. 2011. Liquidity risk, price impacts and the replication problem, *Finance and Stochastics* 15(3): 399–419.
<http://dx.doi.org/10.1007/s00780-011-0156-x>
- Schiller, R. J. 2003. From efficient market theory to behavioral finance, *Journal of Economic Perspectives* 17(1): 83–104.
<http://dx.doi.org/10.1257/089533003321164967>
- Stádník, B. 2011. Explanation of S&P500 index distribution deviation from a gaussian curve (dynamic financial market model), *Journal of Accounting and Finance* 11(2): 69–77. ISSN: 2158-3625.
- Stádník, B. 2012. Testing of market price direction dependence on us stock market, *Business, Management and Education* 10(2): 205–219.
- Stádník, B. 2013a. Market price forecasting and profitability – how to tame random walk?, *Business: Theory and Practice* 14(2): 166–176.
- Stádník, B. 2013b. Spring oscillations within financial markets, *Procedia – Social and Behavioral Sciences* 110: 1176–1184. Available from Internet: <http://www.sciencedirect.com/science/article/pii/S1877042813056048>
- Stankevičienė, J.; Gembickaja, N. 2012. Market behavior: case studies of NASDAQ OMX Baltic, *Business, Management and Education* 10(1): 110–127. ISSN 2029-7491 print / ISSN 2029-6169 online.
- Tsenga J.-J.; Li, S. P. 2011. Asset returns and volatility clustering in financial time series, *Physica A: Statistical Mechanics and its Applications* 390(7): 1300–1314.
- Witzany, J. 2013. Estimating correlated jumps and stochastic volatilities, *Prague Economic Papers* 2: 251–283.

APPENDIX

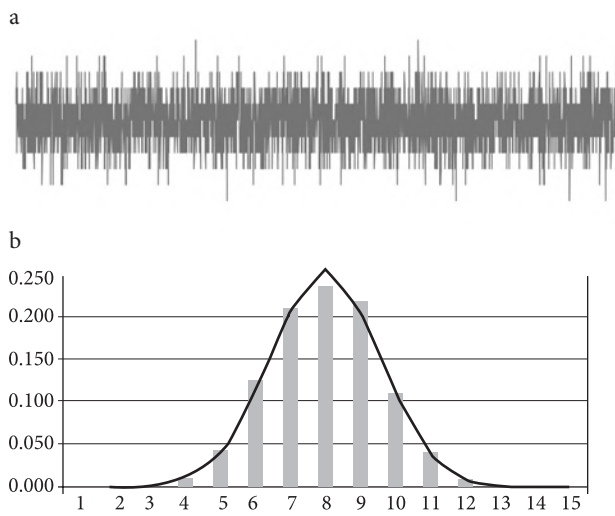


Fig. 13. Example of pure symmetric random walk volatility series (a), autocorrelation: 0.012 and price distribution (b) with average value: -0.0356 , skewness: -0.0092 , kurtosis: -0.252 (source: own research)

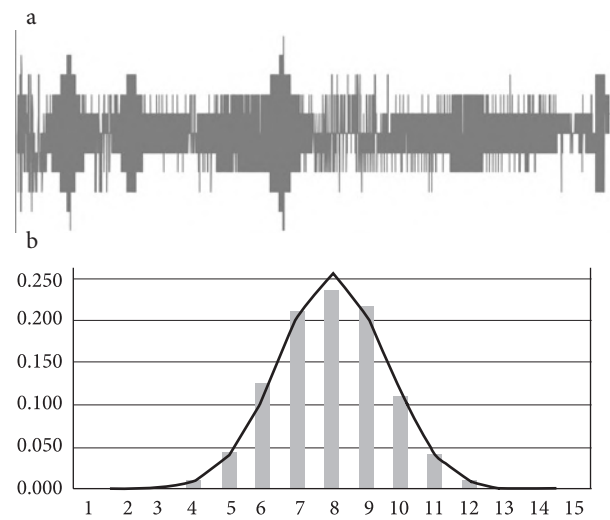


Fig. 14. Artificial example of volatility clustering with Gaussian distribution, volatility autocorrelation: -0.563 , skewness: -0.0092 , kurtosis: -0.252 (source: own research)

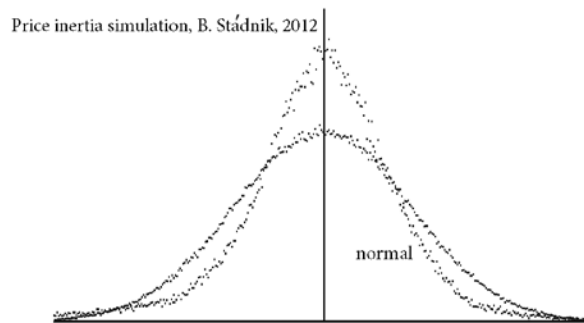


Fig. 15. 1 day returns distribution of S&P500 (b) SIMULATIONS USING FEEDBACKS (WITHOUT VOLATILITY CLUSTERING), volatility autocor.: 0.0236 (a), skewness: -1.057 , kurtosis: 5.259, acuteness: 1.665 (source: own research)

Bohumil STÁDNÍK, Ph.D. Senior lecturer at University of Economics in Prague. Research interests: financial engineering, modeling of financial dynamical processes, market price development and forecasting, theory and practice of fixed income securities.



Early online detection of high volatility clusters using Particle Filters



Karel Mundnich^a, Marcos E. Orchard^{a,*}

Electrical Engineering Department, Universidad de Chile, Av. Tupper 2007, Santiago 8370451, Chile

ARTICLE INFO

Keywords:

Bayesian inference
Risk-sensitive particle filters
Stochastic volatility estimation
Event detection

ABSTRACT

This work presents a novel online early detector of high-volatility clusters based on uGARCH models (a variation of the GARCH model), risk-sensitive particle-filtering-based estimators, and hypothesis testing procedures. The proposed detector utilizes Risk-Sensitive Particle Filters (RSPF) to generate an estimate of the volatility probability density function (PDF) that offers better resolution in the areas of the state-space that are associated with the incipient appearance of high-volatility clusters. This is achieved using the Generalized Pareto Distribution for the generation of particles. Risk-sensitive estimates are used by a detector that evaluates changes between prior and posterior probability densities via asymmetric hypothesis tests, allowing early detection of sudden volatility increments (typically associated with early stages of high-volatility clusters). Performance of the proposed approach is compared to other implementations based on the classic Particle Filter, in terms of its capability to track regions of the state-space associated to a greater financial risk. The proposed volatility cluster detection scheme is tested and validated using both simulated and actual IBM's daily stock market data.

© 2016 Elsevier Ltd. All rights reserved.

1. Introduction

Volatility of returns is a well-studied variable in Finance, mainly because its relevance in pricing and risk management. Since the work of Mandelbrot in the 1960's, it has been widely accepted that volatility presents itself in temporal clusters, where large price variations are followed by large variations (Cont, 2005; Mandelbrot, 1963). Multiple researchers have tried to model the complex behavior of volatility, being the GARCH model (Bollerslev, 1986) the first to capture these temporal cluster properties. The wide recognition for the GARCH models has given rise to a whole family of structures, in which stochastic variations have been lately introduced.

On the one hand, from an engineering perspective, early online detection of high-volatility clusters in a stochastic environment poses an interesting problem, since detection algorithms must be designed to monitor a latent (non-observable) state; simultaneously tracking disturbances introduced by other non-measurable variables that are always present in complex systems (such as stock markets). In fact, from the standpoint of state-space modeling for financial time series, volatility is a non-observable state, while continuously compounded returns can be associated with daily measurements. Given that inference on financial volatility

is necessary to detect high risk events, the challenge is then to propose detection frameworks based on accurate and precise estimates of this non-observable state.

On the other hand, in Finance, the words “early online detection” have reached unsuspected relevance in a world where is now possible to use information from high-volatility cluster detectors (which could have been originally focused on very specific and critical markets) for the implementation of online predictive strategies at a global-scale. Consider, for example, the implementation of intelligent expert systems that could recommend optimal corrective actions for Latin American markets based on online anomaly detectors analyzing Asian markets during the early morning. Indeed, the development of tools for online early detection of high-volatility clusters (such as the one proposed in this article) generates appropriate conditions for the implementation of novel online schemes for optimal decision-making in Finance; a task where the whole community working on expert and intelligent systems may contribute in the near future.

These fundamental questions have motivated in recent years substantial research with focus in the detection of structural breaks (or model parameter changes) in financial variables, with the purpose of understanding market shocks or anomalies (Chan & Koop, 2014; Chen, Gerlach, & Liu, 2011; He & Maheu, 2010; Rapach & Strauss, 2008; Ross, 2013). Given the complexities involved in modeling volatility, several approaches have been proposed, including new models such as the structural break GARCH (SB-GARCH). For these models that include stochastic volatility and

* Corresponding author. Tel.: +56 229784215; fax: +56 226720162.

E-mail addresses: kmundnic@ing.uchile.cl (K. Mundnich), morchard@ing.uchile.cl (M.E. Orchard).

breaks, the most common approach for the estimation of volatility has been sequential Monte Carlo methods (a.k.a. Particle Filters) (Arulampalam, Maskell, Gordon, & Clapp, 2002; Doucet, Godsill, & Andrieu, 2000), because of its good performance, flexibility, and the possibility to estimate model parameters online (Liu and West, 2001, chap. 10). Further efforts have been spent in the study of jumps (or discontinuities) of returns and volatility (Andersen, Tim, & Diebold, 2007; Eraker, Johannes, & Polson, 2003; Laurent, Lecourt, & Palm, 2014; Lee & Mykland, 2008), although these approaches impose restrictions for the quality of data that may be difficult to address. In fact, most of the available tests for detection of jumps include high-frequency, intra-day information of the studied variables or high liquidity of the assets (Laurent et al., 2014), or offline tests.

In this regard, we propose a novel online early detector of high-volatility clusters based on unobserved GARCH models (Tobar, 2010) (uGARCH, a variation of the GARCH model), Risk-Sensitive Particle-Filters (RSPF) estimators (Thrun, Langford, & Verma, 2002), and hypothesis testing procedures. The proposed detector utilizes risk-sensitive particle filters to generate an estimate of the volatility probability density function (PDF) that offers better resolution in the areas of the state-space that are associated with the incipient appearance of high-volatility clusters. Risk-sensitive estimates are used by a detector that evaluates changes between prior and posterior probability densities via asymmetric hypothesis tests, allowing early detection of sudden volatility increments (typically associated with early stages of high-volatility clusters). This algorithm is tested in simulated data (where volatility is known), as well as IBM's stock market data, where volatility has to be estimated (since ground truth cannot be measured). To the best of our knowledge, this is the first attempt in financial econometrics to perform online detection of events by contrasting the information that is present in priors and posterior probability densities estimates in Bayesian estimation frameworks.

The main contributions of this article are:

- Implementation and assessment of a novel method for the generation of volatility estimators, based on RSPF, that provides better resolution in the areas of the state-space associated with the appearance of high-volatility clusters.
- Implementation and assessment of early detection schemes for high-volatility clusters based on the comparison between prior and posterior particle-filtering-based estimates.
- A throughout performance comparison between RSPF and classic sequential Monte Carlo methods in terms of their effectiveness when used in early detection of high-volatility clusters.

The structure of this article is as follows. Section 2 presents a literature review on the use of Bayesian frameworks for Financial volatility estimation. Section 3 presents the proposed method for early detection of high-volatility clusters. Section 4 presents performance measures to be used in the assessment of obtained results, provides a sensitivity analysis for the proposed method using simulated data (where the ground truth value of the unmeasured state is known), and finalizes with a throughout performance analysis for the proposed method based on actual IBM stock data. Section 5 presents a few interesting general remarks, while Section 6 shows the main conclusions related to this research.

2. A Bayesian framework for volatility estimation

Monte Carlo (MC) and Markov Chain Monte Carlo (MCMC) methods have been widely used to approximate integrals and probability density functions (Tobar, 2010). Nevertheless, their use in Bayesian inference is not direct, since this problem involves a sequence of time-variant probability density functions; while MCMC assumes that the objective density is time-invariant. This prompted

the development of a sequential version of Monte Carlo integration, one that is able to use measurements to improve recursive estimation.

The first section of this section introduces the uGARCH model, a stochastic volatility model based on the well-known GARCH(1,1) model (Bollerslev, 1986). Then, the tracking problem is presented in Section 2.2, providing insight about the problems encountered in a Bayesian filtering framework. Also, Monte Carlo integration and the importance sampling method are presented. This opens the possibility to explore the Particle Filter and the Risk Sensitive Particle Filter, which may be employed in a stochastic volatility estimation framework. Finally, Section 2.3 explains the need for online parameter estimation.

2.1. The uGARCH model

The uGARCH model can be seen as a state-space structure that allows the implementation of a Bayesian framework for the purpose of volatility estimation.

The uGARCH model (Tobar, 2010) assumes that the dynamics of volatility are not driven by the observed process $u_k = r_k - \mu_{k|k-1}$. Instead, they are driven by a non-observable process u'_k which has the same distribution as u_k . The uGARCH model is defined as:

$$\sigma_k^2 = \omega + \alpha \sigma_{k-1}^2 \eta_k^2 + \beta \sigma_{k-1}^2, \quad (1)$$

$$r_k = \mu + \sigma_k \epsilon_k, \quad (2)$$

where r_k is a process of returns, σ_k is the stochastic volatility, $\mu \in \mathbb{R}^+$, $\omega \in \mathbb{R}^+$, and $\alpha, \beta > 0$ are parameters, with $\alpha + \beta < 1$. Furthermore, $\epsilon_k \sim \mathcal{N}(0, 1)$ and $\eta_k \sim \mathcal{N}(0, \sigma_\eta^2)$ are *i.i.d.*¹ processes for every time step k .

It is necessary to note from Eqs. (1) and (2) that the subscripts are not written conditionally: at time step k , σ_k^2 is not known without uncertainty, given Σ_{k-1} .

To completely define the model, it is necessary to present the state transition distribution $p(\sigma_k^2 | \sigma_{k-1}^2)$ and the likelihood $p(r_k | \sigma_k^2)$:

$$p(\sigma_k^2 | \sigma_{k-1}^2) = \frac{1}{\sqrt{2\pi \sigma_\eta^2 \alpha \sigma_{k-1}^2 (\sigma_k^2 - \omega + \beta \sigma_{k-1}^2)}} \cdot \exp \left[-\frac{\sigma_k^2 - \omega + \beta \sigma_{k-1}^2}{2\sigma_\eta^2 \alpha \sigma_{k-1}^2} \right], \quad \sigma_k^2 \geq \omega + \beta \sigma_{k-1}^2. \quad (3)$$

$$p(r_k | \sigma_k^2) = \frac{1}{\sqrt{2\pi \sigma_k^2}} \exp \left(-\frac{(r_k - \mu)^2}{2\sigma_k^2} \right). \quad (4)$$

For the complete derivation of Eq. (4), please refer to Mundnich (2013). The calculation and presentation of Eq. (4) makes the use of a generic Particle Filtering approach for volatility estimation in this model possible.

2.2. The Particle Filter

State-space models consider a transition equation that describes the prior distribution of a hidden Markov process $\{x_k; k \in \mathbb{N}\}$, called the state process, and an observation equation describing the likelihood of the observation $\{z_k; k \in \mathbb{N}\}$ (Doucet et al., 2000):

$$x_k = f(x_{k-1}, v_{k-1}), \quad (5)$$

$$z_k = h(x_k, w_k), \quad (6)$$

where $f(\cdot, \cdot)$ is a state-transition function with corresponding $\{v_{k-1}, k \in \mathbb{N}\}$ *i.i.d.* innovation process, and $h(\cdot, \cdot)$ is the observation

¹ Independent and identically distributed.

function with $\{w_k, k \in \mathbb{N}\}$ its corresponding *i.i.d.* noise process. In particular, the objective of tracking is to recursively estimate x_k from all available measurements $z_{1:k} = \{z_i; i = 1, \dots, k\}$ up to time k .

Within a Bayesian estimation framework, all relevant information about $x_{0:k}$ given the observations $z_{0:k}$ can be obtained from the posterior distribution $p(x_{0:k}|z_{0:k})$. In many applications, nevertheless, it is sufficient to calculate the marginal conditional distribution $p(x_k|z_{0:k})$. In particular, the intention of the Bayesian approach is to recursively construct $p(x_k|z_{1:k})$, using [Arulampalam et al. \(2002\)](#):

$$p(x_k|z_{1:k}) = \frac{p(z_k|x_k)p(x_k|z_{1:k-1})}{p(z_k|z_{1:k-1})}, \quad (7)$$

$$= \frac{p(z_k|x_k) \int p(x_k|x_{k-1})p(x_{k-1}|z_{1:k-1})dx_{k-1}}{\int p(z_k|x_k)p(x_k|z_{1:k-1})dx_k}. \quad (8)$$

Eq. (8) forms the basis for the Bayesian optimal solution in the mean square error sense. In most cases, this expression is only conceptual, and cannot be determined analytically. In a restricted set of cases, the optimal solution may be found ([Kalman, 1960](#)). This is possible only if the noises v_k and w_k are additive and Gaussian and the functions $f(\cdot, \cdot)$ are $h(\cdot, \cdot)$ are linear.

Particle Filters are a class of algorithms developed to solve Eq. (8) through sequential Monte Carlo simulations when the integrals are intractable due to possible nonlinearities in the model involved or noise processes that do not possess standard distributions. Solving these integrals is achieved through the *Importance Sampling* principle. The key idea is to represent the required posterior density function by a set of random samples which serve as support points with associated weights and to compute estimates based on these samples and weights, this is:

$$p(x_k|z_{1:k}) \approx \sum_{i=1}^{N_s} w_k^{(i)} \delta(x_k - x_k^{(i)}), \quad (9)$$

The former approximation may be obtained using an *importance density* $q(x_{0:k}|z_{1:k})$ to generate random samples $x_k^{(i)}$, where the weights $w_k^{(i)}$ are calculated using:

$$w_k^{(i)} \propto \frac{p(x_{0:k}^{(i)}|z_{1:k})}{q(x_{0:k}^{(i)}|z_{1:k})}, \quad (10)$$

$$\propto w_{k-1}^{(i)} \frac{p(z_k|x_k^{(i)})p(x_k^{(i)}|x_{k-1}^{(i)})}{q(x_k^{(i)}|x_{k-1}^{(i)}, z_k)}. \quad (11)$$

This algorithm is generally called *Sampling Importance Sampling* (SIS), and denotes the simplest form to solve Eq. (8).

The position of the particles and consequent performance of the filter is greatly determined by the importance density $q(x_k|x_{k-1}^{(i)}, z_k)$ from which particles are drawn. The structure of the Particle Filter algorithm and importance densities usually employed do not regard the problem of high risk and low-likelihood event tracking. In the case where unlikely events may conduce to great loss or high costs, it is natural extend the Particle Filter algorithm to track these low probability states.

The Risk Sensitive Particle Filter is proposed as an extension of the 'Classic' Particle Filter, where the particles are generated from an importance density that is the product of the combination of the posterior density function and a risk functional.

Risk Sensitive Particle Filters generate samples that are distributed according to [Thrun et al. \(2002\)](#):

$$q(x_k|x_{k-1}^{(i)}, z_k) = \gamma_k r(x_k) p(x_k|z_{1:k}), \quad (12)$$

where

$$\gamma_k = \frac{1}{\int r(x_k) p(x_k|z_{1:k})} \quad (13)$$

is a normalizing constant that ensures that the importance density is indeed a probability density function. Hence, the position of samples are generated according to the likelihood of a certain state event $x_k^{(i)}$ and its risk $r(x_k^{(i)})$.

Considering the former approach, the Classic Particle Filter needs a simple modification. First, the initial set of particles $x_0^{(i)}$ is generated from $\gamma_0 r(x_0) p(x_0)$, and Eq. (11) is updated to

$$w_l^{(i)} = \frac{r(x_k^{(i)}) p(z_k|x_k^{(i)})}{r(x_{k-1}^{(i)})}. \quad (14)$$

In this work, the authors propose an importance density $q(x_k|x_{k-1}^{(i)}, z_k)$, for which they assume that a risk functional $r(x_k^{(i)})$ exists.

2.3. Online parameter estimation with Particle Filters

In the context of state estimation, it is sometimes necessary to handle an online estimation scheme for a model parameter vector. Although parameters α and β have been presented as fixed in the uGARCH model, this is not necessarily adequate, given possible structural breaks in the data. The stock market suffers from variations and regime shifts, and these variations may be considered as parameter changes through time. This is true not only for time series derived from the stock market, but for a diverse range of applications where state tracking is intended.

To understand the problems of parameter estimation outside a Bayesian context, let θ be a vector parameter. The maximum likelihood estimate of the vector parameter θ is obtained by maximizing the log-likelihood function ([Kitagawa & Sato, 2001](#), chap. 9):

$$l(\theta) = \log[L(\theta)] = \sum_{k=1}^K \log[p(z_k|z_{1:k-1}, \theta)], \quad (15)$$

where

$$p(z_k|z_{1:k-1}, \theta) = \int p(z_k|x_k, \theta) p(x_k|z_{1:k-1}, \theta) dx_k \quad (16)$$

needs to be approximated through Monte Carlo.

The maximization of Eq. (15) for the estimation of θ is not always direct, and approximations over Eq. (16) make this method impractical, due to the high computational costs involved if parameter estimation is intended for every time step. Thus, a different perspective is necessary to approach the online parameter estimation problem. This idea is attacked through the artificial evolution of parameters.

The first ideas about introducing random disturbances to particles were proposed by [Gordon, Salmond, and Smith \(1993\)](#), and are currently widely used in financial econometrics. In their work, the authors propose to introduce random disturbances to the positions of particles (called *roughening penalties*) in order to combat degeneracy. This idea has been extended in order to estimate online a vector of fixed model parameters, which is referred to as *artificial evolution* ([Liu & West, 2001](#), chap. 10). Artificial evolution of parameters is a simple and powerful idea, nevertheless, it requires careful handling because of the inherent model information loss given by the consideration of time-varying parameters that are fixed.

Instead of estimating the vector parameter θ through maximum likelihood, the Bayesian framework may be introduced to estimate θ online. This is achieved by augmenting the state vector x_k with unknown parameters θ as:

$$x'_k = \begin{bmatrix} \theta_k \\ x_k \end{bmatrix}, \quad (17)$$

where $\theta_k = \theta$ implies the consideration of an extended model where parameters are time-varying. Then, an independent,

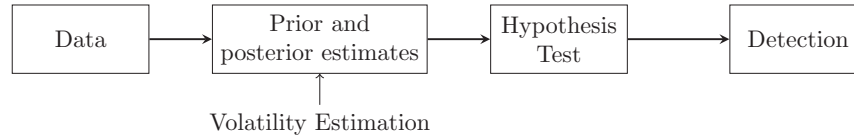


Fig. 1. Detection flow chart. Data is served as an input for the PF-based estimation, which produces prior and posterior estimates that are given as the input for the hypothesis test, which results in the early detection of high volatility clusters.

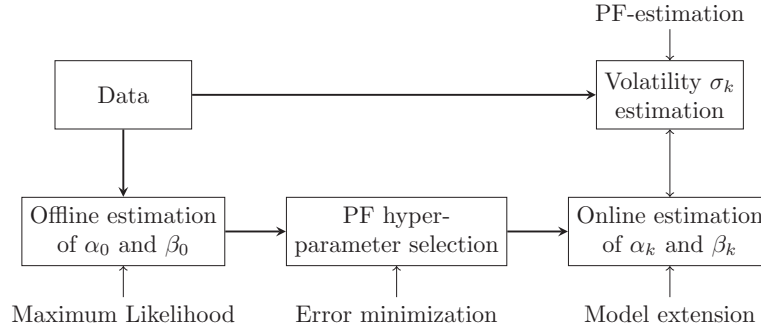


Fig. 2. Estimation flow chart. In an initialization step, PF hyper-parameter selection is performed through error minimization. Then, offline parameter estimation is performed using maximum likelihood. Finally, the PF estimates in parallel the model parameters α_k and β_k , as well as the stochastic volatility σ_k .

zero-mean normal increment is added to the parameter at each time step (Liu & West, 2001, chap. 10):

$$\theta_k = \theta_k + \zeta_k, \tag{18}$$

$$\zeta_k \sim \mathcal{N}(0, W_k), \tag{19}$$

where W_k is a variance matrix and θ_k and ζ_k are conditionally independent given Σ_k . The key motivation is that the artificial evolution of parameters gives new values for each iteration, and thus, weight assignment in Particle Filters considers the likelihood of the state and parameter values.

3. Detection of high volatility clusters using PF-based estimation methods

This chapter describes the implementation details followed to create an online high volatility cluster detection scheme. In the context of Bayesian estimation in state-space models, volatility arises as a non-observable state. Therefore, simulated stock market data is used to correctly implement, analyze and assess the proposed Bayesian filtering framework.

Our approach proposes the use of the GARCH(1,1) volatility model to create a volatility time series – after defining the value of some model parameters – and consequently generate a returns series for the given volatility at every time step. This is useful to measure the effectiveness of estimation frameworks and detection schemes.

The detection scheme presented in this section is founded upon a Bayesian estimation framework, which is based in Particle Filter-based estimation (Fig. 1). Therefore, it is mandatory to comprehend the details of the estimation process in order to understand the construction of the detection scheme. These details include the online hyper-parameter estimation and volatility estimation in the uGARCH model, and the construction of prior and posterior estimates (Arulampalam et al., 2002). To introduce these concepts, Section 3.1 first describes the data used in the development of this work. Then details about offline hyper-parameter estimation are given. This offline estimation is used as the input for online hyper-parameter estimation, which is performed in parallel to the volatility estimation (Fig. 2).

3.1. Data

The assessment of Bayesian estimation frameworks and detection schemes requires data sets where observations and the state are known for every instant in a given period. This allows the evaluation of filtering schemes and consequent comparison of the implemented techniques. Given that the volatility of a returns series is not observable, it is mandatory to generate data sets where the algorithms can be tested and fine-tuned. This section provides details about artificially generated data used during this work, and presents the acquisition and post-processing necessary to apply the proposed algorithms in stock market data.

3.1.1. Simulated data

The simulated data has been generated using a GARCH(1,1) model, where model parameters α and β are chosen in such a way that $\alpha + \beta$ is a value close to 1. In observed financial time series, it is not possible to ensure that the values of the model parameters α and β are fixed for a given time window. For this reason, volatility time series are created using time-dependent parameters over the studied time span. In particular, time series of 500 steps have been generated, with a parameter change in the step 250 (see Table 1). This change resembles a regime shift (or structural break) in the market (Tobar, 2010).

The model used for data generation is:

$$\sigma_{k|k-1}^2 = \omega + \alpha u_{k-1}^2 + \beta \sigma_{k-1|k-2}^2, \tag{20}$$

$$r_k = \mu + u_k, \tag{21}$$

Table 1
GARCH(1,1) model parameters for each data set. The arrow (→) indicates a change in the parameter value at time step 250. Note that parameters μ and ω are constant for each set.

Parameter	GARCH1	GARCH3
μ	9×10^{-4}	9×10^{-4}
ω	10×10^{-6}	10×10^{-6}
α	0.20 → 0.10	0.20 → 0.12
β	0.60 → 0.85	0.60 → 0.80

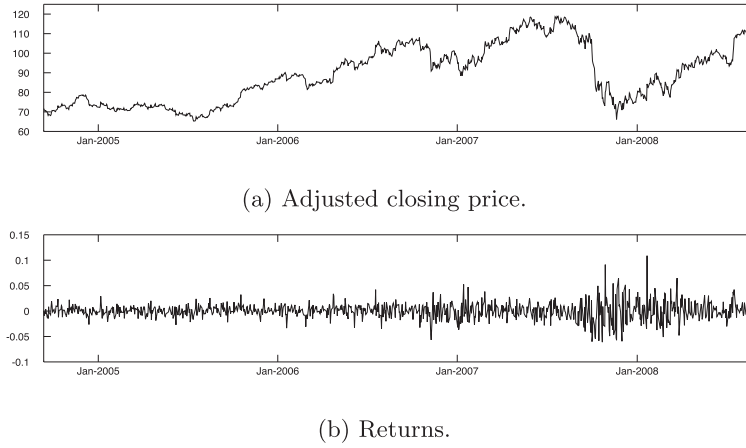


Fig. 3. IBM's adjusted closing stock prices and corresponding daily returns from September 12th, 2005 to September 1st, 2009.

where $\mu_{k|k-1} = \mu$ and ω are considered constant parameters in the studied time span, and $\sigma_0^2 = 0.5 \times 10^{-4}$.

The implemented method for data generation creates data sets in which there are large volatility variations and small volatility variations. These are necessary for the correct assessment of the proposed detection algorithm, as well as providing the necessary environment to assess the robustness of the method against model variations.

3.1.2. Stock market data

A section of IBM daily stock prices is used to apply the developed algorithm for early high volatility cluster detection. The data is extracted from (Yahoo!, 2013), with information between January 1st, 1962 and May 17th, 2013 for a total of 12,933 data points. The data considered for filtering is the *adjusted closing price*, which is commonly used for analysis of historical data. Data in which the proposed algorithm is applied is shown in Fig. 3, which corresponds to 1000 data points between September 12th, 2005 and September 1st, 2009. This data set includes the dramatic market fall occurred in October 2008.

3.2. Implementation issues related to Bayesian filtering

3.2.1. Estimation of model parameters α and β

Model parameters α and β have a high impact on volatility series. These parameters have the power to drive the variation speed of a volatility series and to control the average of the series over time. Hence, it is of great importance to have good estimates of both model parameters to adequately estimate volatility.

In financial time series, it is impossible to know if model parameters α and β are fixed for a given time window in a data set. Therefore, it is necessary to estimate these model parameters online. This work includes two stages of model parameter estimation: estimation through maximum likelihood in a training set and online estimation in test data points.

Estimation of model parameter initial conditions through maximum likelihood. Model parameter estimation has been performed in both simulated data sets and stock market data through maximum likelihood. This is plausible due to the similar structure in both the GARCH(1,1) model and the uGARCH model. In particular, this task has been accomplished using the `garchfit` function available in the Financial Toolbox of MATLAB®.

In the simulated data sets, model parameter estimation is performed using the first 150 steps for each returns time series. For

IBM's stock prices, model parameter estimation is performed over the first 200 time steps of the returns time series. These estimations are used as the initial conditions for online model parameter estimation.

Online model parameter estimation. Section 2.3 describes the reasons for using online model parameter estimation in a Particle Filtering scheme. In this work, parameters α and β of the uGARCH model are allocated into an extended state vector,

$$(x_k)' = \begin{bmatrix} \alpha_k \\ \beta_k \\ \sigma_k^2 \end{bmatrix}, \quad (22)$$

where α_k and β_k are parameters considered to be time-variant, and are called pseudo-particles.

Maximum likelihood estimates α_0 and β_0 are used to compute the initial conditions α_1 and β_1 , which include a random perturbation for every particle (i):

$$\alpha_1^{(i)} = \mathcal{N}(\alpha_0, 0.1 \cdot \alpha_0), \quad (23)$$

$$\beta_1^{(i)} = \mathcal{N}(\beta_0, 0.1 \cdot \beta_0). \quad (24)$$

The initial conditions are used to drive the noise variance of the parameters in the extended state vector (see Eq. (17)):

$$\alpha_k^{(i)} \sim \mathcal{N}(\alpha_{k-1}^{(i)}, \alpha_1^{(i)} \sigma_{\alpha,\beta}^2) \quad (25)$$

$$\beta_k^{(i)} \sim \mathcal{N}(\beta_{k-1}^{(i)}, \beta_1^{(i)} \sigma_{\alpha,\beta}^2) \quad (26)$$

There are two major drawbacks with this method:

- $\mathbb{P}(\alpha_k^{(i)} < 0) > 0$ and $\mathbb{P}(\beta_k^{(i)} < 0) > 0 \quad \forall i, k$,
- $\mathbb{P}(\alpha_k^{(i)} + \beta_k^{(i)} > 1) > 0 \quad \forall i, k$,

both of which are not permitted in the uGARCH model. In particular, they have been addressed in the following way:

- For each $\alpha_k^{(i)} < 0$, let $\alpha_k^{(i)} = 10^{-5}$. Similarly, for each $\beta_k^{(i)} < 0$, let $\beta_k^{(i)} = 10^{-5}$.
- The Particle Filter self-regulates from the cases where $\alpha_k^{(i)} + \beta_k^{(i)} > 1$, provided that these cases have very low likelihood, which translate into very low values of corresponding weights. Hence, no saturation condition has been used for the upper bound.

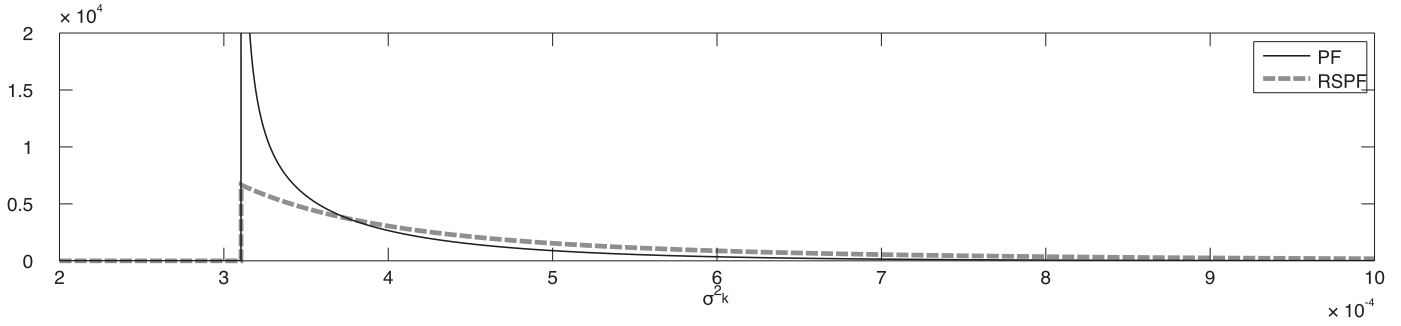


Fig. 4. Comparison between $q_{PF}(\sigma_k^2 | \sigma_{k-1}^{2(i)})$ and $q_{RSPF}(\sigma_k^2 | \sigma_{k-1}^{2(i)})$. In this example, $\sigma_{k-1}^{2(i)} = 5 \times 10^{-4}$, $\alpha = 0.2$, $\beta = 0.6$, $\omega = 1.0468 \times 10^{-5}$, and $\sigma_\eta^2 = 0.7$. The RSPF obtains particles from a fat-tailed distribution to ensure a higher resolution in risk-sensitive areas.

3.2.2. Particle Filters

Volatility estimation in both simulated data and stock market data has been performed using two different Particle Filtering schemes, including classic and risk sensitive approaches. The estimation is performed using 100 particles. Due to the inherent randomness of the filtering processes, these are repeated 10 times. Also, both filters are implemented with a resampling stage, where residual resampling is used. Next, details about each particular filter are presented.

Classic Particle Filter. The Classic Particle Filter (PF) for volatility estimation in the uGARCH model has been implemented using an importance density equal to

$$q_{PF}(x_k | x_{k-1}^{(i)}, z_k) = p(\sigma_k^2 | \sigma_{k-1}^{2(i)}). \tag{27}$$

A closed expression for $p(\sigma_k^2 | \sigma_{k-1}^{2(i)})$ has been given in Eq. (4). Thus, samples are generated according to:

$$\sigma_k^{(i)} \sim p(\sigma_k^2 | \sigma_{k-1}^{2(i)}), \tag{28}$$

which leads to the following weight update equation:

$$w_k^{(i)} = w_{k-1}^{2(i)} p(r_k | \sigma_k^{2(i)}). \tag{29}$$

Risk Sensitive Particle Filter. In the search for an importance density function that could be used to propose a risk sensitive approach towards volatility estimation, it was necessary to find a distribution with very specific characteristics. First, the probability density function needs a localization parameter that lets both the Classic Particle Filter's (PF) and Risk Sensitive Particle Filter's (RSPF) importance density have the same support. Second, the RSPF's importance density should have a fatter tail than the PF's density. The proposed RSPF uses the Generalized Pareto Distribution as the importance density function, which is commonly used to model the tails of other distributions; since it is able to model exponential, polynomial and even finite tails.

The Generalized Pareto Distribution is defined as follows (Ebrechts, Kluppelberg, & Mikosch, 1997; Mathworks, 2013):

$$f_{GPD}(x | k, \sigma, \theta) = \begin{cases} \frac{1}{\sigma} \left[1 + k \frac{x - \theta}{\sigma} \right]^{-1 - \frac{1}{k}} & \text{if } \begin{cases} k > 0, & \text{for } \theta < x \\ k < 0, & \text{for } \theta < x < \sigma/k \end{cases} \\ \frac{1}{\sigma} \exp \left[-\frac{x - \theta}{\sigma} \right] & \text{if } k = 0, \text{ for } \theta < x \end{cases} \tag{30}$$

This distribution has two special cases, where it is reduced to other distributions:

- If $k = 0$ and $\theta = 0$, the generalized Pareto distribution is equivalent to the exponential distribution.

- If $k > 0$ and $\theta = \sigma/k$, the generalized Pareto distribution is equivalent to the Pareto distribution.

The probability density function of the GPD has three parameters. These can be interpreted as follows:

- k : Shape parameter,
- σ : Scale parameter,
- θ : Threshold (location) parameter.

These parameters cannot take any value if one wants to ensure the convergence of the first and second moments of the GDP, since

$$\begin{aligned} \mathbb{E}[X] &= \theta + \frac{\sigma}{1+k}, \text{ for } k < 1, \\ \text{Var}[X] &= \frac{\sigma^2}{(1-k)^2(1-2k)}, \text{ for } k < 1/2, \end{aligned} \tag{31}$$

Considering that the variance is defined for $k < 1/2$, the parameters of the probability density function of the GPD have been used in the following way to utilize it as the importance density of the RSPF:

$$k = 0.49, \tag{32}$$

$$\sigma = 0.3\sigma_{k-1}^{2(i)}, \tag{33}$$

$$\theta = \omega + \beta_{k-1}^{(i)}\sigma_{k-1}^{2(i)}, \tag{34}$$

where $\beta_k^{(i)}$ is the (i) th pseudo-particle for the online estimation of the uGARCH parameter β . Parameter k has been fixed in the aforementioned value to reproduce the shape of $p(\sigma_k^2 | \sigma_{k-1}^{2(i)})$ (see Eq. (4)). Parameter σ gives the scale to $f_{GPD}(x | k, \sigma, \theta)$. Given that $\max\{f_{GPD}(x | k, \sigma, \theta)\} = 1/\sigma$, using a scaled previous-step particle, a desired fat tail with similar shape to $p(\sigma_k^2 | \sigma_{k-1}^{2(i)})$ is obtained. Parameter θ sets the location of the density of the GPD and is set to be equivalent to $\omega + \beta_{k-1}^{(i)}$ (see Eq. (4)), this is, the support of $f_{GPD}(x | k, \sigma, \theta)$ is set to be equivalent to the support of $p(\sigma_k^2 | \sigma_{k-1}^{2(i)})$. Hence, the importance density function employed is

$$q_{RSPF}(x_k | x_{k-1}^{(i)}, z_k) = f_{GPD}(\sigma_k^2 | 0.49; 0.3\sigma_{k-1}^{2(i)}; \omega + \beta_{k-1}^{(i)}\sigma_{k-1}^{2(i)}). \tag{35}$$

Particles are drawn from

$$\sigma_k^{2(i)} \sim f_{GPD}(\sigma_k^2 | 0.49; 0.3\sigma_{k-1}^{2(i)}; \omega + \beta_{k-1}^{(i)}\sigma_{k-1}^{2(i)}), \tag{36}$$

and the weight update equation is

$$w_k^{(i)} = w_{k-1}^{(i)} \frac{p(r_k | \sigma_k^{2(i)})p(\sigma_k^{(i)} | \sigma_{k-1}^{(i)})}{f_{GPD}(\sigma_k^{2(i)} | 0.49; 0.3\sigma_{k-1}^{2(i)}; \omega + \beta_{k-1}^{(i)}\sigma_{k-1}^{2(i)})}. \tag{37}$$

A visual comparison of $q_{PF}(x_k | x_{k-1}^{(i)}, z_k)$ and $q_{RSPF}(x_k | x_{k-1}^{(i)}, z_k)$ is shown in Fig. 4. Notice that both importance densities are defined over the same support, and $q_{RSPF}(x_k | x_{k-1}^{(i)}, z_k)$ has a fatter tail than $q_{PF}(x_k | x_{k-1}^{(i)}, z_k)$. Hence, the design conditions for the RSPF's importance density are met.

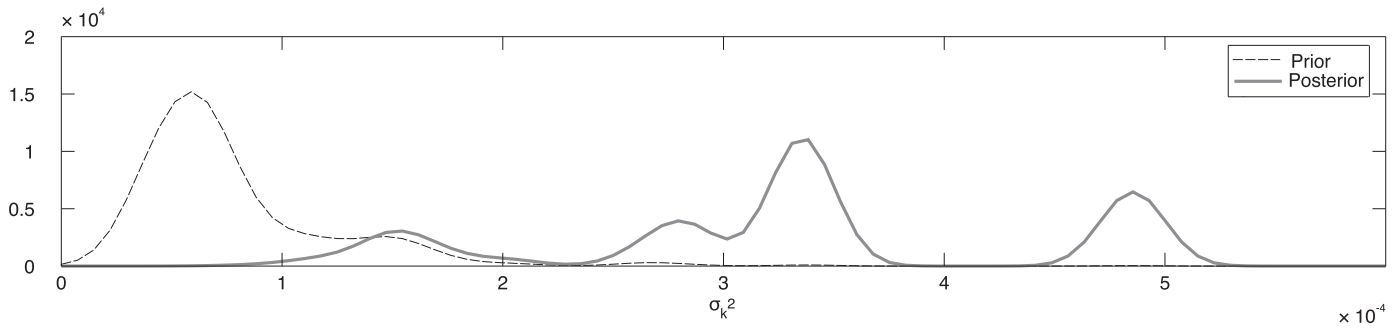


Fig. 5. Examples of prior and posterior densities of the RSPF in a volatility filtering process.

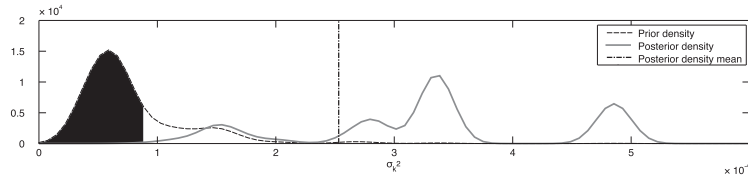


Fig. 6. Hypothesis test example. The filled area under the smoothed prior density represents the 70% confidence interval for the smoothed prior density. Here, the null hypothesis is accepted.

3.3. Detection using a hypothesis test

The Particle Filter, such as any other Bayesian filtering framework, predicts through model dynamics (Eq. (5)), and updates the estimation with the new measurement. Therefore, for every time step, the Particle Filter produces a prior estimate and a posterior estimate:

$$\text{Prior: } \hat{p}(x_k | z_{1:k-1}) = \sum_{i=1}^{N_s} w_{k-1}^{(i)} \delta(x_k - x_k^{(i)}), \tag{38}$$

$$\text{Posterior: } \hat{p}(x_k | z_{1:k}) = \sum_{i=1}^{N_s} w_k^{(i)} \delta(x_k - x_k^{(i)}), \tag{39}$$

Differences between prior and posterior densities may be considerable if model dynamics diverge from actual measurements. This is the case when unlikely events such as unexpected market falls or machine ruptures occur. Fig. 5 shows the vast differences that may occur between prior and posterior density estimates. A detection scheme through hypothesis test exploits these differences to design rapid change detectors in the estimated state.

To accept or reject the null hypothesis \mathcal{H}_0 , the implemented test considers the 70% confidence interval of the prior density, and contrasts it with the mean of the posterior density. The confidence interval is calculated using Parzen windows and a Normal kernel, whose bandwidth σ_{kernel} is obtained through Silverman’s thumb rule (Principe, 2010). If the mean of the posterior density is greater than the 70% interval bound of the prior density, the null hypothesis is accepted. Fig. 6 shows an example of the designed hypothesis test, where an unlikely event occurs and the null hypothesis \mathcal{H}_0 is accepted.

4. Results obtained for the proposed detection strategy

This section describes the results obtained for volatility estimation using Particle Filters, and detection of high volatility clusters using information derived from the filtering process. During the training stage, hyper-parameter selection for the setup of the PF algorithm is achieved through a sensibility analysis and subsequent selection through the smallest associated estimation error (in percentage). These results are used to select the PF algorithm hyper-parameters to be utilized in the detection scheme,

where estimation through PF is crucial. After the hyper-parameter selection stage, results for three different detection approaches are presented.

The performance measure introduced in this chapter may only be used in simulated data, where the true volatility is known. Hence, quantitative results showing performance measures results are presented for simulated data, and qualitative results are presented for returns series derived from IBM stock prices.

4.1. Performance measure: accuracy indicator

Section 2 describes the non-observability property of the state associated with financial volatility. The performance measure described in this section assume knowledge of the ground truth data, and as a consequence, results may be analyzed only in simulated data. The following sections consider $\hat{\sigma}_k^2$ as the estimated volatility and σ_k^2 as the true volatility (this is, the ground truth).

Accuracy of Particle Filters, including the Classic and Risk Sensitive approaches, is compared in terms of error (in percentage). The accuracy indicator is defined as follows:

$$i^{EX}(k) = \frac{|\hat{\sigma}_k^2 - \sigma_k^2|}{\sigma_k^2} \cdot 100. \tag{40}$$

Given that $i^{EX}(k)$ is defined for every time step k of the filtering process, one can obtain an average of $i^{EX}(k)$ over the filtering time window T_i, \dots, T_f :

$$I^{EX} = \frac{1}{T_f - T_i} \sum_{k=T_i}^{T_f} i^{EX}(k) = \frac{1}{T_f - T_i} \sum_{k=T_i}^{T_f} \frac{|\hat{\sigma}_k^2 - \sigma_k^2|}{\sigma_k^2} \cdot 100. \tag{41}$$

Furthermore, given that I^{EX} is defined only for one filtering process, one can obtain an average of I^{EX} over the amount of realizations of the filtering process, which include 10 in this work:

$$\bar{I}^{EX} = \frac{1}{10} \sum_{n=1}^{10} I^{EX}(n). \tag{42}$$

In particular, index \bar{I}^{EX} serves as the base to compare the error (in percentage) for each filtering process, for each set of hyper-parameters. Hence, the best set of parameters is obtained by observing the smaller index \bar{I}^{EX} .

Table 2
Parameter estimation using MATLAB®'s `garchfit` function from the Financial Toolbox.

Parameter	GARCH1	GARCH3
α	0.1477	0.2612
β	0.2768	0.6699
$\alpha + \beta (< 1)$	0.4245	0.9311

4.2. Volatility estimation through Particle Filters for an early high volatility cluster detection scheme

4.2.1. Fitting model parameters

The first step towards a filtering process starts with the estimation of model parameters that are used as the initial conditions in the extended GARCH model (refer to Section 3.2.1). As previously mentioned, for the uGARCH model this can be achieved by maximum likelihood, assuming that the model is in fact a GARCH model (Table 1).

Table 2 shows the results of model parameter estimation for the simulated data sets. The parameters are obtained using the `garchfit` function of MATLAB® over the training window of each data set. The true values for this time window are $\alpha = 0.2$ and $\beta = 0.6$ for every data set. From Table 2, GARCH1 is the data set that obtains the poorest parameter estimates from data contained within the training window.

This estimation has direct incidence over the filtering process, since these values are used as initial conditions for the extended uGARCH model, where the dynamics are non-observable. Initial conditions in non-observable systems are of great importance in the outcome of the a Bayesian filtering process. If the system is non-observable, the state may follow one of an infinite number of possible paths that match the current observations. Therefore, accurate initial conditions are necessary to achieve an unbiased estimate of the state.

4.2.2. Particle Filter hyper-parameter selection

This section presents the results of the sensibility analysis of hyper-parameters of the Classic Particle Filter. These parameters have been tested to find the combination that minimizes the estimation error $\bar{\mu}^{EX}$. The tested parameters include R_{th} (resampling threshold), $\sigma_{\alpha, \beta}$ (pseudo-particle standard deviation), and σ_{η} (process noise).

To find the hyper-parameter values that minimize the estimation error, the following hyper-parameter mesh is used:

- $R_{th} = \{0.5, 0.6, 0.7\}$,
- $\sigma_{\alpha, \beta} = \begin{Bmatrix} 0.0010, & 0.0015, & 0.0020, & 0.0025, & 0.0030 \\ 0.0035, & 0.0040, & 0.0050, & 0.0075, & 0.0100 \\ 0.0125, & 0.0150, & 0.0175, & 0.0200, & 0.0225 \\ 0.0250, & 0.0275, & 0.0300, & 0.0350, & 0.0400 \end{Bmatrix}$,
- $\sigma_{\eta} = \{0.5, 0.6, 0.7\}$.

It should be noted that the selected values that are employed to create the mesh for $\sigma_{\alpha, \beta}$ were placed at irregular intervals. Since there is a tendency to have better estimations with lower values of $\sigma_{\alpha, \beta}$, a better resolution has been given to the interval of smaller values.

Every set of hyper-parameters is used to run 10 times each filtering process over the complete time window $T = \{1, \dots, 500\}$ of every set of simulated data (GARCH1 and GARCH3). The error is computed over the interval $T' = \{151, \dots, 500\}$, which excludes the training interval.

Table 3a and b shows the percentage error for the mean of the 10 filtering routines for each set of parameters. Since results are 3-dimensional, the tables show the results for $\sigma_{\eta} = 0.7$, which is the noise process value that minimizes the error for every data set.

Table 3
Estimation error $\bar{\mu}^{EX}$ for different parameter values $\sigma_{\alpha, \beta}$ for the two data sets. These tables show the results for $\sigma_{\eta} = 0.7$.

R_{th}	0.0010	0.0015	0.0020	0.0025	0.0030	0.0035	0.0040	0.0050	0.0075	0.0100	0.0125	0.015	0.0175	0.02	0.0225	0.025	0.0275	0.03	0.035	0.04	
Data set GARCH1. The minimum error is obtained for $\sigma_{\alpha, \beta} = 0.0350$, $R_{th} = 0.6$.																					
0.5	51.0611	51.2075	50.1367	50.1331	47.4300	48.0407	46.5103	44.3850	38.7528	30.2866	26.1898	23.0201	21.7539	21.6545	21.4255	20.5647	20.3163	19.9770	19.7330	19.9307	
0.6	51.4037	50.8755	50.6492	49.4681	49.1941	47.3560	47.2149	45.0067	36.1592	31.3635	27.4839	25.0151	22.8430	21.6427	20.7188	21.0935	20.1355	19.7223	19.4162	20.1503	
0.7	51.4245	50.8909	50.8915	49.6318	48.5846	47.6203	47.2209	45.2000	36.7997	30.1693	27.4139	24.1124	22.9076	21.5613	21.4261	20.0818	20.5648	20.6290	19.9582	20.0205	
Data set GARCH3. The minimum error is obtained for $\sigma_{\alpha, \beta} = 0.0035$, $R_{th} = 0.7$.																					
R_{th}	0.0010	0.0015	0.0020	0.0025	0.0030	0.0035	0.0040	0.0050	0.0075	0.0100	0.0125	0.015	0.0175	0.02	0.0225	0.025	0.0275	0.03	0.035	0.04	
0.5	19.3664	20.0746	17.8894	17.7761	18.0384	17.3640	16.3491	18.7394	19.4852	22.1763	24.1930	26.4535	27.9966	31.0447	32.1416	33.1691	35.9803	38.5001	38.3597	41.2628	
0.6	18.1588	17.5985	17.4676	17.9119	17.2962	17.4517	18.1153	17.9320	19.3590	20.3719	24.5801	25.5974	29.5183	31.5754	32.1902	32.8693	37.5007	37.0170	39.5580	42.0956	
0.7	19.7638	18.9000	18.2602	18.5192	17.4313	16.1627	17.2223	18.4436	18.9302	21.1907	24.3899	26.4036	27.6496	29.5650	35.0783	31.5716	37.9800	35.0379	39.5324	43.3656	

Table 4
Summary of the sensibility analysis for the Classic Particle Filter.

Parameter	GARCH1	GARCH3	Mean
R_{th}	0.7	0.7	0.63
$\sigma_{\alpha, \beta}$	0.0350	0.0035	0.0141
σ_{η}	0.7	0.7	0.7
Minimum error \bar{E}^{EX}	19.4162	16.1627	22.9247
$\alpha + \beta (< 1)$	0.4245	0.9311	0.7609

The first thing to note in Table 3a and b is that the minimum percentage error for the filtering process on these data sets is bounded approximately between 16% and 19%. Second, it is very important to notice that errors are very similar for each one of the columns of the tables. This means that the resampling threshold R_{th} has a limited impact on the estimates when contrasted to the ground truth from an accuracy perspective. This is very important since one can simply employ an average of R_{th} over all data sets without losing estimation accuracy, or simply select the value that is most often the best value. Also, data shows that minimization occurs over a convex space which lets one assume that there is in fact a set of parameters which minimize the estimation error. These results also demonstrate that higher noises (this is, greater particle variability) do not translate into better estimates. In fact, there is a small subset of the parameter space where Bayesian filters such as the Particle Filter may work properly.

Table 4 shows the summary of selected hyper-parameters for each data set and its arithmetic mean, calculated using the information for every data set. Error values increase hugely towards the left side of the columns of Table 3a. This most probably occurs due to the poor estimation of initial conditions through maximum likelihood. Since the initial conditions are far from the ideal values, more variability is needed in the artificial evolution equations included within the Particle Filter algorithm in order to effectively learn and find the correct intervals where these parameters lie. On the other hand, error values increase hugely towards the right side of Table 3b. Initial conditions are very close to the ideal values, low noise variabilities are needed in order to find the correct intervals where these parameters lie.

The inherent non-observability issues of volatility imply that using an average value for $\sigma_{\alpha, \beta}$ over all the data sets where the filtering process is applied will result in poor estimations for the certain data sets.

To choose specific hyper-parameter values R_{th} , $\sigma_{\alpha, \beta}$ and σ_{η} , it is necessary to consider that hyper-parameters R_{th} and σ_{η} have a very small incidence in the estimation error given the parameter mesh. Thus, both of these parameters are set to 0.7. For parameter $\sigma_{\alpha, \beta}$, if one considers the arithmetic mean, results for the GARCH1 data set are far from optimum. Nevertheless, this is the proposed value used in the detection scheme. As a summary, the values considered for the proposed detection algorithms are the following:

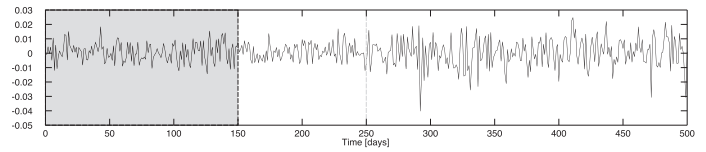
$$R_{th} = 0.6, \tag{43}$$

$$\sigma_{\alpha, \beta} = 0.0141, \tag{44}$$

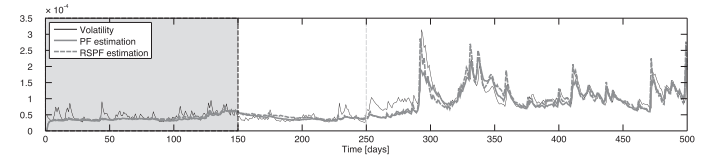
$$\sigma_{\eta} = 0.7. \tag{45}$$

4.2.3. PF and RSPF-based volatility estimation results

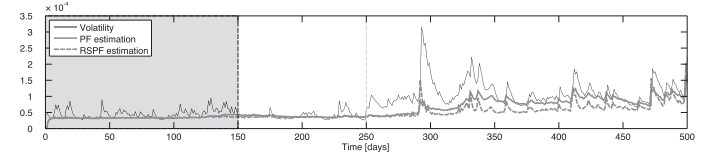
Filtering results with optimum hyper-parameters for each data set. This section presents the results obtained for volatility estimation using the hyper-optimum parameters for the Classic Particle Filtering processes, described in Section 4.2.2. These hyper-parameters have also been applied and used in the RSPF. Results are shown in Figs. 7b and 8b.



(a) Returns.

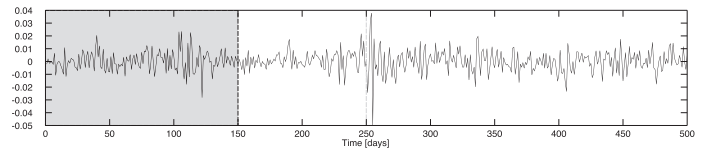


(b) Volatility estimation with optimum parameters.

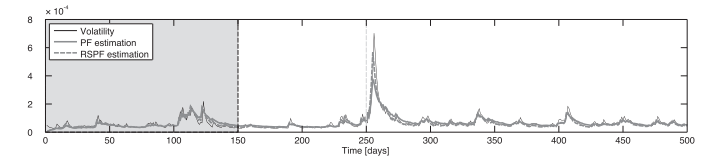


(c) Volatility estimation with averaged hyper-parameters.

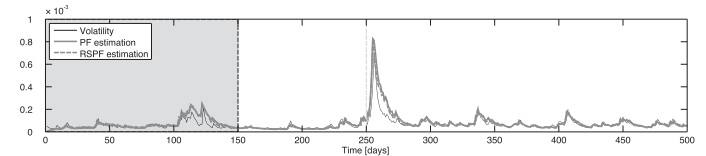
Fig. 7. Volatility estimation in GARCH1 data set. Thin line represents ground truth volatility, coarse line represents the PF estimation, and coarse dashed line represents the RSPF estimation.



(a) Returns.



(b) Volatility estimation with optimum parameters.



(c) Volatility estimation with averaged hyper-parameters.

Fig. 8. Volatility estimation in data set GARCH3. Thin line represents ground truth volatility, coarse line represents the PF estimation, and coarse dashed line represents the RSPF estimation.

Analysis of the estimation performance in each data set uncovers many interesting findings that need to be addressed. The comments about results are discussed separately for every data set.

- GARCH1 (Fig. 7): In this data set, there is a large change in the model parameters α and β for the simulated data at time step 250. Up to time step 250, both the PF and RSPF are only able to track the trend of the volatility curve, but there is no reaction to sudden changes. This behavior changes in time step 250, where there is a tendency towards capturing rapid volatility changes. The filter demonstrates the results of the learning process at time step 290, where a hefty volatility cluster

occurs. There is correct tracking of volatility shape with a very small estimation bias. This occurs between time steps 290 and 500, which corresponds to the end of the time window.

- GARCH3 (Fig. 8): There is excellent filtering performance throughout the time window. Accurate estimation, excellent shape tracking. For this data set, only about 100 time steps are necessary for the algorithm to learn and adapt.

The algorithms need at most 300 data points to learn and correctly adapt to the observed data. In general, there is good tracking of trends before this turning point, but if the algorithm is able to adapt properly, both tendency and shape are correctly tracked.

One important aspect from these results is that estimation performance depends vastly on the value $\sigma_{\alpha, \beta}$. Previous experiments demonstrate that low values of $\sigma_{\alpha, \beta}$ (this is, lower than the optimum) result in underestimation of financial volatility in both PF approaches, while higher values of $\sigma_{\alpha, \beta}$ are conducive to overestimation of volatility. From the purpose of tracking the shape of the envelope that characterizes the evolution of volatility in time, this is irrelevant, unless the filters lose the ability to track due to lack of particle variability. Given these results, it could be convenient to separate $\sigma_{\alpha, \beta}$ into σ_{α} and σ_{β} (this is, to consider separate sources of uncertainty on each pseudo-particle that extends the model). This is important for two reasons: First, is it necessary to understand that α multiplies the process noise σ_{η} in Eq. (1) and therefore, the process noise in the extended uGARCH model is the result of the multiplication of two random variables: $\alpha_k \sim \mathcal{N}(\alpha_{k-1}, \alpha_1 \sigma_{\alpha})$ and η_k^2 . Second, variables α and β introduce different behaviors in the model, since the former is associated to innovations and the latter is associated to the memory of the model.

According to Rachev, Hsu, Bahasheva, and Fabozzi (2008), the value of $\alpha + \beta$ in the GARCH model is the “process persistence parameter, since it determines the speed of the mean-reversion of volatility to its long-term average. A higher value for $\alpha + \beta$ implies that the effect of the shocks of volatility, u_k^2 , dies out slowly”. In Table 4, the estimated value of $\alpha + \beta$ was included for each data set. Although there is no apparent relation between the filtering performance of the Particle Filters and the value of $\alpha + \beta$, there is in fact one relation that needs attention: The data set in which the estimated value of α was bigger, the filtering performance was more accurate and errors were systematically lower (Table 3b).

From a detection perspective, it is necessary to notice that the RSPF is usually more capable of tracking correctly sudden rises of volatility. In these cases, estimations of the RSPF are better than the PF estimations, since the latter tends to under estimate. This seems a natural result considering the construction of both PFs: The RSPF grants more resolution to high volatility areas, resulting in a better estimation of sudden volatility rises.

Continuing with the PF and RSPF comparison, the PF usually outperforms the RSPF in terms of estimation accuracy. Albeit sudden volatility changes from low to high values, the PF is less biased than the RSPF.

As a final comment, one should notice that the RSPF outperforms the Classic PF in terms of 1-step prediction in cases where volatility experiences sudden increments. This occurs due to the construction of the uGARCH model, in comparison to the GARCH model. Comparing both dynamics equations,

$$\text{GARCH: } \sigma_{k|k-1}^2 = \omega + \alpha u_{k-1}^2 + \beta \sigma_{k-1|k-2}^2,$$

$$\text{uGARCH: } \sigma_k^2 = \omega + \alpha \sigma_{k-1}^2 \eta_k^2 + \beta \sigma_{k-1}^2,$$

where $u_k = \sigma_{k|k-1} \epsilon_k$, the innovations process in the GARCH model depends on the value of the previous step of the returns process, while the volatility dynamics of the uGARCH model are time independent of the returns series. Since the simulated data was generated according to a GARCH model and cases associated with filter-

ing through PF schemes is based on the uGARCH model, this 1-step prediction in sudden volatility rises is possible.

Filtering results with averaged hyper-parameters (as used in detection scheme). This section presents the results obtained for financial volatility estimation using the averaged hyper-parameters in the Classic Particle Filtering implementation (Eqs. (43)–(45)). The use of averaged hyper-parameter values is performed as an attempt to provide a more realistic solution to the problem of interest. This algorithm is intended to be used in stock market data and the hyper-parameters need to be estimated. These hyper-parameters have also been applied and used in the RSPF. Results are shown in Figs. 7c and 8c.

The previous section describes the phenomenon of over and underestimation related to the selected value of $\sigma_{\alpha, \beta}$. Given that the previous experiment showed results for the optimum value of this parameter, this situation was not apparent. Nonetheless, the new experiment makes this behavior palpable. A detailed analysis for each filtering process is given below.

- GARCH1 (Fig. 7c): The corresponding figure clearly shows underestimation of the state. Nevertheless, an interesting result is that shape tracking is extremely accurate, which is essential for the correct operation of the proposed detection algorithms.
- GARCH3 (Fig. 8c): Results for this data set are extremely interesting because of the ample robustness of the filtering performance to variations of the value $\sigma_{\alpha, \beta}$. Shape tracking and estimation accuracy are almost intact in contrast to the use of optimum parameters.

The anomalous behavior occurring in data set GARCH1 (Fig. 7c) may be explained again by the estimation through maximum likelihood of parameter α .

Comparing the performance of the PF and RSPF, there is again a clear response from the RSPF towards estimating correctly sudden changes in volatility from low to high values. This is correct for sudden changes, since the PF tends to be less biased in average. This behavior is extremely important for the detection scheme, since correct performance from the proposed detection techniques can be obtained even though the optimal parameters are not used in simulated or real data.

4.3. Early detection of high volatility clusters using a hypothesis test

This section presents results obtained from the proposed hypothesis test to capture early rises in volatility. Figs. 9 and 10 show these results. These figures contain 3 subfigures, which correspond to (a) returns series, (b) volatility series, RSPF prior and posterior estimation, and confidence interval, (c) detection points.

Figs. 9 to 10 show that the detector works correctly, since it is able to capture early rises of volatility which transform into high volatility clusters. The detector can also be interpreted as a local peak detector in the returns series, which is expected. Since the hypothesis test contrasts the dynamics of the model (prior) and the updated dynamics through the observations (posterior), it is clear that detections will occur mainly when local peaks of returns occur.

A detailed analysis of the results for each of the data sets is given ahead.

- GARCH1 (Fig. 9): All of the high volatility clusters are detected, except for the high volatility variation due to regime shift at time step 250. This regime shift introduces a notorious mean variation in volatility, which the test is not able to capture, since there are no vast variations in the returns series. High volatility sub-clusters around time step 350 are also detected.

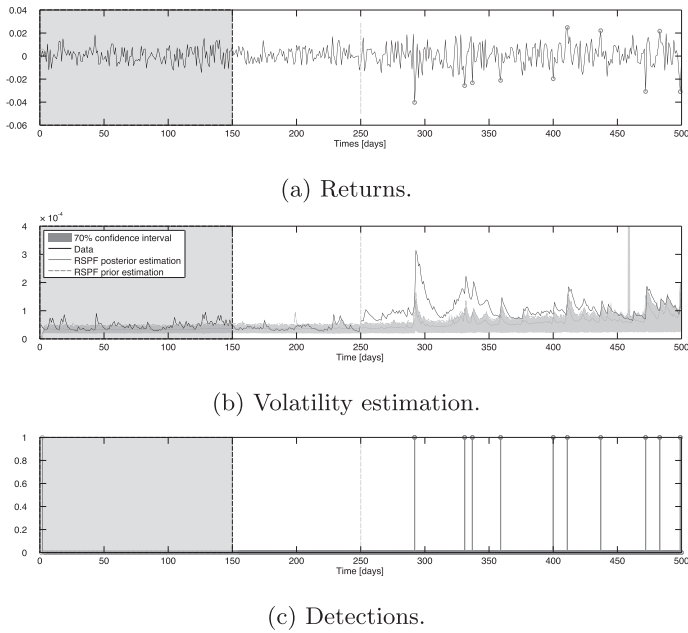


Fig. 9. Hypothesis test-based detection for data set GARCH1.

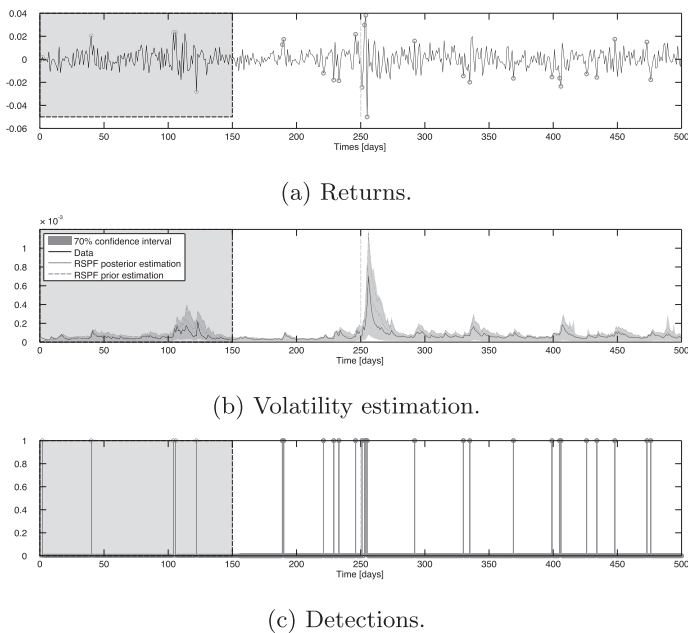


Fig. 10. Hypothesis test-based detection for data set GARCH3.

- GARCH3 (Fig. 10): All of the major sudden volatility rises are detected, except for the higher volatility episode starting at approximately time step 320. Continuing over this line of thought, the detector works as expected, although the performance measures do not correctly express the actual detector capacity.

The detection results obtained through a proposed hypothesis test show that the detector is very sensitive even to mild high volatility clusters, when the estimation framework works properly. This translates into the difficulty of measuring correctly the performance of the algorithm, since there is no possible definable hard limit between low and high volatility clusters. In fact, one can only use a diffuse definition.

Other results that need to be addressed correspond to the robustness of the algorithm and the employed value of $\sigma_{\alpha, \beta}$ in

Table 5
Parameter estimation of the GARCH(1,1) model through maximum likelihood for IBM's returns series between September 12th, 2005 and September 1st, 2009.

GARCH parameter	Value
ω	2.5690×10^{-6}
α	0.0647
β	0.9234
μ	6.9333×10^{-4}

the estimation stage. This parameter has tremendous implications over the estimation performance, but not over detection performance. If shape is tracked correctly, the hypothesis test-based detector performs exceptionally well, even under extreme estimation biases.

4.4. Case study: early detection of high volatility clusters in IBM's stock data

IBM stock price series are usually used as examples for the study of returns series and volatility series (Tsay, 2010). There are various episodes since the year 1962 which are interesting events to explore, including the market falls of 1987 and 2008. As mentioned in Section 3.1.2, the data employed for this case study involves adjusted closing prices between September 12th, 2005 and September 1st, 2009.

The data observed here does not include the ground truth values for volatility, which means that volatility can only be estimated and therefore, there is no possibility to quantify the detector's performance. Analysis is solely based upon observation of the obtained results and qualitative interpretation of the data.

Table 5 displays the estimated parameters for the GARCH(1,1) model in the first 200 data points of the series, which serve as the training period. The parameters ω and μ are left fixed in the extended uGARCH model, while estimations of α and β are used as initial conditions for the online estimation of these parameters. The estimation exhibits a very low value for α , while β has a large value. Given that $\alpha + \beta = 0.9881$ and that evidence shows that usually $\alpha + \beta$ is close to 1, one might assume that the estimation is good. Given that the value of α is small, the pseudo-particle standard deviation used is equal to $\sigma_{\alpha, \beta} = 0.04$. Moreover, $R_{th} = 0.7$ and $\sigma_{\eta} = 0.7$.

Fig. 11 exhibits the obtained results from volatility estimation and early detection of high volatility clusters. In particular, details about the adjusted price series, returns series, volatility estimation, detections and the training window may be observed. Analysis of this Fig. 11c shows that volatility estimation of both the PF and the RSPF are extremely close, and the differences between most estimations occur, although mildly, in sudden volatility rises, where the RSPF has a faster reaction towards unlikely values. This is more visible at the beginning of bigger high volatility clusters, from time step 500 and onwards.

Estimations obtained from the RSPF are used as the base of the hypothesis test-based detector, which showed the best results in the previous sections. One may observe that most of the small high volatility clusters between time steps 200 and 500 are detected. There are some false positives and false negatives, but these are minor. In the time window that includes time steps 500–1000, all of the major volatility clusters are detected in a very early stage, including the high volatility cluster starting at time step 750, conducive to the big stock market drop of the year 2008. Moreover, in this time window, there are only 2 false positives, which occur after the last high volatility cluster. All of the other detections need to be considered true positives.

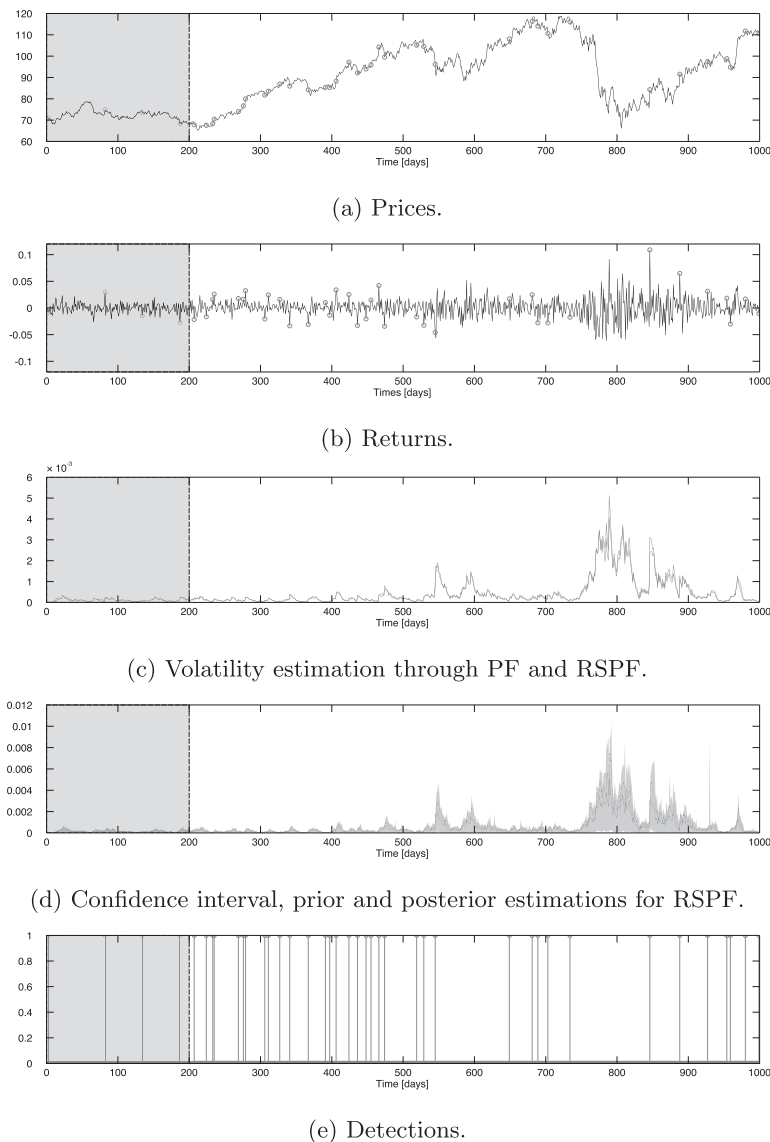


Fig. 11. Early hypothesis test-based detection of high volatility clusters in IBM's stock data.

5. Discussion

The results obtained from the PF and RSPF are aligned with the literature: they are suitable frameworks that may offer excellent estimation performance for stochastic volatility estimation. Nevertheless, non-observability issues may produce poor results, a problem that needs to be correctly addressed. Analysis of the parameter estimation of the GARCH model together with the sensitivity analysis including noise values demonstrate that estimation performance is extremely dependent on four aspects:

1. Correct initial conditions for particle population.
2. Adequate characterization of process noise sources.
3. Correct initial conditions of pseudo-particles if the state-space model has been extended to include online parameter estimation.
4. Adequate characterization of process noise sources for pseudo-particle variability within artificial evolution-based approaches.

Inadequate values can lead to algorithms with inability to learn, or extremely biased estimates. Moreover, there is an important relationship between points 3 and 4: if estimates of the GARCH model (which in this case are used as the initial conditions) are too

low or inaccurate, higher noise values for these pseudo-particles are needed to improve the learning capabilities of the PF algorithm. As a consequence, the parameter $\sigma_{\alpha, \beta}$ should be separated into σ_{α} and σ_{β} , this is, use a separate dispersion value for the noise process of each pseudo-particle which extends the model.

A performance comparison between the Classic Particle Filter and the proposed Risk Sensitive approach shows that the Risk Sensitive algorithm behaves better for purposes of tracking sudden volatility changes from low to high values. The greater particle resolution offered by the Risk Sensitive Particle Filter in areas of high volatility give this algorithm a very high performance in these cases.

This filtering approach, combined with the proposed detection technique based on the contrast of prior and posterior estimations of the Risk Sensitive Particle Filter through a hypothesis test proves that early detection of high volatility clusters is possible with a small error. Important aspects associated with the performance ensure that the detection is extremely robust to biased estimates, which are related to sub-optimal dispersion values of noise. In particular, if the Particle Filter does not lose the ability to learn and track the shape of volatility, the proposed hypothesis test-based detector excels in early detection of high volatility clusters.

6. Conclusions

This work presents and explores the use of Particle Filtering frameworks for the online detection of variations in financial returns that may conduce to high volatility clusters. Our approach uses a novel volatility estimator based on a Risk Sensitive Particle Filters (RSPF) that employs the Generalized Pareto Distribution to generate particles in areas associated to higher risk.

The methods proposed include the use of a simple stochastic variation of the GARCH model – the uGARCH model– in order to capture volatility variations of financial returns that may lead to high-volatility clusters. This model has been chosen in order to diminish the complexity of our method, while simultaneously helping to track disturbances introduced by other non-measurable factors (often found in complex systems such as the stock markets). This efforts result in a simple, but effective, detection scheme based on the comparison of prior and posterior PDF estimates through a hypothesis test. The proposed method proves (both with simulated and actual financial data) that early detection of high volatility clusters is possible with a small error using low-complexity models and risk-sensitive approaches in the detection framework.

Future work will focus on exploring connections with the problem of jumps detection in financial variables. Our approach offers a framework that is independent from the stochastic volatility model structure; thus representing a plausible option for online jumps detection in financial econometrics.

Acknowledgements

This work has been partially supported by FONDECYT Chile Grant No. 1140774 and Advanced Center for Electrical and Electronic Engineering, Basal Project FB0008.

References

- Andersen, T. G., Tim, & Diebold, F. X. (2007). Roughing it up: including jump components in the measurement, modeling, and forecasting of return volatility. *The Review of Economics and Statistics*, 89, 701–720.
- Arulampalam, M. S., Maskell, S., Gordon, N., & Clapp, T. (2002). A tutorial on particle filters for online nonlinear/non-Gaussian Bayesian tracking. *IEEE Transactions on Signal Processing*, 50, 174–188.
- Bollerslev, T. (1986). Generalized autoregressive conditional heteroskedasticity. *Journal of Econometrics*, 31, 307–327.
- Chan, J. C., & Koop, G. (2014). Modelling breaks and clusters in the steady states of macroeconomic variables. *Computational Statistics and Data Analysis*, 76, 186–193.
- Chen, C. W., Gerlach, R., & Liu, F.-C. (2011). Detection of structural breaks in a time-varying heteroskedastic regression model. *Journal of Statistical Planning and Inference*, 141, 3367–3381.
- Cont, R. (2005). Volatility clustering in financial markets: empirical facts and agent-based models. *Long memory in economics*. Springer.
- Doucet, A., Godsill, S., & Andrieu, C. (2000). On sequential monte carlo sampling methods for Bayesian filtering. *Statistics and Computing*, 10, 197–208.
- Embrechts, P., Kluppelberg, C., & Mikosch, T. (1997). Modelling extremal events for insurance and finance. *Stochastic modelling and applied probability*: vol. 33 (1st ed.). Springer-Verlag.
- Eraker, B., Johannes, M., & Polson, N. (2003). The impact of jumps in volatility and returns. *The Journal of Finance*, 58(3), 1269–1300.
- Gordon, N., Salmond, D., & Smith, A. (1993). Novel approach to nonlinear/non-Gaussian Bayesian state estimation. *IEE Proceedings F: Radar and Signal Processing*, 140, 107–113.
- He, Z., & Maheu, J. M. (2010). Real time detection of structural breaks in GARCH models. *Computational Statistics and Data Analysis*, 54, 2628–2640.
- Kalman, R. E. (1960). A new approach to linear filtering and prediction problems. *Transactions of the ASME – Journal of Basic Engineering*, 82, 35–45.
- Kitagawa, G., & Sato, S. (2001). Monte carlo smoothing and self-organizing state-space model. In A. Doucet, N. de Freitas, & N. Gordon (Eds.), *Sequential Monte Carlo methods in practice in statistics for engineering and information science* (pp. 177–195). Springer-Verlag.
- Laurent, S., Lecourt, C., & Palm, F. C. (2014). Testing for jumps in conditionally gaussian ARMA-GARCH models, a robust approach. *Computational Statistics and Data Analysis*. doi:10.1016/j.csda.2014.05.015. (in press).
- Lee, S. S., & Mykland, P. A. (2008). Jumps in financial markets: a new nonparametric test and jump dynamics. *The Review of Financial Studies*, 21(6), 2535–2563.
- Liu, J., & West, M. (2001). Combined parameter and state estimation in simulation-based filtering. In A. Doucet, N. de Freitas, & N. Gordon (Eds.), *Sequential monte carlo methods in practice in statistics for engineering and information science* (pp. 197–223). Springer-Verlag.
- Mandelbrot, B. (1963). The variation of certain speculative prices. *The Journal of Business*, 36, 394–419.
- Mathworks (2013). Generalized pareto distribution. retrieved from <http://www.mathworks.com/help/stats/generalized-pareto-distribution.html>.
- Mundnich, K. (2013). Early detection of high volatility clusters using particle filters. Electrical Engineering thesis. Department of Electrical Engineering, University of Chile. retrieved from <http://tesis.uchile.cl/handle/2250/115486>.
- Principe, J. C. (2010). Information theoretic learning: Renyi's entropy and kernel perspectives. *Information Science and statistics* (1st ed.). Springer.
- Rachev, S., Hsu, J., Bahasheva, B., & Fabozzi, F. (2008). Bayesian methods in finance. *The Frank J. Fabozzi Series* (1st ed.). John Wiley & Sons, Inc..
- Rapach, D. E., & Strauss, J. K. (2008). Structural breaks and GARCH models of exchange rate volatility. *Journal of Applied Econometrics*, 23, 65–90.
- Ross, G. J. (2013). Modelling financial volatility in the presence of abrupt changes. *Physica A*, 392, 350–360.
- Thrun, S., Langford, J., & Verma, V. (2002). Risk sensitive particle filters: vol. 14. *Advances in Neural Information Processing Systems* (pp. 961–968). MIT Press.
- Tobar, F. A. (2010). *Inferencia de volatilidad de retornos financieros usando filtro de particulas*. Master's thesis Universidad de Chile.
- Tsay, R. (2010). Analysis of financial time series. *Wiley Series in Probability and Statistics* (3rd ed.). Chicago: John Wiley & Sons, Inc.
- Yahoo! (2013). International Business Machines Corporation – NYSE. retrieved from <http://finance.yahoo.com/q?s=IBM>.

Volatility clustering at the Johannesburg Stock Exchange: Investigation and Analysis

Olivier Niyitegeka

Regent Business School, Graduate Student

D.D.Tewari

Professor School of Accounting,
Economic and Finance the College of Law and Management
University of KwaZulu-Natal, Durban, South Africa.
Email. davetewari@gmail.com

Doi:10.5901/mjss.2013.v4n14p621

Abstract

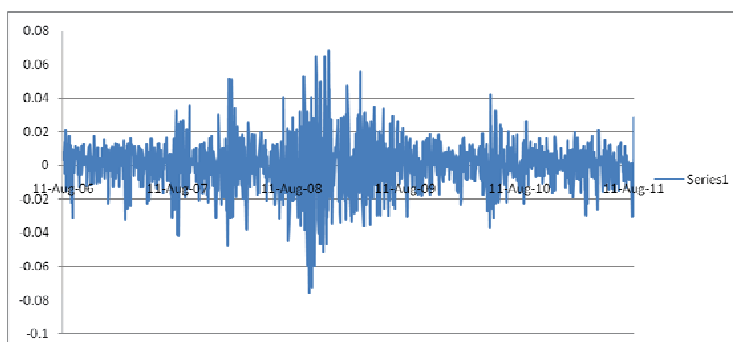
This paper examines the existence and the nature of the volatility clustering phenomenon in the Johannesburg Stock Exchange (JSE). Volatility clustering is one of the most common stylized facts in financial time series; this phenomenon has intrigued many researchers and oriented in a major way the development of stochastic models in finance. The study uses GARCH-type models to detect volatility clustering. GARCH-type models are widely used to test the volatility clustering phenomenon. Their popularity stems from their healing power for heteroskedasticity in regression models and their ability to model nonlinear dynamics. Various studies on volatility clustering suggest that negative shocks to stock prices will generate more volatility than positive shocks of equal magnitude. In this regard the study also examines the asymmetric effect of positive and negative shocks in the JSE. The results indicate the presence of volatility clustering in the JSE. An asymmetric effect of positive and negative shocks on conditional volatility could not be identified.

Keywords: Volatility clustering, leverage effect, GARCH, asymmetric GARCH models.

1. Introduction

Uncertainty plays a crucial role in financial theories. Many models in the field of academic finance use variance (or standard deviation) as a measure of uncertainty. In most of these models variance is assumed to be constant through time; this is known as homoscedasticity (Brooks, 2002: 386). However, empirical evidences have rejected this assumption. It has been established that time series exhibit volatility clustering, where calm and volatile episodes are observed, such that at least the variance appears to be predictable. Figure 1 represents the daily return of the FTSE/JSE's All Share Index, for a period of five years. This raw time series data suggests that there are periods of volatility clustering where days of large movement are followed by days with the same feature.

Figure.1. Daily returns for FTSE/JSE All Share Index during for the period between 10 August 2006 and 10 August 2011



Source: McGregor BFA, 2012

Statistically, volatility clustering entails a strong autocorrelation in squared returns. A technical term given to this phenomenon is Autoregressive Conditional Heteroskedasticity (ARCH) or simply the ARCH effect.

Modelling volatility is important when it comes to risk management and portfolio selection as well as pricing of assets. Volatility makes investors more averse to holding stocks due to uncertainty; investors in turn demand a higher risk premium to insure against the increased uncertainty. A greater risk premium results in a higher cost of capital, which subsequently leads to less private investment (Emenike, 2010). Therefore, modelling volatility improves the usefulness of measuring the intrinsic value of securities and in the process it becomes easy for a firm to raise funds in the market. Additionally, the detection of volatility provides an insight for a better way to design an appropriate investment strategy (Emenike, 2010). On the basis of the aforementioned, it is essential to know the behaviour of volatility of the Johannesburg Stock Exchange (JSE) returns. This paper adds to the existing literature on the persistence of market return volatility at the JSE. Previous studies by Samouilhan (2007) and Louw (2008), found that volatility clustering is present clustering on the FTSE/JSE top 40 index. This study broadens the analysis by examining volatility in the South African stock exchange using the FTSE/JSE All Share Index (ALSI) as a proxy for the entire shares listed on the South African stock market.

The study is organised as follows: Section Two provides a brief review of the relevant literature on volatility clustering. Section Three covers data and methodology. Section Four provides a discussion of the empirical findings, and Section Five concludes.

2. Volatility Clustering: A Review

As mentioned above, empirical research has provided strong evidence that volatility is time-varying and that changes in volatility are predictable to some extent. A ground-breaking study by Mandelbrot (1963), and later confirmed by Fama (1965), found that there is a memory effect the size of price change. Large price changes were followed by large price changes of either sign, or that small price changes were followed by small price changes of either sign. Another study by Christie (1982) established that, owing to financial leverage, there is a negative relationship between the volatility of the rate of return on equity and the value of equity. This meant that an increase in financial leverage was accompanied by an increase in volatility (Louw, 2008). Christie's (1982) findings were in sharp contrast with Black's (1976) results that indicated that positive and bad news had a symmetrical impact on volatility (Louw, 2008).

An easy method for detecting volatility clustering is to capture changing variance using Autoregressive Conditional Heteroskedasticity (ARCH) and Generalized ARCH (GARCH), models developed by Engle (1982), and extended by Bollerslev (1986) and Nelson (1991).

Various studies investigated volatility clustering on financial markets using GARCH-type models, and include, among others, Jacobsen and Dannenburg (2003) who used temporal aggregation on monthly stock returns for daily, weekly, bi-weekly and monthly data from France, Germany, Italy, Netherlands, United Kingdom and the United States. They identified a significant GARCH effect at monthly levels, which was confirmed by a Monte Carlo simulation. Jagajeevan (2012) examined the persistence of volatility, risk-return trade off and asymmetric volatility in returns, on daily and monthly returns on the All Share Price Index of the Colombo stock exchange. He only identified volatility clustering in daily returns, but not in monthly returns. Jagajeevan (2012) also identifies a leverage effect in daily returns, where the stock market becomes more volatile when negative shock takes place as compared the positive shock.

By using agent-based models¹, academics have established that agents' herd behaviour² causes volatility clustering in stock markets. For instance, Alfarano and Lux (2001) noted that the existence of herd behaviour among market participants modifies the distribution of market returns. As they explained further, this is characterized by the presence of fat tails and volatility clustering in these financial data. Yamamoto (2011) used an agent-based model to run simulations on an artificial stock market. The simulations consisted of two economies: one with and the other without herding. He established that a herding economy can engender volatility clustering, but volatility could be found when agents do not herd others at all. Park (2008) demonstrated that herd behaviour leads to a high increase in volatility but not trading volume.

As far as African stock markets are concerned, a considerable number of studies investigated volatility clustering. Emenike (2010) investigated volatility clustering, leptokurtosis and leverage effect for the Nigerian Stock Exchange returns series. Using GARCH (1,1) he found that volatility of stock returns is persistent in Nigeria. Using the GJR-GARCH

¹ Computer simulation that represents individual actors in a dynamic social system.

² Herd behaviour occurs when managers simply mimic the investment decision of other managers, ignoring substantive private information.

(1,1) model he also identified leverage effects in Nigerian stock returns. A study by Floros (2008) examined volatility in the Egyptian stock market using daily data for Egypt's CMA general index. Using GARCH –type models, he found strong evidence of volatility clustering. He also noted that a leverage effect exists and that bad news increased volatility. A study by Samouilhan (2007) found a large degree of persistence of volatility on equity returns on the JSE for the broad ALSI40 index and its various sub-sectors. Using a Component ARCH (CARCH) model, he found significant evidence of volatility clustering over both the long and the short run for each series and for the broad index. Louw (2008) examined volatility clustering on the FTSE/JSE top 40 index. He used various models to test the phenomenon, namely, linear regression, exponential smoothing, GARCH (1,1) and EGARCH(1,1). After conducting an analysis of the distribution qualities, the autocorrelation of volatility for five return intervals, as well as the results of forecasting models, he found sufficient evidence that volatility clustering exists on the FTSE/JSE top 40 index. He also concluded that more complex models, such as GARCH (1,1) and EGARCH(1,1), marginally outperform less complex models. Ahmed and Suliman (2011) used both symmetric and asymmetric GARCH models to investigate conditional variance in daily returns of the Khartoum Stock Exchange (KSE). They found a high degree of persistence in the conditional volatility of stock returns on the KSE.

3. Data and Methodology

3.1 Data

In this study, daily returns based on closing prices of the FTSE/JSE All Share Index for the period between August 2006 and August 2011 was used. They represent 1250 observations. The data was downloaded from database of McGregor BFA.

Table 1 presents descriptive statistics for the series, they are: sample means, standard deviations, skewness, kurtosis and the Jarque-Bera test for normality (with their p-value). It is clear that the distribution of the series is non-normal and has leptokurtic distribution, features that are common with most financial data (Chinzara, 2008).

Table 1. Descriptive statistics for the log return of FTSE/JSE All Share Index

Number of observation	mean	Median	Minimum	Maximum	Standard deviation	Skewness	Kutosis	Jarque-Bera
1250	0.012	0.0465	-3.292	2.968	0.651	-0.121	140.639	404***

***, ** and * indicate significance at the 1%, 5% and 10% levels respectively.

3.2 Methodology

The study uses a Generalised Autoregressive Conditional Heteroskedasticity (GARCH) type model to test volatility clustering. As mentioned above, the GARCH models are widely used to test the volatility clustering phenomenon. Their popularity stems from their healing power for heteroskedasticity in regression models and their ability to model nonlinear dynamics (Hourvoulides, 2007).

The GARCH model, employs the maximum likelihood procedure, and allows the conditional variance to be dependent upon previous own lags. The conditional variance equation is expressed as follows:

$$\sigma_t^2 = \alpha_0 + \sum_{j=1}^p \beta_j \sigma_{t-j}^2 + \sum_{i=1}^q \alpha_i \varepsilon_{t-i}^2 \dots\dots\dots (1)$$

where α_0 is a constant term, σ_t^2 is the volatility at time t , ε_{t-1}^2 is previous period's squared the error term, and σ_{t-1}^2 is the previous period's volatility. For any GARCH (p, q), the order is normally chosen through the Schwarz Bayesian Information Criteria (SBIC) and is based on the following formula:

$$SBIC = 1 + \ln(2\pi) + \ln\left(\frac{ESS}{T}\right) + \frac{k}{T} (\ln T) \dots\dots\dots (2)$$

where T is the sample size, k is the number of estimated parameters and ESS is the sum of the squared residuals in the regression. The SBIC is usually chosen over the Akaike Information Criterion (AIC) because it penalizes more heavily for degrees of freedom, therefore, it tends to select more parsimonious models. The model with the smallest criterion value for each GARCH specification is used (Chinzara, Azakpioko, 2009).

Interestingly enough, first-order GARCH models, that is, GARCH (1,1) models, are so often empirically adequate

to test volatility clustering that they have achieved something of a canonical status (Diebold, 2012) .

3.2.1 GARCH (1,1)

Working under the assumption that volatility depends on the last period's conditional volatility, the GARCH (1,1) model is expressed as follows:

$$Y = \mu_t + \varepsilon \dots\dots\dots (3)$$

$$\sigma_t^2 = \alpha_0 + \alpha_1 \varepsilon_{t-1}^2 + \beta \sigma_{t-1}^2 \dots\dots\dots (4)$$

Where Equation 3 is the mean equation and Equation 4 is the conditional variance equation, α_0 is a constant term, σ_t^2 is the volatility at time t , ε_{t-1}^2 is previous period's squared error term, and σ_{t-1}^2 is the previous period's volatility. Statistically significant positive parameter estimates α_1 and β (with the constraint $\alpha_1 + \beta < 1$) would indicate the presence of clustering, with the rate of persistence expressed by how closer $\alpha_1 + \beta$ is to unity, the bigger the persistence of conditional volatility.

The constraint $\alpha_1 + \beta < 1$ allows the process to remain stationary, with the upper limit of $\alpha_1 + \beta = 1$ which represents an integrated process.

It should be noted that a key feature for an appropriate mean Equation 3 is that it should be "white noisy" meaning that its error terms should be serially uncorrelated. In this regard the mean Equation 3 will have to be tested for autocorrelation using the Durbin Watson (DW) test and the LM autocorrelation test. Should there be evidence of autocorrelation, lagged values of the dependent variable will be added to the right-hand side of Equation 4 until serial correlation is eliminated (Chinzara, Azakpioko, 2009). The appropriate mean equation will also be tested for ARCH effect to ensure that it is necessary to proceed to estimating GARCH models.

The GARCH (1,1) model assumes that good and bad news have a symmetrical effect on volatility and this is not always the case in various financial time-series. In this regard, the study estimated EGARCH and GJR GARCH models.

3.2.2 GJR GARCH (1,1,1)

The GJR GRCH model is a simple extension of GARCH with the additional term added to account for possible asymmetries. The conditional variance is given by:

$$\sigma_t^2 = \alpha_0 + \alpha_1 \varepsilon_{t-1}^2 + \beta \sigma_{t-1}^2 + \gamma \mu_{t-1}^2 + I_{t-1} \dots\dots\dots (5)$$

where $I_{t-1} = 1$ if $\mu_{t-1}^2 < 0$ and $I_{t-1} = 1$ otherwise.

I is the asymmetry component and γ is the asymmetry coefficient. The presence of leverage effects is indicated by significantly positive γ . The idea behind this is that good news ($\varepsilon_t > 0$) and bad news ($\varepsilon_t < 0$) will have different impacts on conditional variance. Good news will have an impact of α_1 , bad news will have an impact of $\alpha_1 + \gamma$. Thus, if γ is significantly different from zero, the impact of good news is different from the impact of bad news on current volatility (Arguile, 2012). It is worth noting that the condition for non-negativity will be $\alpha_0 \geq 0$, $\alpha_1 \geq 0$, $\beta \geq 0$, and $\alpha_1 + \beta$.

3.2.3 EGARCH (1,1,1)

Another GARCH model that accounts for an asymmetric affect is Exponential GARCH (1,1,1) (EGARCH). It is expressed as follows:

$$\ln(\sigma_t^2) = \alpha_0 + \alpha_1 \left(\frac{|\varepsilon_{t-1}|}{\sigma_{t-1}} - \sqrt{\frac{2}{\pi}} \right) + \beta \ln(\sigma_{t-1}^2) + \gamma \frac{\varepsilon_{t-1}}{\sigma_{t-1}} \dots\dots\dots (6)$$

Where α_1 and β are still interpreted as they are in the GARCH (1, 1) model and γ is the asymmetry coefficient. The

inclusion standardized residual $\frac{\varepsilon_{t-1}}{\sigma_{t-1}}$ allows the EGARCH model to be asymmetric for $\gamma \neq 0$. This is captured by the fact that the ARCH effect represented by $\alpha_1 + \gamma$ will be obtained for positive residuals and the ARCH effect represented by $\gamma - \alpha$ will be obtained for negative residuals. In other words, the leverage effect, which is a special case of asymmetric impacts, would exist if $\gamma < 0$ (Chinzara, 2008).

4. Results and Analysis

Before running GARCH-type models, the mean equation was estimated and tested for autocorrelation for FTSE/ ALSI index and ARCH effect. The results are reported in Table 2.

Table 2: Test for autocorrelation and ARCH effects

	DW stat test	Arch LM test
ALSI	1.92	45.230 [0.000]***

***, ** and * indicate significance at the 1%, 5% and 10% levels respectively.

The result of the DW stat test is 1.92 implying that there is no evidence of autocorrelation in the mean equation. It is also clear that ALSI shows significant evidence of the ARCH effect, implying that the mean equation did not adequately capture volatility, hence we estimate the GARCH models based on this mean equation.

GARCH(1,1), EGARCH(1,1,1) and GJR GARCH(1,1,1,1) are therefore estimated and the results are reported in Table 3

Table 3. Testing for volatility clustering

	GARCH(1,1)	EGARCH(1,1,1)	GJR GARCH(1,1,1)
α_0	0.0064***	- 0.104 ***	0.0063***
α_1	0.108 ***	0.105 ***	0.031
β	0.876***	0.982 ***	0.906***
$\alpha_1 + \beta$	0.984	1.807	0.937
γ	n/a	-0.114 ***	1.199
AIC	2067.009	2027.480	2033.276
BIC	2092.664	2035.196	2053.801

***, ** and * indicate significance at the 1%, 5% and 10% levels respectively.

The sum of the α_1 and β coefficients is high in all models, indicating the presence of volatility clustering. For instance, in the GARCH model the sum of $\alpha_1 + \beta$ is 0.984 indicates the presence of volatility clustering. In the EGARCH model, however, the stationarity condition ($\alpha + \beta < 1$) is violated, since the sum of α and β is more than unity. For this reason, the EGARCH model should not be used to test the leverage effect. As for the GJR model, although the asymmetry coefficient is positive, it is not significant at conventional levels of significance. Given the fact that GJR GARCH and EGARCH could not reach conclusive results, we conclude that asymmetric effects of news on conditional volatility are not prevalent in the JSE.

5. Conclusion

This paper investigated the volatility of stock market returns in the JSE using three variants of the GARCH model, namely, GARCH(1,1) GJR GARCH(1,1,1) and EGARCH(1,1,1). Volatility clustering and leverage effects were examined for the JSE returns series from August 2006 to August 2011. The results from the GARCH (1,1) model show that volatility of stock returns is persistent in South Africa. The result of EGARCH and GJR-GARCH (1,1) fail to indicate the existence of leverage effects in South African stock returns. This is in line with Louw's (2008) work that acknowledged the presence of volatility clustering in the FTSE/JSE top 40 index.

References

- Alfarano, S. and Lux, T. (2001), "A minimal noise trader model with realistic time series properties". Economics Working Papers, Christian-Albrechts-University of Kiel, Department of Economics.
- Arguile, W. P. (2012), *Performance of defensive shares on the JSE during financial crisis: evidence from analysis of returns and volatility* (Doctoral dissertation, Rhodes University).
- Black, F. (1976), "Capital market equilibrium with restricted borrowing" *The Journal of Business*. 5(3): 444-455.
- Bollerslev, T. (1986), "Generalized Autoregressive Conditional Heteroskedasticity". *Journal of Econometrics*. 31, 307-327.
- Brooks, C. (2002), *Introductory Econometrics for Finance*. Cambridge: Cambridge University Press.
- Diebold, F. (2012), 100+ Years of Financial Risk Measurement and Management. University of Pennsylvania and NBER. Available from: <http://www.ssc.upenn.edu/~fdiebold/papers/paper108/DieboldElgar.pdf> [Accessed 12/12/2012]
- Chinzara, Z. (2008), An empirical analysis of the long-run comovement, dynamic returns linkages and volatility transmission between the world major and the South African stock markets. Unpublished Masters thesis. Grahamstown: Rhodes University.
- Chinzara, Z., and Aziakpono, M. J. (2009), "Dynamic returns linkages and volatility transmission between South African and world major stock markets". *Journal of Studies in Economics and Econometrics*, 33(3), 69-94.
- Christie, A. A. (1982), "The stochastic behavior of common stock variances: Value, leverage and interest rate effects". *Journal of financial Economics*, 10(4), 407-432.
- Emenike, Kalu O. (2010), Modelling stock returns volatility in Nigeria using GARCH Models. Published in: Proceeding of International Conference on Management and Enterprise Development, Ebitimi Banigo Auditorium, University of Port Harcourt - Nigeria, Vol. 1, No. 4 (10. February 2010): pp. 5-11.
- Engle, R. F. (1982), "Autoregressive conditional Heteroskedasticity with estimates of the variance of United Kingdom inflation". *Econometrica*. 50, 987-1007.
- Fama, E. F. (1965), "The behavior of stock-market prices". *The journal of Business*, 38(1), 34-105.
- Floros, C. (2008), "Modeling volatility using GARCH models: Evidence from Egypt and Israel. *Middle Eastern Finance and Economics*, 2: 31-41
- Hourvouliaides, N. L., (2007), "Volatility Clustering in the Greek Futures market: Curse or Blessing?" *International Research Journal of Finance and Economics*. 11, Available from: <http://www.eurojournal>[Accessed on 03/05/2011]
- Jacobsen, B. and Dannenburg, D. (2003), "Volatility clustering in monthly stock returns." *Journal of Empirical Finance*. 10(4): 479-503.
- Jagajeevan, S. (2012), Return Volatility and asymmetric news effect in Sri Lankan Stock Market. *Staff Studies*, 40(1), 37-57
- Louw, J.P (2008), Evidence of volatility clustering on the FTSE/JSE top 40 index. Masters dissertation. Stellenbosch: University of Stellenbosch.
- Mandelbrot, B. (1963), "The Variation of Certain Speculative Prices," *Journal of Business*, 36, 394-419.
- Nelson, D. B. (1991), "Conditional Heteroskedasticity in Asset returns: A new Approach". *Econometrica*, 59 (2): 347-370.
- Park, B. J. (2008), Herd behavior and volatility in financial markets. In *The 3rd International Conference on Asia-Pacific Financial Markets*.
- Samouilhan, N. (2007), The persistence of SA equity volatility: A Component ARCHperspective. *Journal of the Study of Economics and Econometrics*, 31(1): 99-117.
- Yamamoto, R. (2011), "Volatility clustering and herding agents: does it matter what they observe?". *Journal of Economic Interaction and Coordination*. 6 :41-59.

Quantifying volatility clustering in financial time series

Jie-Jun Tseng^a, Sai-Ping Li^{a,b}

^a*Institute of Physics, Academia Sinica, Nankang, Taipei 115, Taiwan*

^b*Department of Physics, University of Toronto, Toronto, Ontario M5S 1A7, Canada*

Abstract

A novel concept is introduced in this work to quantify and compare the volatility clustering among various financial time series. We further give examples to demonstrate that comparing to conventional methods, our approach can extract more details from the financial time series, such as the rise/fall and large/small asymmetry. For example, one obvious feature can be observed from our analysis is that the big losses in financial markets usually lump more severely than big gains. In addition, we also find that instead of the heavy tails in asset return distributions, the slow decay behaviour in autocorrelation functions of absolute returns is actually directly related to the degree of clustering of large fluctuations within the financial time series.

Keywords: Econophysics, Volatility clustering, Heavy-tailed distribution, Financial stylized facts

PACS: 89.65.Gh, 89.75.Da, 05.45.Tp

1. Introduction

In financial markets, prices of stocks and commodities fluctuate over time which then produce financial time series. These time series are in fact of great interest both to practitioners and theoreticians for making inferences and predictions. Using modern day technologies, one can now obtain a vast amount of financial data that record every transaction in financial markets which was not possible a couple of decades ago. The analysis involved is also far more complicated. With the tremendous amount of information obtained over the past decade, researchers have now come to agree on several stylized

Email address: gen@phys.sinica.edu.tw (Jie-Jun Tseng)

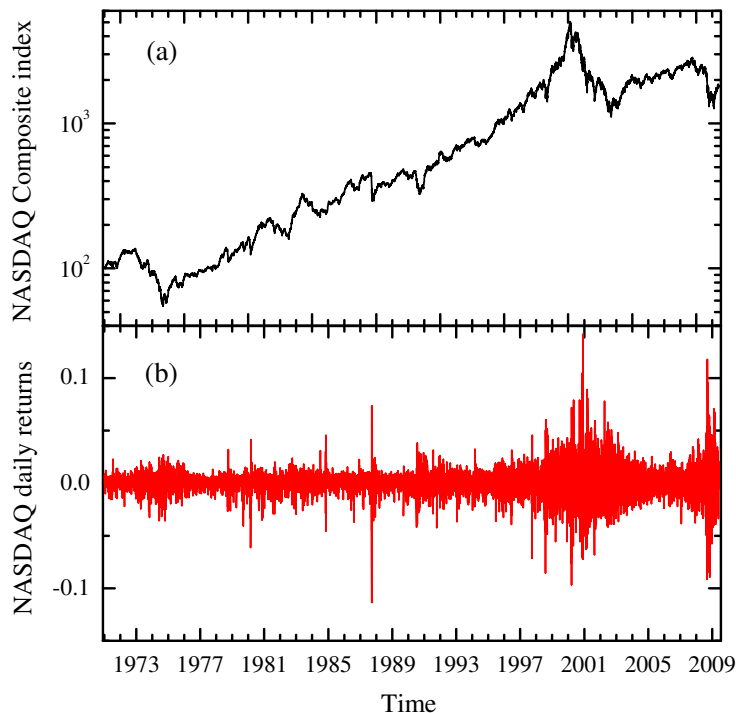


Figure 1: The empirical data of the NASDAQ Composite index from February 8, 1971 through June 30, 2009. (a) shows the historical daily closing price while (b) plots the daily returns during this period.

facts about financial markets, i.e., heavy tails (or fat tails in the terminology of finance) in asset return distributions, absence of auto-correlations of asset returns, volatility clustering, aggregational normality and asymmetry between rises and falls [1, 2, 3, 4, 5]. Figure 1 (a) shows a plot of the historical daily closing values of NASDAQ Composite index from February 8, 1971 through June 30, 2009 while figure 1 (b) is its daily price returns during this period. The price return $R_\tau(t)$ at time t is defined as the difference between the price $p(t)$ of a financial asset (here it is the index value of NASDAQ) at time t and its price a time τ before, $p(t - \tau)$, divided by $p(t - \tau)$,

$$R_\tau(t) = \frac{p(t) - p(t - \tau)}{p(t - \tau)}. \quad (1)$$

Therefore, one can obtain the daily returns $R_1(t)$ by setting $\tau = 1$ trading day and these returns reflect the price fluctuations in this time series. We will use daily returns to define fluctuations in a financial price series throughout this

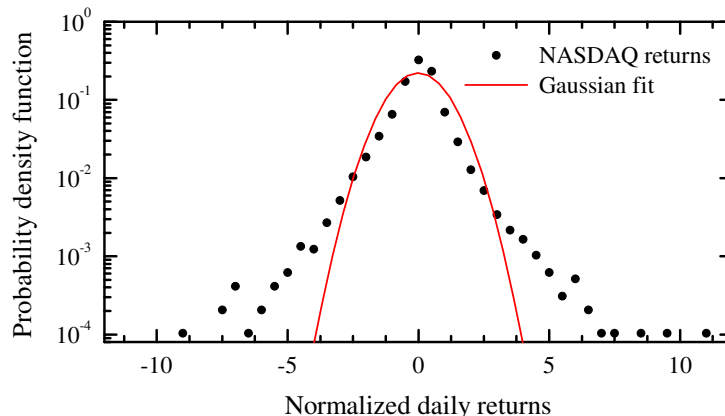


Figure 2: The probability density function of the normalized daily returns of the NASDAQ index in figure 1.

article. As one can see in figure 1 (b) that the daily returns are varying over time. A naive thinking would be that these fluctuations are independent, identically distributed (iid) variables generated by some random processes (i.e., random walks [6]) and therefore the probability density function of the returns should follow a Gaussian distribution. However, it turns out that the empirical distributions of the returns are indeed heavy-tailed. In figure 2, we depict the probability density function of normalized daily returns of the NASDAQ index. The normalized daily return is defined as $(R_1(t) - \mu_R) / \sigma_R$, where μ_R and σ_R denote the average and the standard deviation of $R_1(t)$. One can clearly see that there are heavy tails at the two ends of the distribution. For comparison, we also include a Gaussian fit with $\mu = 0$ and $\sigma = 1$. This is one of the stylized facts that was discovered back in 1960s [7, 8]. Many studies have been carried out over the years on different financial time series and the heavy tails in return distributions have always been observed. There have been many suggestions on the form of the distributions but no general consensus has been reached on the exact form of the tails so far. We will not continue our discussion on this issue here but refer our reader to the literature [4, 5, 9, 10].

In addition to those heavy tails in return distributions, large fluctuations in prices seem to lump together as well [11, 12]. If one examines the empirical time series shown in figure 1, it is easy to observe that large fluctuations in prices are more often followed by large ones while small fluctuations are more likely followed by small ones. This stylized fact is known as volatility

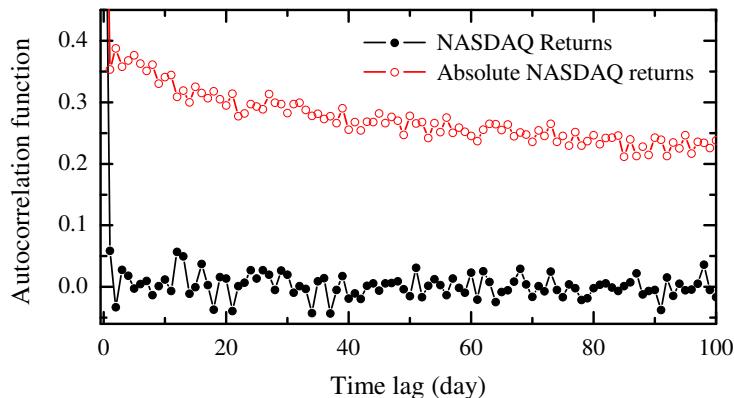


Figure 3: The autocorrelation functions of the returns and its absolute value.

clustering [13]. In financial time series, it is not just that there are more large fluctuations than pure random processes but also these large fluctuations tend to cluster together. It is often suggested that a more quantitative way to view this property is to look at the autocorrelations of the return series [12]. The autocorrelation function $C(x_t, x_{t+\tau})$ is defined as

$$C(x_t, x_{t+\tau}) \equiv \frac{\langle (x_t - \langle x_t \rangle) (x_{t+\tau} - \langle x_{t+\tau} \rangle) \rangle}{\sqrt{\langle x_t^2 \rangle - \langle x_t \rangle^2} \sqrt{\langle x_{t+\tau}^2 \rangle - \langle x_{t+\tau} \rangle^2}}, \quad (2)$$

where $\langle x \rangle$ denotes the expectation value of the variable x . While the returns themselves do not show the evidence of temporal correlations, the absolute returns or their squares do display a positive, pronounced slowly decaying autocorrelation which indeed exhibit power-law decay behaviour. The autocorrelations of the absolute value or the square, etc of the asset returns are often known as the nonlinear autocorrelations. We will only consider the autocorrelation of the absolute returns as an example of the nonlinear autocorrelation in this paper.

Figure 3 are plots of the autocorrelation functions of the returns and its absolute value for the time series shown in figure 1. It is easy to see that there is no correlation among the returns since the autocorrelation function drops to the noise level within a couple of days. On the other hand, the autocorrelation function of the absolute returns, i.e., the nonlinear autocorrelation does exhibit a much slower decay behaviour. Researchers have fitted this with a power law decay, and it is not clear at this moment whether the slow decay should imply long time memory of the financial time series [13]. However,

Table 1: The probability of the occurrence of large and small fluctuations following the occurrence of large or small ones on the previous day (the first column). The result here is for NASDAQ time series.

20%	Largest	Smallest	Rest
Largest	0.3947	0.1156	0.4897
Smallest	0.1265	0.2401	0.6334
Rest	0.1597	0.2148	0.6255

one should also keep in mind that if the time series do possess the properties of the long time memory and the heavy-tailed distribution, many standard estimation procedures (i.e., examining sample autocorrelations.) may fail to work [13, 14, 15]. Therefore, in order to have a more reliable measurement of the volatility clustering, an alternative approach is also needed while dealing with financial time series. For instance, if only the clustering behaviour is concerned, one can simply characterize this property by the concept of probability. Table 1 is an example which shows the probability of the occurrence of large and small fluctuations following the occurrence of large or small fluctuations on the previous day. By large (small) fluctuations, we here choose them to be the largest (smallest) 20% of all the returns and the remaining returns are denoted as the rest. Therefore, each row in table 1 sums to unity. It is easy to see that the probability that there will be a large (small) return following a large (small) one on the previous day is significantly higher (larger than 20% in this case) than that of a pure random process.

A natural question to ask is whether the above stylized facts are indeed related to each other and if so, is it possible for one to understand its origin. In the following, we will give an attempt to answer the first question which would hopefully shed light on searching for an answer to the second question. This paper is organized as follows. In section 2, we will give detailed analysis of volatility clustering in financial time series. In particular, we give arguments on what ingredient in financial time series is responsible for reproducing the nonlinear autocorrelations of price returns such as the one shown in figure 3. We then introduce, in section 3, an index as a quantitative measure of volatility clustering in financial time series. This would allow us to directly compare the degree of volatility clustering across different financial time series. The asymmetry between rises (gains) and falls

(losses) in the time series will be discussed in section 4. Section 5 will be the summary and discussion. In this work, we have carried out the analysis on seven different representative financial time series. They include (i) NASDAQ Composite Index (NASDAQ), (ii) Standard & Poor's 500 index (S&P500), (iii) Hang Seng Index (HSI), (iv) Microsoft stock price (MSFT), (v) US Dollar/New Taiwan Dollar (USD/NTD), (vi) Australian Dollar/New Taiwan Dollar (AUD/NTD) and (vii) West Texas Intermediate (WTI). While we use NASDAQ as an example throughout the paper, we will include the results of other financial time series in the appendix.

2. Volatility clustering and autocorrelation functions

We now begin our study by looking into the question of whether there is a relationship among the heavy tails of return distributions, volatility clustering and autocorrelation functions, if the answer is yes, how they are related. Let us begin by asking the following question: Is it necessary for one to have a heavy-tailed distribution in order for the nonlinear autocorrelation function to exhibit the slow decay? To answer this question, let us now assume that the return distribution follow a Gaussian distribution instead of the empirical distribution shown in figure 2. In this case, we assume the Gaussian distribution to have its mean and standard deviation to be the same as the mean and the standard deviation of the daily returns series in figure 1. One can easily perform a simulation on this. We now draw an equal number of returns from this Gaussian distribution and call it the simulated data set. After this is done, we sort both the empirical set and the simulated set in the descending order of absolute returns. We then substitute the values in the empirical data set by the simulated data set one by one from the largest fluctuation to the smallest one and calculate the nonlinear autocorrelation function of this rearranged Gaussian data. The result is presented in figure 4. For comparison, we also include the nonlinear autocorrelation of the empirical data and the result from a pure Gaussian noise which is drawn from a Gaussian distribution but without arranging the data according to the positions of empirical data set like we do for the rearranged Gaussian data. The pure Gaussian noise shows no temporal correlations as expected. What is surprising is that the rearranged Gaussian returns shows the same kind of slow decay behaviour as the empirical data set. On the other hand, if we randomize the temporal positions of the empirical returns, namely, we reshuffle the original financial time series, the result we obtain is always sim-

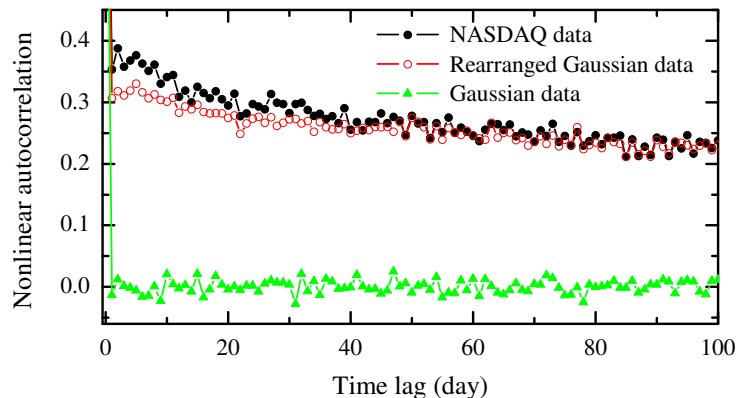


Figure 4: The nonlinear autocorrelation function of the empirical data and of the rearranged Gaussian data.

ilar to the case of the pure Gaussian noise, which means that there is no temporal correlation. The above analysis therefore strongly suggests that the heavy tails in return distributions are not responsible for the slow decay behaviour of the nonlinear autocorrelation functions.

If the heavy tails in the distributions are not responsible for slow decay in nonlinear autocorrelation functions, what possible ingredients in the financial time series would be responsible for such a slow decay behaviour. We here try to provide an answer to this question. Let us begin by looking at the clustering of large price fluctuations in figure 1. We begin by picking out the largest $p\%$ (where p is a constant) fluctuations (whether they are positive or negative) in the time series¹ and see whether their clustering behaviour would affect the nonlinear autocorrelation function of the returns. Since we are only interested in the clustering behaviour, which in turn means the temporal positions but not the values of the large fluctuations in the financial time series, we can here simply use 1 to represent the largest $p\%$ fluctuations and 0 for all the other smaller fluctuations. In this way, we will have a sequence which contains only 0 and 1. This will in turn make our analysis much easier to interpret. Figure 5 shows the nonlinear autocorrelation of figure 1 using 1 for the largest $p\%$ fluctuations and 0 for the rest. We here include the results

¹A similar treatment is to pick the large fluctuations that are outside q standard deviations of the average value of the returns, where q is a pure number, see e.g., H.E. Stanley [16].

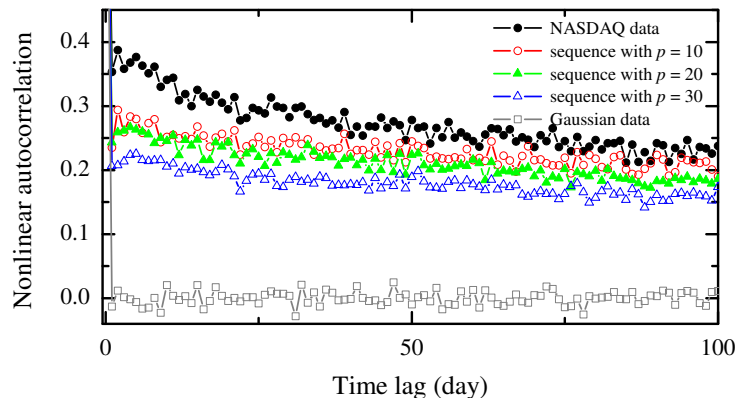


Figure 5: The nonlinear autocorrelation functions of the empirical data, the Gaussian data and the sequences of 1s and 0s with $p = 10, 20$ and 30 . p here refers to the largest $p\%$ fluctuations in the empirical returns and are represented by 1s while the rest are represented by 0s.

for sequences with $p = 10, 20$ and 30 . To facilitate our discussion, we also include both the nonlinear autocorrelation for empirical data and the Gaussian noise for comparison. One can see that all these sequences show similar slow decay behaviour as the original empirical data set, though with smaller values. This analysis thus shows that the positions of the large fluctuations are essential for a slow-decaying nonlinear autocorrelation function. Therefore, one can conclude that it is the clustering of large fluctuations rather than the heavy tail in the return distribution which should be responsible for the slow decay behaviour of nonlinear autocorrelation functions. This fact has also been observed in the other financial time series in our study and the results are presented in the appendix.

Before we end this section, we would also like to make a further study of the clustering of fluctuations in financial time series. Instead of looking at the clustering of large fluctuations, we now focus on the clustering of the small fluctuations in time series. Since small fluctuations are smaller in value and basically do not contribute to the nonlinear autocorrelation functions, they are often left out in the discussion in the literature. However, whether their temporal positions in a time series can have similar effects as the large fluctuations is an interesting question that one can ask. In figure 6 (a), we plot the historical daily return time series of the currency exchange rate USD/NTD from July 2, 2001 through June 30, 2009, where the black line denotes the original empirical returns while the red one represents the

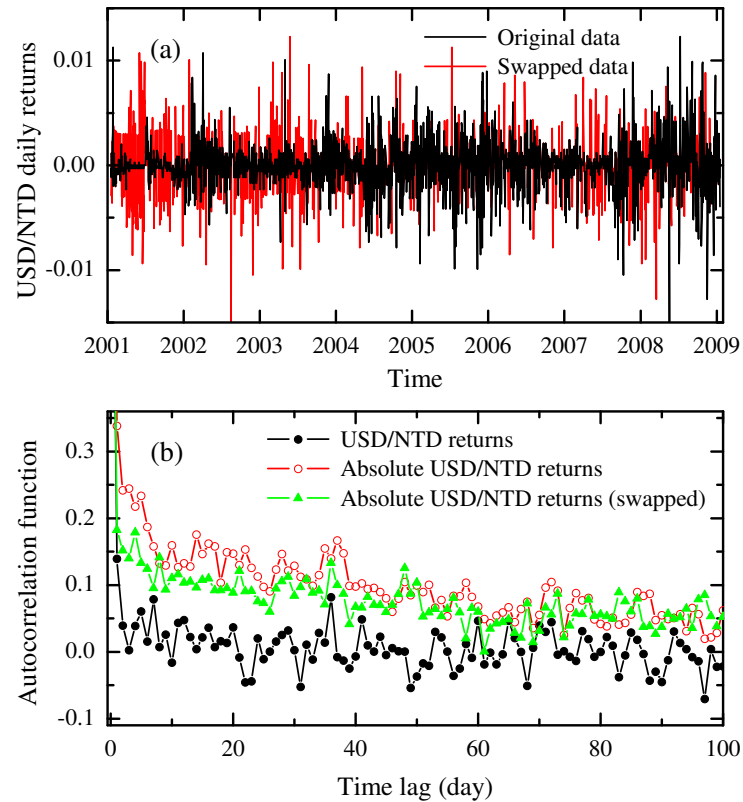


Figure 6: (a) The historical daily return series for the currency exchange rate USD/NTD (black) and the series with the largest 20% and smallest 20% of the returns being swapped (red). (b) The nonlinear autocorrelations of the original returns (line with open circles) and the swapped returns (line with triangles).

same set but with the largest 20% and smallest 20% of the returns being swapped. The nonlinear autocorrelations of the original empirical returns (line with open circles) and the swapped returns (line with triangles) are drawn in figure 6 (b). We also include in this figure the autocorrelation function of the original returns for comparison. One can see that although the line with triangles has values smaller than the original data set, both lines have similar slow decay behaviour. This in turn means that the clustering of small fluctuations in this returns series has basically the same kind of feature as that of their large fluctuation counterparts. On the other hand, as we swap the large and small fluctuations in the other six financial time series that we have been investigating, the nonlinear autocorrelation functions of the swapped returns series show no sign of slow decay. They basically drop very fast, similar to the kind of Gaussian noise in figure 4. This interesting fact will be discussed in more detail in the next section as we introduce a clustering index to quantitatively study the clustering behaviour of different financial time series. The introduction of this index would then allow us to directly compare the degree of clustering across different financial time series.

3. Quantitative measurement of volatility clustering

As mentioned above, in order to discuss the volatility clustering in a more quantitative way, it is better to introduce some parameters to quantitatively measure the volatility clustering of different financial time series that we can make comparison with. We here introduce an index to quantify the volatility clustering in the financial time series. We begin by introducing a moving window with a certain window size to scan through a given time series. As an example, one can pick a window with size of n (where n is fixed throughout the scanning process) trading days. Similar to what we have done in previous section, we can count the total number of trading days that are among the largest $p\%$ fluctuations in returns within this window as we scan through the time series. As we will see, one can interpret this as the degree of volatility clustering of the largest $p\%$ fluctuations with respect to this particular window with size n .

Figure 7 is an illustration of the clustering of the largest 20% fluctuations in figure 1 with a window size of 10 trading days, a span of two weeks in real daily life. The statistics here is obtained by using the so called moving window method. This means that we begin by putting the window on the first day of the whole series and count the number of days among largest

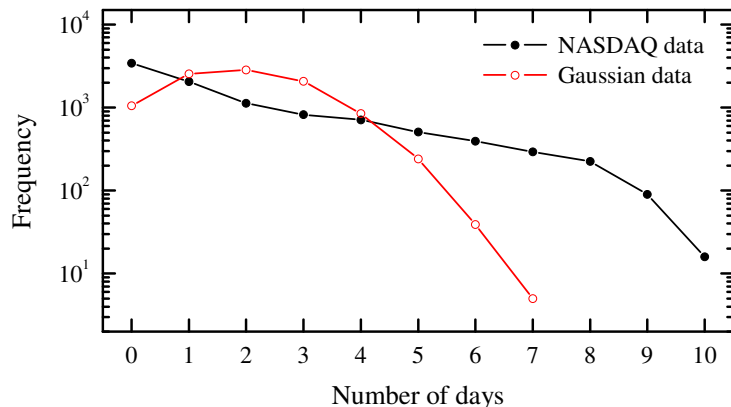


Figure 7: The plot of the frequency distribution of the number of days with largest 20% fluctuations within a window of 10 trading days.

20% fluctuations within this 10-day window. This is the first step. We then move on to the second day of the whole series and again count the number of days among largest 20% fluctuations within this next 10-day window, the second step. We repeat the same procedure until we finish scanning through the whole time series. The curve with full circles in figure 7 is a plot of the frequency distribution of the number of days among the largest 20% fluctuations within a 10-day period by using this moving window method. To make it into a quantitative measure of the degree of clustering, we need to compare it with a randomly generated time series for example, a Gaussian noise series. The curve with open circles in figure 7 is the frequency distribution of the number of days of the largest 20% fluctuations within a 10-day period from a simulated Gaussian noise series. From figure 7, one can already visually tell the difference between these two curves. To be more concise, we take the ratio of the standard deviation of the number of days of the largest $p\%$ fluctuations within the n -day window between the empirical and the simulated data sets. Mathematically, it is defined as $R_n \equiv \sigma_e/\sigma_G$, where σ_e and σ_G are the standard deviation of the number of days of the largest $p\%$ fluctuations within an n -day period for the empirical and simulated Gaussian data sets respectively. The larger the ratio is, the larger the degree of clustering will be. This result can be understood easily. The average number of days of largest $p\%$ fluctuations within a window size of n is equal to $p \times n/100$. This is true irrespective of whether it is the empirical data set or the simulated one. One can indeed see this for the simulated data set which has a peak

near this value. However, if the time series displays the phenomenon of clustering of large fluctuations, there will be a higher frequency of occurrence that the number of days of the largest $p\%$ fluctuations within this window is much larger than the average value $p \times n/100$. Similarly, there will also be a higher frequency of occurrence that the number of days of the largest $p\%$ fluctuations within this window is much smaller than the average value $p \times n/100$. This scenario will indeed be reflected in the value of the standard deviation of the frequency distribution in figure 7. Thus, one can simply take the ratio of the standard deviation of the empirical and simulated data sets to get a quantitative measure of the degree of clustering of the largest $p\%$ fluctuations of the financial time series that one is interested in.

The ratio or index R_n that we introduce here can in fact be studied analytically. It has both theoretical upper and lower bounds and the standard deviation of the simulated Gaussian noise can also be calculated analytically. Let us first derive the theoretical value of the standard deviation of the simulated Gaussian noise. Recall from above that the mean value of the average number of days of the largest $p\%$ fluctuations within a n -day window is equal to $p \times n/100$. For a total of n days, the probability that there are m days with fluctuations among the largest $p\%$ fluctuations can be written as

$$\frac{n!}{m!(n-m)!} P^m (1-P)^{n-m}, \quad (3)$$

where P denotes $p/100$. We here convert the percentage into decimals for simplicity. The standard deviation of the average number of days of the largest $p\%$ fluctuations within a n -day window is therefore equal to

$$\sigma_G = \left[\sum_{m=0}^n (m - Pn)^2 P^m (1-P)^{n-m} \right]^{1/2} = \sqrt{nP(1-P)}, \quad (4)$$

which is the familiar result in statistics for the standard deviation of a sequence of n random events with occurrence probability P . The theoretical lower bound for the index corresponds to the case when the time series is completely random, which is therefore equal to 1.

To get a theoretical upper limit of the standard deviation of the average number of days of the largest $p\%$ fluctuations within a n -day period, we proceed as follows. We look for an extreme case when all the largest $p\%$ fluctuations are ordered one after the other, then follow by the rest of the

data points (one can of course reverse the order of the largest $p\%$ fluctuations and the rest). The first $p\%$ of the data points will then be represented by 1 and the rest will be by 0, as what we have done in the above. This is the case when we should have the largest possible degree of clustering. If one plots this extreme case in figure 7, one will have two peaks in the frequency distribution function, one is at 0, and the other is at n (10 in the case in figure 7). Let us now use a window of size n and begin with the first data point, which is a 1, and count the n data points in this window, all of which are 1s (assuming that the length of the time series N is much longer than the window size n). Recall that we call this procedure to be step one. We then let the window slide to the next data point, the second step, and so on. As the moving window continues to move along the time series, it will have moved $PN - n + 1$ steps before it reaches the first 0. We again have P here to be equal to $p/100$ for simplicity. As it continues to move along the time series, the number of 1s will decrease while the number of 0s will increase until the window consists of all 0s. There are then $(1 - P)N - n + 1$ steps which has all 0s within the moving window. For the whole time series, we have a total of $N - n + 1$ steps so we have to average over these steps. It is now easy to calculate the standard deviation in this extreme case, which is the square root of the expression in Eq. (5). Recall that the average 1s within the moving window is Pn . We then have

$$\begin{aligned} & \frac{1}{N-n+1} \{ (PN - n)(n - Pn)^2 + [(1 - P)N - n] (Pn)^2 + \sum_{m=0}^n (m - Pn)^2 \} \\ & = \frac{1}{N-n+1} \{ n^2(N - n - 1)P(1 - P) + \frac{n(n+1)(2n+1)}{6} - n^3 [P^2 + (1 - P)^2] \}. \end{aligned} \quad (5)$$

In the limit PN and $(1 - P)N \gg n$, the right hand side of Eq. (5) reduces to $n^2P(1 - P)$. Therefore, the theoretical limit of the standard deviation σ_{lim} as N goes to infinity is

$$\sigma_{\text{lim}} = \sqrt{n^2P(1 - P)}. \quad (6)$$

The theoretical upper limit of R_n is then equal to

$$R_n^{\text{lim}} = \frac{\sigma_{\text{lim}}}{\sigma_G} = \sqrt{n}. \quad (7)$$

Figure 8 shows the value of the clustering index for NASDAQ time series in figure 1 for various largest $p\%$ fluctuations as a function of window size n . The different curves represent the different largest $p\%$ of the fluctuations in

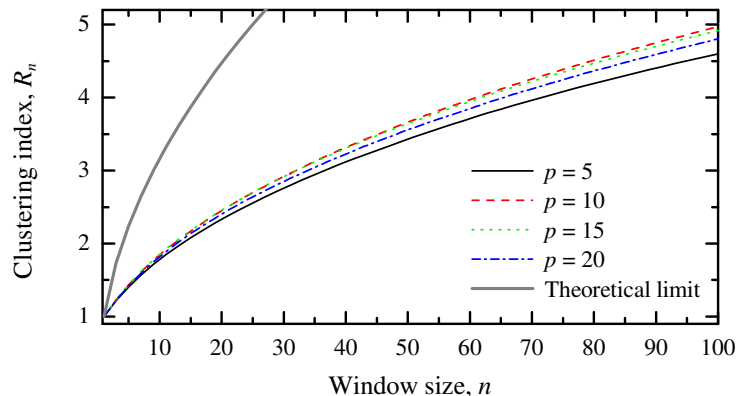


Figure 8: The clustering index, R_n , for the NASDAQ return series with $p = 5$ (solid), 10 (dash), 15 (dot) and 20 (dash dot). The theoretical limit of the index is drawn as a thick line for comparison.

the time series. We have included here the results for $p = 5, 10, 15$ and 20 . Also included is the curve of the theoretical limit of the index. The index values all start from unity when the window size n corresponds to 1 trading day, and gradually increase as the window size increases.

With the clustering index in hand, one can practically study the behaviour of clustering of any sort of fluctuations in a financial time series. Other than the largest $p\%$ that we have looked into, one can also look at the degree of clustering for small fluctuations. To give the reader an idea of how one can use the index to study the properties of financial time series, we go back to a case which we considered in previous section. Recall that we have studied a time series in which we swapped the largest $p\%$ and smallest $p\%$ of the returns in the series, as indicated in figure 6. It turns out that the nonlinear autocorrelation function of the swapped data set still exhibits similar slow decay behaviour. On the other hand, we have analyzed the other six time series that we consider in this paper and there is practically no such kind of slow decay behaviour of the swapped data sets. Using the index that we introduce here, the difference becomes clear. Figure 9 shows the curves for the index value of the smallest 20% returns vs. window size in all the seven financial time series that we study in this work. One can now see that the value of the index is rather small for each of the other six financial time series when compared with the curve for USD/NTD. This means that the clustering of the smallest 20% returns of these other financial time series indeed behave not much different from random sequences. On the other

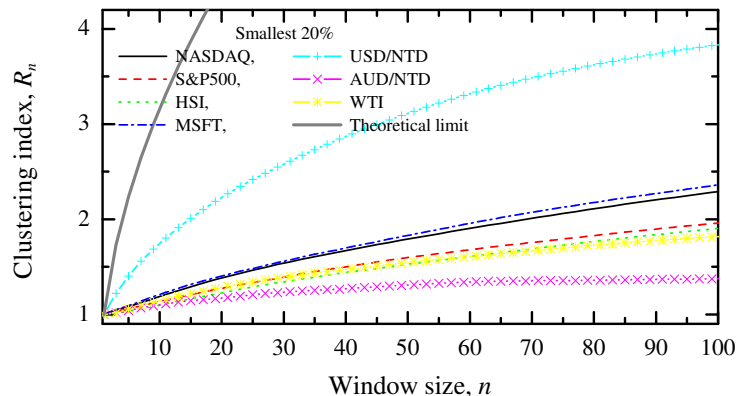


Figure 9: The clustering index for smallest 20% returns of the NASDAQ, S&P500, HSI, MSFT, USD/NTD, AUD/NTD and WTI series. The theoretical limit of the index is drawn as a thick line for comparison.

hand, the clustering of the time series USD/NTD as shown in figure 6 is significantly larger which in turn reflects the slow decay behaviour of the swapped data set in figure 6. This example suggests that the index that we introduce here is a good indicator to quantify the degree of clustering of fluctuations in financial time series. In the next section, we will see that the index that we introduce here indeed contains more information than people have previously observed in financial time series.

4. Rise/Fall asymmetry

There exist discussions in the literature [17, 18, 19, 20] about the asymmetry of asset returns such as the skewness of the returns distribution in figure 2. In the study of financial time series, one can for example, ask whether there are more days that the returns are gains (rises) rather than losses (falls) as some kind of asymmetry. One can further ask whether the returns in gains would like to cluster more or the other way round, how large the difference is, and whether large fluctuations tend to cluster more, etc. These can all be viewed as asymmetries in a financial time series. With the index introduced in previous section, one should hopefully be able to extract more information on the asymmetries in financial time series and to study these asymmetries on a more quantitative basis. To study the asymmetries in financial time series, let us first give the definitions here. In the case of the asymmetry between the largest/smallest returns, we adopt the notation that

the largest and smallest fluctuations refer to the absolute returns as before. We first obtain the clustering index for the largest and smallest $p\%$ returns. The asymmetry of largest/smallest returns A_{ls} is then defined as

$$A_{ls} = \frac{R_l - R_s}{R_l + R_s}, \quad (8)$$

where R_l and R_s are the indices for the largest and smallest $p\%$ fluctuations respectively. This asymmetry will give us an idea whether the large fluctuations or the small fluctuations would like to cluster more as we increase the size of the moving window. From this definition, it is clear that A_{ls} is equal to zero when the window size is equal to 1, since there are an equal number of largest and smallest fluctuations.

In a similar fashion, one can define the asymmetry between the largest positive and negative returns, which we call A_{+-} as follows

$$A_{+-} = \frac{R_+ - R_-}{R_+ + R_-}, \quad (9)$$

where R_+ and R_- are the indices for the largest positive and negative returns respectively. We should remind our reader here that in the case of A_{+-} , we first pick up the largest $p\%$ fluctuations from the absolute returns and then separate the fluctuations (returns) into positive and negative categories. In this way, we can see the asymmetry between the large positive and negative returns as well as their degree of clustering. Notice that the asymmetries as defined above are bounded by 1 and -1. Figure 10 contains the plots of the asymmetries A_{ls} and A_{+-} for $p = 15$ and 20 for the NASDAQ time series in figure 1. From the figure, it is easy to observe that the two curves for A_{ls} are always positive, which means that the degree of clustering is more obvious for large fluctuations than for small fluctuations in the NASDAQ times series. On the other hand, the two curves for A_{+-} are always below zero. This reflects the fact that negative returns, or big losses are likely to cluster together than big gains in the case of NASDAQ. This is in agreement with some observations [2, 19] indicating that there are more big losses rather than big gains in financial markets since we have more big losses and these big losses are more likely to lump together. We should remark here that the window size equals to 1 corresponds to the asymmetry of distribution of returns in figure 2. In the case of NASDAQ, the asymmetry is negative. There are however, examples of financial time series that the asymmetry

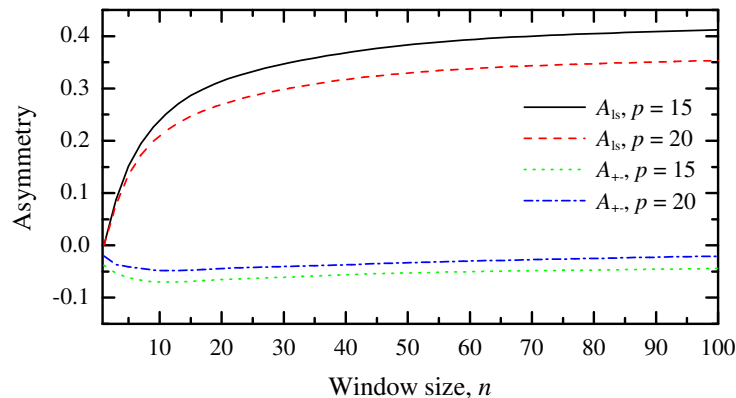


Figure 10: The asymmetry A_{ls} and A_{+-} with $p = 15$ and 20 for NASDAQ return series.

for the probability density function is positive and they are included in the appendix below. By increasing the size of the moving window, one can also study the asymmetry of returns with respect to the clustering of large and small fluctuations. Therefore, the use of the index to study asymmetries in financial time series allows one to extract more information comparing to conventional methods.

The asymmetry between rises (gains) and falls (losses) in returns can also be observed in the probability of the occurrence of large and small fluctuations following the occurrence of large or small ones on the previous day, which is shown in table 2. Unlike table 1, we now separate the rise and fall of the fluctuations into separate categories. Each row in this table sums to unity as before. In this way, one can easily detect the difference.

5. Summary and discussion

In this paper, we have made a detailed analysis of the stylized facts in financial time series. We have found that the slow decay behaviour is directly related to the degree of clustering of the large fluctuations (absolute returns) within the financial time series while the heavy tails in return distributions do not seem to play a role here. We have also introduced an index to quantitatively measure the clustering behaviour of fluctuations in financial time series and have given examples to demonstrate its advantages over the conventional methods. This index has both theoretical lower and upper bounds. It is equal to unity if the fluctuations are independent, identically distributed within the financial time series. On the other hand, its upper bound can also

Table 2: The probability of the occurrence of large and small rise/fall following the occurrence of large or small rise/fall on the previous day (the first column).

20%	Largest (rise/fall)	Smallest (rise/fall)	Rest (rise/fall)
Largest (rise)	0.2054/0.1514	0.0551/0.0724	0.3319/0.1838
Largest (fall)	0.1856/0.2438	0.0365/0.0681	0.2122/0.2538
Smallest (rise)	0.0451/0.0573	0.1437/0.1023	0.3624/0.2892
Smallest (fall)	0.0790/0.0767	0.1226/0.1100	0.3471/0.2646
Rest (rise)	0.0742/0.0582	0.1269/0.0934	0.4475/0.1998
Rest (fall)	0.0737/0.1255	0.1183/0.0888	0.2888/0.3049

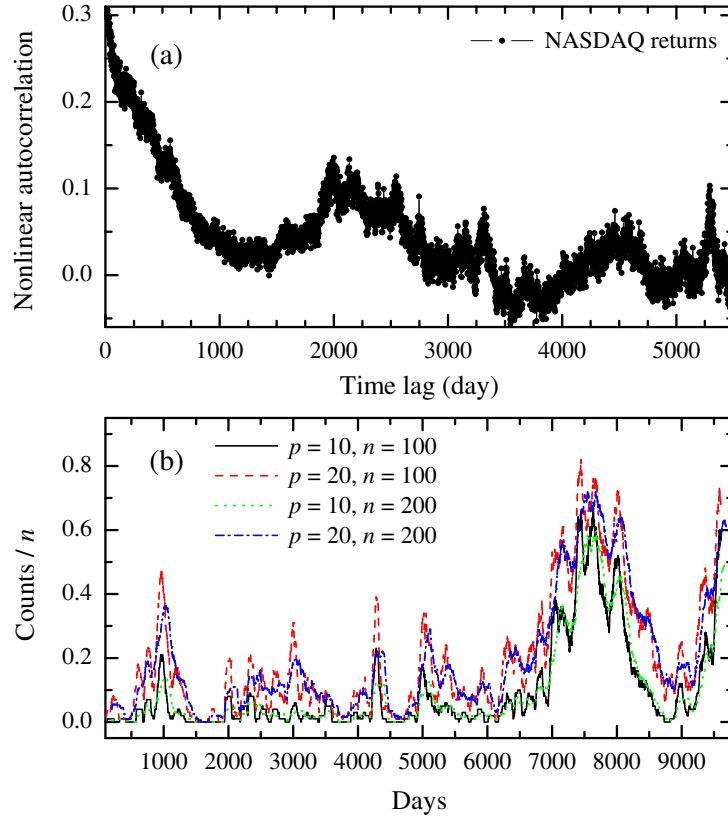


Figure 11: (a) The nonlinear autocorrelation of the NASDAQ returns with large time lags. (b) The event counts for the largest $p\%$ fluctuations in the NASDAQ returns within a moving window of size of n days.

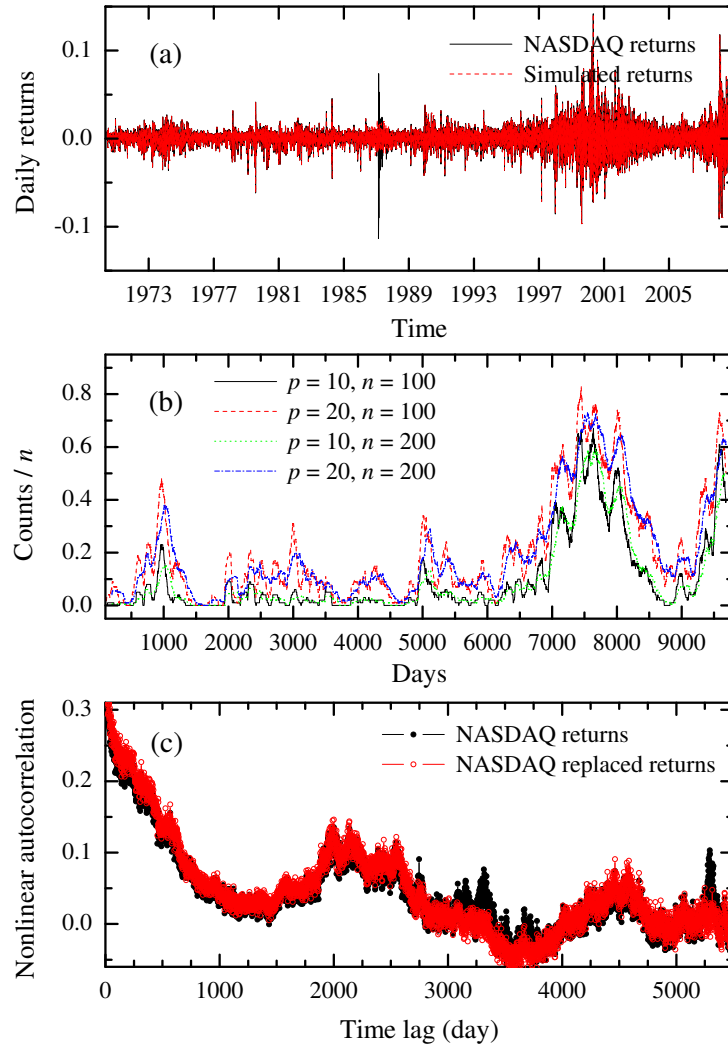


Figure 12: (a) The comparison between the NASDAQ returns (solid) and the simulated returns (dash) with the cluster of large fluctuations around the 4300th day replaced by Gaussian noise fluctuations. (b) The event counts for the largest $p\%$ fluctuations in the corresponding simulated NASDAQ returns within a moving window of size of n days. (c) The nonlinear autocorrelation for the NASDAQ (line with dots) and the simulated returns (line with open circles) with large time lags.

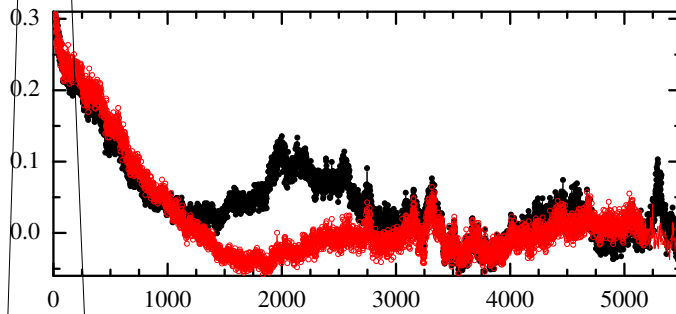


Figure 13: (a) The comparison between the NASDAQ returns (solid) and the simulated returns (dash) with the cluster of large fluctuations around the 9600th day replaced by Gaussian noise fluctuations. (b) The event counts for the largest $p\%$ fluctuations in the corresponding simulated NASDAQ returns within a moving window of size of n days. (c) The nonlinear autocorrelation for the NASDAQ (line with dots) and the simulated returns (line with open circles) with large time lags.

be analytically calculated and in the limit when the time scale of the given series is much longer than the window size n , the index R_n is simply equal to \sqrt{n} . With this index in hand, one not only can study the asymmetry of the asset returns but also the effect of clustering on the asymmetry properties in financial time series. One can see that the larger fluctuations tend to cluster more than the smaller ones. Similarly, big losses tend to lump together more severely than big gains. These findings should be helpful to people who make investments in financial markets.

There are also interesting features that appear in the autocorrelation functions of financial time series that are related to the clustering of large fluctuations. Figure 11 (a) again shows the nonlinear autocorrelation vs. time lag of NASDAQ, which already appeared in figure 4 earlier. However, we here show the time lag up to 5000+ days. The interesting feature that appear in figure 11 (a) are the bumps that appear at time lags around the 2000th day, the 3300th day, the 5300th day, and etc. These bumps can in fact be understood from the properties of clustering of large fluctuations in financial time series. Figure 11 (b) shows the event counts for the largest $p\%$ fluctuations in the NASDAQ returns within a n -day moving window. (For comparison among the results with different n , we have here divided the event counts by n .) One can observe that there are clusters of large fluctuations around the 1000th, the 4300th, the 7500th and the 9600th day. The appearance of these clusters is the cause of bumps appearing in the nonlinear autocorrelation. To demonstrate that this is indeed the case, we have replaced the large fluctuation clusters around the 4300th and the 9600th day by Gaussian noise fluctuations while the results are shown in figures 12 and 13, respectively. In figure 12, the 4300th day cluster is replaced by simulated Gaussian noise fluctuations and the simulated time series is plotted in figure 12 (a) together with the empirical NASDAQ returns for comparison. Figure 12 (b) is the event counts for the corresponding simulated series while figure 12 (c) shows the nonlinear autocorrelation for both the empirical (line with dots) and simulated (line with open circles) returns. It is clear that both bumps near the 3300th and the 5300th day disappear in the simulated NASDAQ series. Therefore, we conclude that the bump near the 3300th (5400th) day in the nonlinear autocorrelation is indeed a result of the correlation between the large fluctuation clusters around the 7500th (9600th) day with the large fluctuation cluster around the 4300th day in the NASDAQ returns.

In a similar fashion, we replace the large fluctuation cluster around the

9600th day by Gaussian noise fluctuations and the result is shown in figure 13. We can now see that the bump around the 2000th day in the nonlinear autocorrelation disappears. One can further verify the bumps that appear at various time lag in the nonlinear autocorrelations are actually results of the correlations between large fluctuation clusters by replacing them by Gaussian noise fluctuations. With this approach, we check through the bumps in the nonlinear autocorrelations for all the financial time series investigated in this work. The results are included in figure A.4 for reference. We expect that this bump behaviour is a general phenomenon in financial time series which have large fluctuation clusters.

Whether the clustering of large fluctuations in financial time series is from long time memory effect or other effects such as human psychology is not clear to us at the moment. Indeed, if only the clustering of large fluctuations is concerned, one is able to find complex systems that are random in nature but can possess the property of large degree of clustering. It is also possible to find simple ways which can give both large degrees of clustering and slow-decaying nonlinear autocorrelations in a simulated time series. We will discuss these issues in a future publication [21].

Acknowledgments

This work was supported in part by the National Science Council of Taiwan under grants NSC#98-2120-M-001-002 and NSC#97-2112-M-001-008-MY3.

Appendix

For comparison, we here show the results of other financial time series as mentioned in section 1 with the same procedures introduced in this paper. They include (i) Standard & Poor's 500 index (S&P500, from January 4, 1950 through June 30, 2009), (ii) Hang Seng Index (HSI, from January 2, 1987 through June 30, 2009), (iii) Microsoft stock price (MSFT, from March 4, 1986 through June 30, 2009), (iv) US Dollar/New Taiwan Dollar (USD/NTD, from July 2, 2001 through June 30, 2009), (v) Australian Dollar/New Taiwan Dollar (AUD/NTD, from July 2, 2001 through June 30, 2009) and (vi) West Texas Intermediate (WTI, from January 6, 1986 through June 30, 2009).

References

- [1] R. Cont, Empirical properties of asset returns: stylized facts and statistical issues, *Quant. Finance* 1 (2001) 223–236.
- [2] R. F. Engle, A. J. Patton, What good is a volatility model?, *Quant. Finance* 1 (2001) 237–245.
- [3] A. Chakraborti, I. M. Toke, M. Patriarca, F. Abergel, *Econophysics: Empirical facts and agent-based models*, arXiv:0909.1974 (2009).
- [4] R. N. Mantegna, H. E. Stanley, *Introduction to Econophysics: Correlations and Complexity in Finance*, Cambridge University Press, Cambridge, 2000.
- [5] J. P. Bouchaud, M. Potters, *Theory of Financial Risk and Derivative Pricing: From Statistical Physics to Risk Management*, Cambridge University Press, Cambridge, 2003.
- [6] L. Bachelier, Théorie de la spéculation, *Ann. Sci. Ec. Normale Supérieure* 17 (1900) 21.
- [7] B. Mandelbrot, The variation of certain speculative prices, *Journal of business* 36 (1963) 394.
- [8] E. F. Fama, The behavior of stock market prices, *Journal of Business* 38 (1965) 34–105.
- [9] L. Gillemot, J. Töyliä, J. Kertész, K. Kaskia, Time-independent models of asset returns revisited, *Physica A* 282 (2000) 304–324.
- [10] B. LeBaron, Robust properties of stock return tails, Tech. rep., International Business School, Brandeis University (2008).
- [11] R. F. Engle, Autoregressive conditional heteroscedasticity with estimates of the variance of united kingdom inflation, *Econometrica* 50 (1982) 987–1009.
- [12] Z. Ding, C. Granger, R. F. Engle, A long memory property of stock market returns and a new model, *Empirical Finance* 1 (1993) 83–106.

- [13] R. Cont, Long Memory in Economics, Springer Berlin Heidelberg, Heidelberg, 2007, Ch. Volatility clustering in financial markets: empirical facts and agent-based models, pp. 289–309.
- [14] S. I. Resnick, A practical guide to heavy tails, Birkhäuser Boston, Boston, 1998, Ch. Why non-linearities can ruin the heavy-tailed modeler's day, pp. 219–239.
- [15] S. Resnick, G. Samorodnitsky, F. Xue, How misleading can sample ACFs of stable MAs be? (very!), Ann. Appl. Probab. 9 (1999) 797–817.
- [16] F. Wang, K. Yamasaki, S. Havlin, H. E. Stanley, Complex Sciences, Vol. 4 of Lecture Notes of the Institute for Computer Sciences, Social Informatics and Telecommunications Engineering, Springer Berlin Heidelberg, Heidelberg, 2009, Ch. Return intervals approach to financial fluctuations, pp. 3–27.
- [17] O. Henry, Modelling the asymmetry of stock market volatility, Appl. Financial Econ. 8 (1999) 145–153.
- [18] A. Peiró, Asymmetries and tails in stock index returns: are their distributions really asymmetric?, Quant. Finance 4 (2004) 37–44.
- [19] J. Chen, H. Hong, J. C. Stein, Forecasting crashes: trading volume, past returns, and conditional skewness in stock prices, J. Financial Econ. 61 (2001) 345–381.
- [20] M. M. Pelagatti, Modelling good and bad volatility, Stud. Nonlinear Dyn. Econ. 13 (2009) Article 2.
- [21] J. J. Tseng, S. P. Li, in preparation.

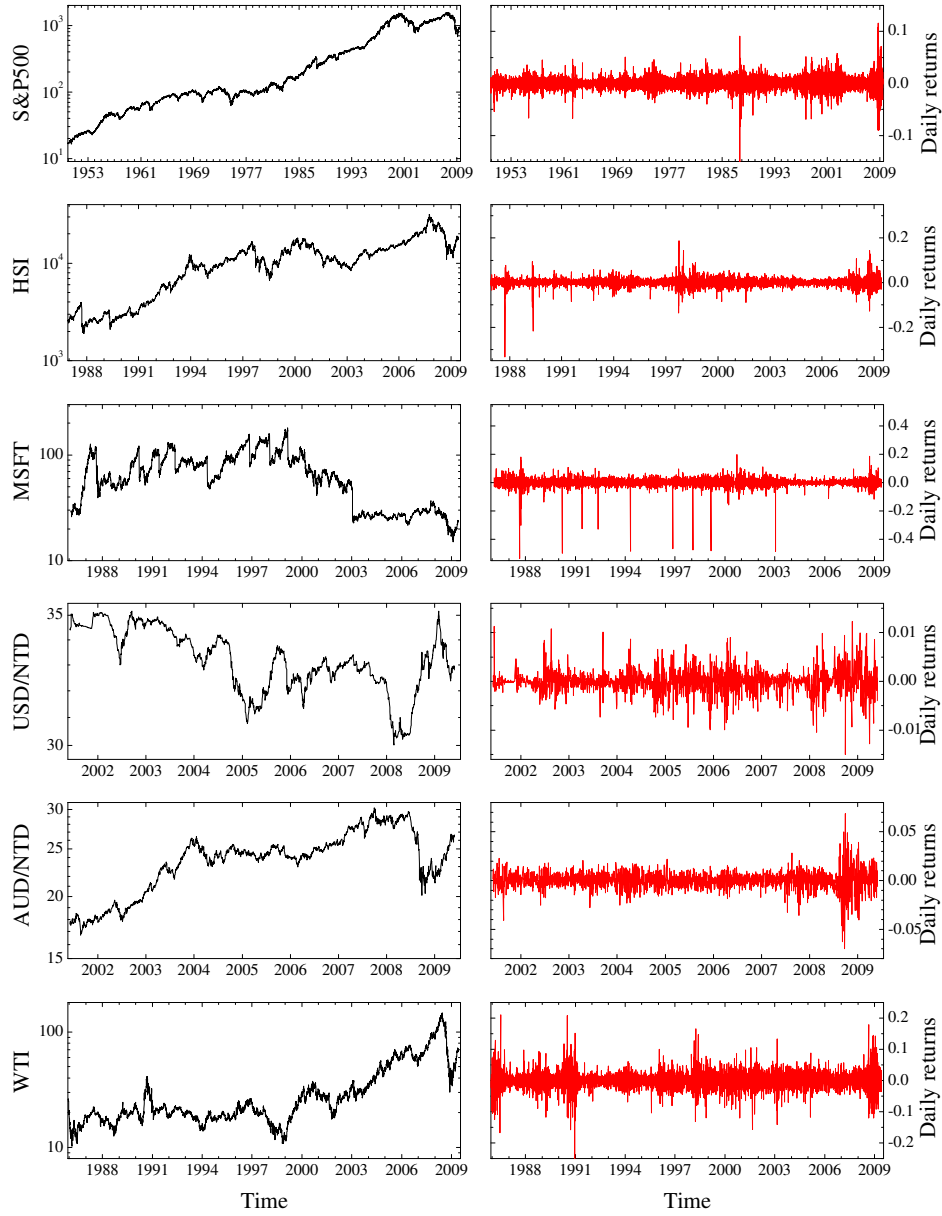


Figure A.1: The left panels are plots of the historical daily closing value for S&P500, HSI, MSFT, USD/NTD, AUD/NTD and WTI (from top to bottom), while the right panels show the daily returns for each of these time series.

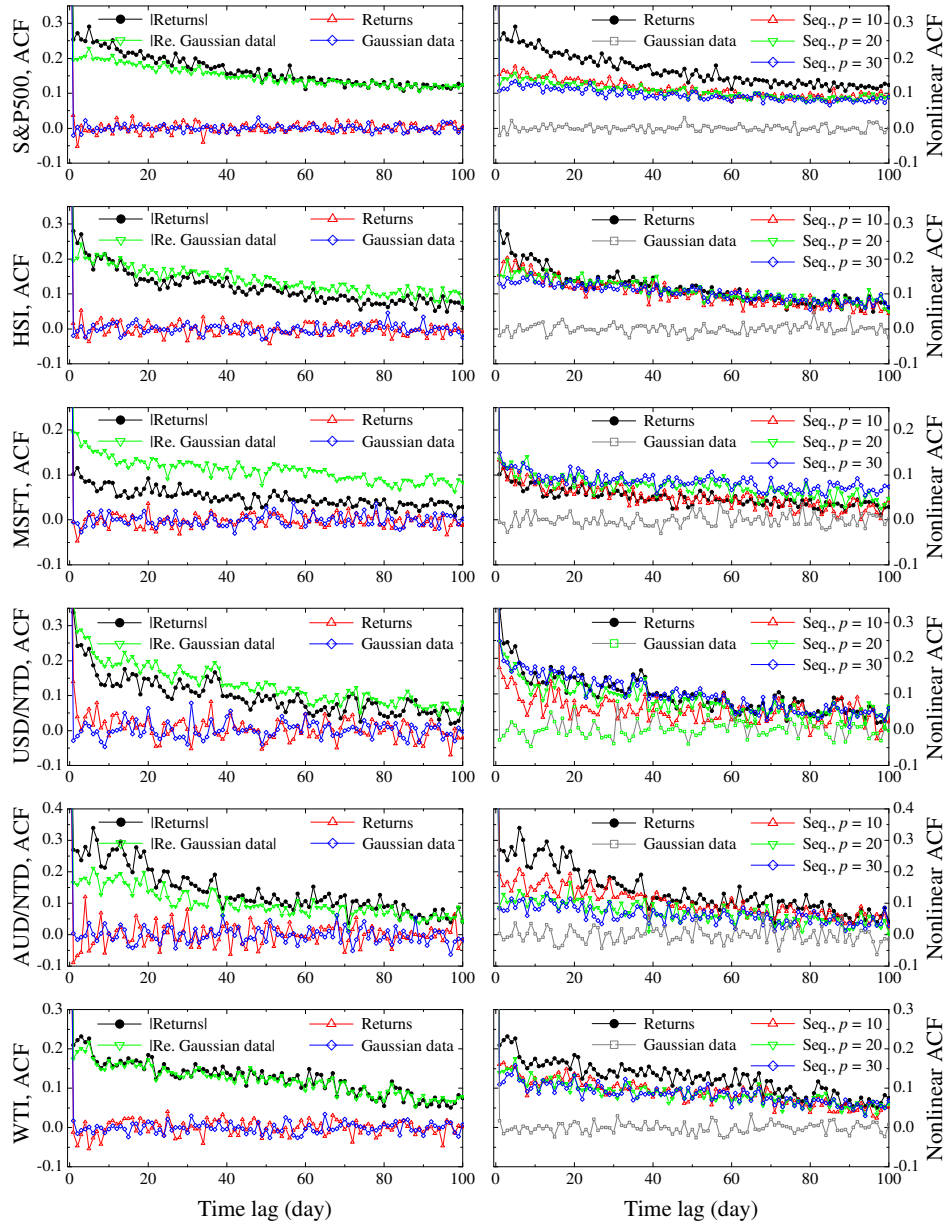


Figure A.2: The left panels are plots of the autocorrelation functions for S&P500, HSI, MSFT, USD/NTD, AUD/NTD and WTI returns (from top to bottom), while the right panels show the nonlinear autocorrelations of the sequences of 1s and 0s with $p = 10, 20$ and 30 as extracted from these returns.

Table A.1: The probability of the occurrence of large and small fluctuations following the occurrence of large or small ones on the previous day (the first column).

S&P500, 20%	Largest	Smallest	Rest
Largest	0.2999	0.1556	0.5445
Smallest	0.1440	0.2305	0.6255
Rest	0.1853	0.2046	0.6101
HSI, 20%	Largest	Smallest	Rest
Largest	0.3226	0.1568	0.5206
Smallest	0.1587	0.2126	0.6287
Rest	0.1730	0.2101	0.6169
MSFT, 20%	Largest	Smallest	Rest
Largest	0.3087	0.1327	0.5586
Smallest	0.1354	0.2419	0.6227
Rest	0.1852	0.2085	0.6063
USD/NTD, 20%	Largest	Smallest	Rest
Largest	0.3985	0.0777	0.5238
Smallest	0.0501	0.4010	0.5489
Rest	0.1840	0.1724	0.6436
AUD/NTD, 20%	Largest	Smallest	Rest
Largest	0.2700	0.1600	0.5700
Smallest	0.1825	0.2200	0.5975
Rest	0.1827	0.2068	0.6105
WTI, 20%	Largest	Smallest	Rest
Largest	0.3120	0.1762	0.5118
Smallest	0.1603	0.2025	0.6372
Rest	0.1761	0.2071	0.6168

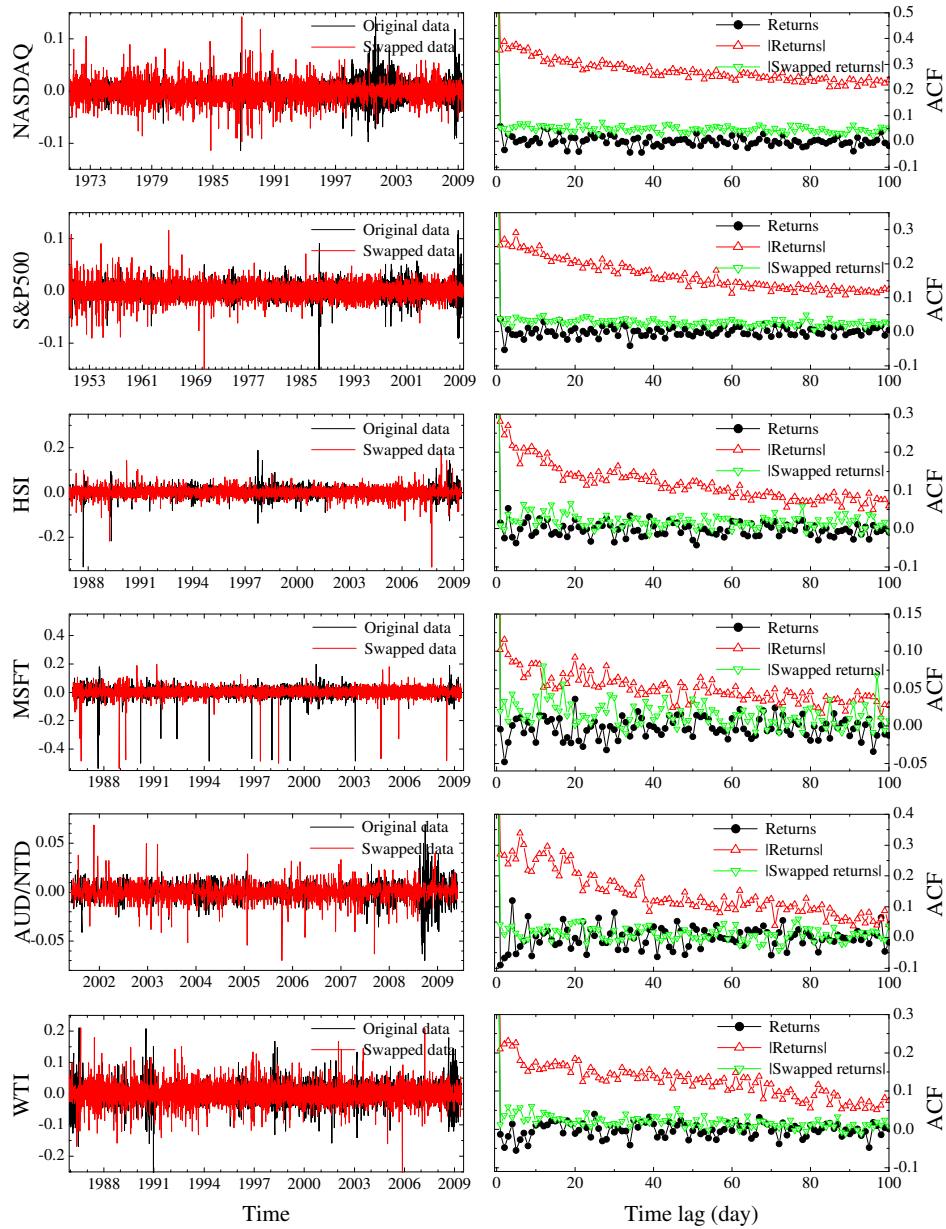


Figure A.3: The left panels show the original returns series and the 20% swapped series for NASDAQ, S&P500, HSI, MSFT, AUD/NTD and WTI (from top to bottom), while the right panels plot the autocorrelations for each of these time series.

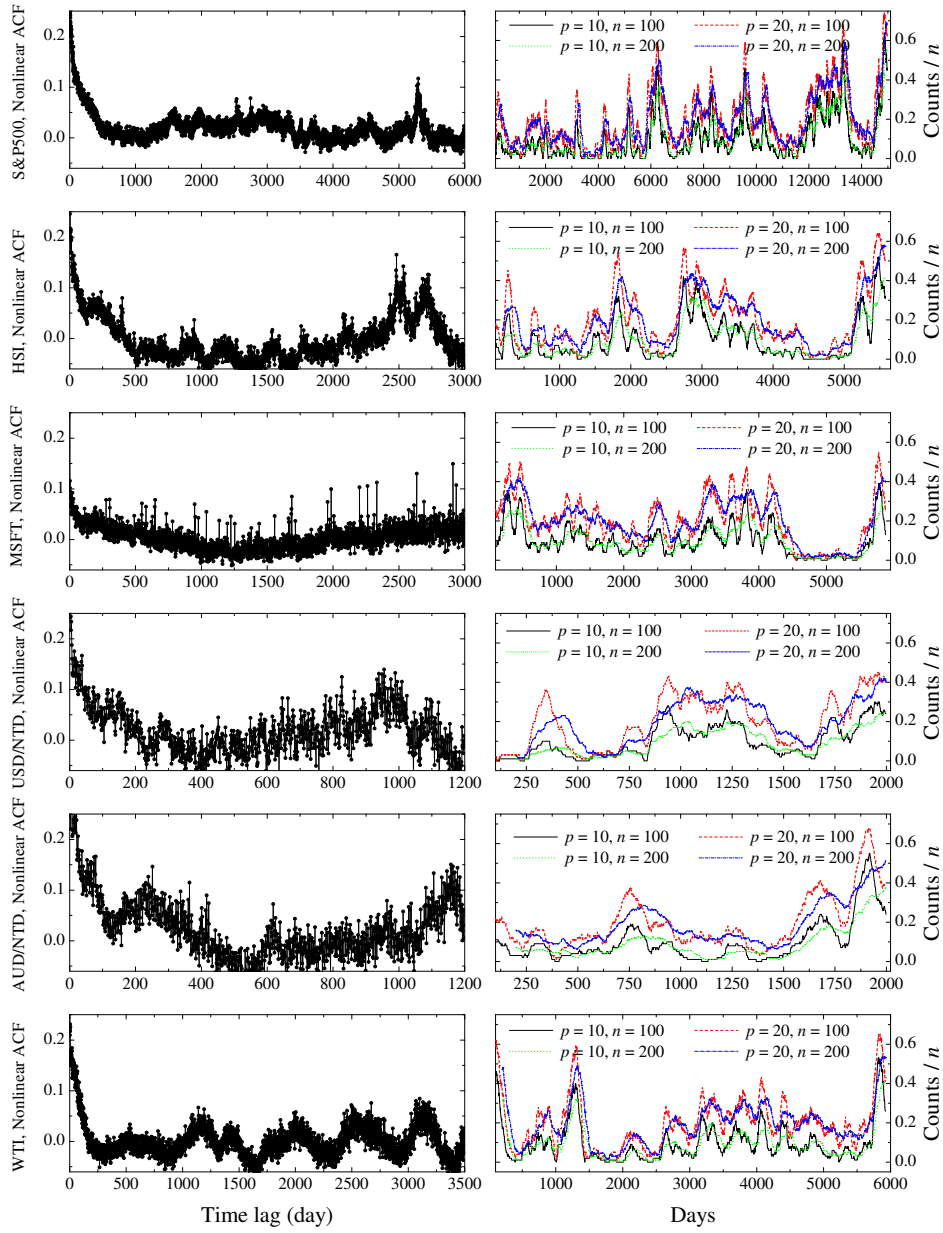


Figure A.4: The left panels show the nonlinear autocorrelation for S&P500, HSI, MSFT, USD/NTD, AUD/NTD and WTI (from top to bottom), while the right panels are the event counts for the largest $p\%$ fluctuations in these time series within a moving window of size of n days.

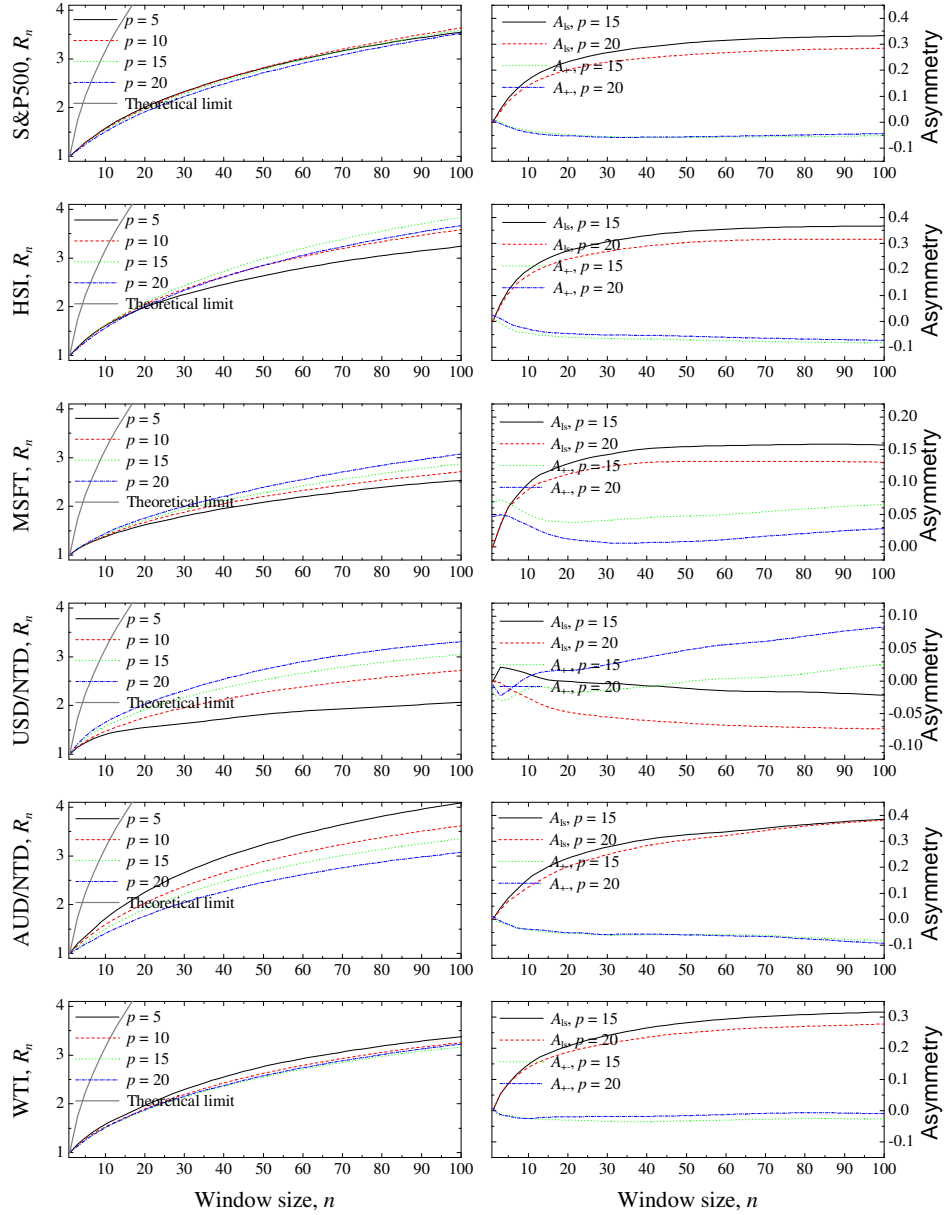


Figure A.5: The left panels show the clustering index R_n for S&P500, HSI, MSFT, USD/NTD, AUD/NTD and WTI (from top to bottom), while the right panels are the asymmetries A_{ls} and A_{+-} for each of these time series.

Table A.2: The probability of the occurrence of large and small rise/fall following the occurrence of large or small rise/fall on the previous day (the first column).

S&P500, 20%	Largest (rise/fall)	Smallest (rise/fall)	Rest (rise/fall)
Largest (rise)	0.1634/0.0954	0.0922/0.0797	0.3150/0.2543
Largest (fall)	0.1598/0.1831	0.0697/0.0690	0.2602/0.2582
Smallest (rise)	0.0678/0.0622	0.1307/0.1195	0.3497/0.2701
Smallest (fall)	0.0808/0.0794	0.1053/0.1025	0.3210/0.3110
Rest (rise)	0.0963/0.0764	0.1224/0.0979	0.3590/0.2480
Rest (fall)	0.0864/0.1139	0.1003/0.0857	0.3047/0.3090

HSI, 20%	Largest (rise/fall)	Smallest (rise/fall)	Rest (rise/fall)
Largest (rise)	0.1684/0.1088	0.1003/0.0884	0.2908/0.2433
Largest (fall)	0.1799/0.1932	0.0625/0.0587	0.2973/0.2084
Smallest (rise)	0.0904/0.0638	0.1099/0.0993	0.3351/0.3015
Smallest (fall)	0.0888/0.0743	0.1087/0.1069	0.3243/0.2970
Rest (rise)	0.0912/0.0642	0.0996/0.1210	0.3388/0.2852
Rest (fall)	0.0842/0.1091	0.1103/0.0886	0.3055/0.3023

MSFT, 20%	Largest (rise/fall)	Smallest (rise/fall)	Rest (rise/fall)
Largest (rise)	0.1726/0.1217	0.0786/0.0586	0.2865/0.2820
Largest (fall)	0.1879/0.1385	0.0835/0.0436	0.2960/0.2505
Smallest (rise)	0.0767/0.0737	0.1293/0.0917	0.3038/0.3248
Smallest (fall)	0.0629/0.0530	0.1257/0.1434	0.2888/0.3262
Rest (rise)	0.1045/0.0858	0.1148/0.0886	0.2983/0.3080
Rest (fall)	0.0963/0.0839	0.1235/0.0901	0.3082/0.2980

Table A.3: The probability of the occurrence of large and small rise/fall following the occurrence of large or small rise/fall on the previous day (the first column).

USD/NTD, 20%	Largest (rise/fall)	Smallest (rise/fall)	Rest (rise/fall)
Largest (rise)	0.2183/0.1371	0.0863/0.0051	0.2741/0.2791
Largest (fall)	0.1584/0.2822	0.0594/0.0050	0.2525/0.2425
Smallest (rise)	0.0268/0.0368	0.2542/0.1171	0.2843/0.2808
Smallest (fall)	0.0112/0.1899	0.0894/0.1117	0.1676/0.4302
Rest (rise)	0.0711/0.1438	0.0321/0.4264	0.2640/0.0626
Rest (fall)	0.0651/0.1127	0.1320/0.0511	0.2975/0.3416

AUD/NTD, 20%	Largest (rise/fall)	Smallest (rise/fall)	Rest (rise/fall)
Largest (rise)	0.0780/0.1220	0.1024/0.0976	0.2585/0.3415
Largest (fall)	0.2359/0.1077	0.0667/0.0513	0.3231/0.2153
Smallest (rise)	0.0679/0.1176	0.1222/0.0950	0.3620/0.2353
Smallest (fall)	0.1056/0.0722	0.1500/0.0778	0.3500/0.2444
Rest (rise)	0.0783/0.0934	0.1130/0.0994	0.3178/0.2981
Rest (fall)	0.1067/0.0899	0.1086/0.0918	0.3633/0.2397

WTI, 20%	Largest (rise/fall)	Smallest (rise/fall)	Rest (rise/fall)
Largest (rise)	0.1331/0.1514	0.0998/0.0815	0.2396/0.2946
Largest (fall)	0.1573/0.1829	0.0940/0.0769	0.2615/0.2274
Smallest (rise)	0.0801/0.0740	0.1193/0.0952	0.3127/0.3187
Smallest (fall)	0.0860/0.0822	0.0994/0.0880	0.3614/0.2830
Rest (rise)	0.0897/0.0756	0.1178/0.1032	0.3252/0.2885
Rest (fall)	0.0969/0.0910	0.1163/0.0757	0.3259/0.2942